EPFL

Thèse n° 10 822

Post-translational regulation of neuronal differentiation

Présentée le 20 décembre 2021

Faculté des sciences de la vie
Unité du Prof. D'Angelo
Programme doctoral en biotechnologie et génie biologique

pour l'obtention du grade de Docteur ès Sciences

par

Jaipreet Singh LOOMBA

Acceptée sur proposition du jury

Prof. B. E. Ferreira De Sousa Correia, président du jury
Prof. G. D'Angelo, directeur de thèse
Prof. D. Teis, rapporteur
Prof. J.-I. Inokuchi, rapporteur
Prof. C. Sandi, rapporteuse

École polytechnique fédérale de Lausanne

2021

Abstract

In English:

Glycosphingolipids (GSLs) are amphipathic lipid moieties that make up only 3% of the total lipid content of the cell and are almost exclusively expressed at the Plasma Membrane(PM). They are key drivers of signalling hotspots known as 'lipid-rafts' as well as acting as primary signalling molecules themselves. Pathologically, perturbations in their synthesis (Knock-Out mice models) and disorders in their metabolism(Lysosomal storage disorders), both converge on neurological symptoms. In fact, during neuronal development, stem cells have been known to completely remodel their glycosphingolipid profiles, so much so, that the developmental stages of the nervous system have been associated with the expression of different glycosphingolipids. This coordinated change in the expression of glycosphingolipids has been previously attributed to the transcriptional shift in the the expression of genes encoding specific Glycosphingolipid Synthesizing Enzymes (GSEs) observed over neuronal development and, more recently, shown to be internally regulated by the GSLs themselves whereby globosides negatively regulate the expression of the ganglioside synthesizing enzyme GM3S via a neuronal transcription factor AUTS2. In this thesis I show that there exists an extra layer of post-translational regulation that is active over neuronal development that destabilizes the Gb3 synthesizing enzyme, Gb3S, on one hand while stabilizing the GM3S on the other. The regulatory mechanism achieves this effect by doubling the rate of degradation of Gb3S in neuronal cells, probably via membrane trafficking events. The exact details of the stabilization effect of GM3S remains to be determined as the results could not ascertain if it was the same mechanism or a completely different one. My study goes on to show that this regulatory mechanism is activated early during development, preceding the changes in canonical stem and neuronal markers. Morphologically, the study points towards a post-compaction but pre-cavitation (E2.5-E3.5) point of activation for the mechanism of Gb3S destabalization, relative to early mouse embryological development. Furthermore, I found that the Gb3S interactor and AUTS2 transcriptional target UCHL1 is a key regulatory unit of the machinery such that inhibiting its activity results in a specific rescue of the Gb3S enzyme.

In French:

Les glycosphingolipides (GSL) sont des fragments lipidiques amphipathiques qui ne représentent que 3% du contenu lipidique total de la cellule et sont presque exclusivement exprimés au niveau de la membrane plasmique (PM). Ils sont les principaux moteurs des points chauds de signalisation connus sous le nom de "radeaux lipidiques" et agissent eux-mêmes en tant que molécules de signalisation primaires. Pathologiquement, les perturbations de leur synthèse (modèles souris Knock-Out) et les troubles de leur métabolisme (troubles du stockage lysosomal), convergent tous deux vers des symptômes neurologiques. En effet, au cours du développement neuronal, les cellules souches sont connues pour remodeler complètement leurs profils de glycosphingolipides, à tel point que les stades de développement du système nerveux ont été associés à l'expression de différents glycosphingolipides. Ce changement coordonné dans l'expression des glycosphingolipides a été précédemment attribué au changement transcriptionnel de l'expression des gènes codant pour des enzymes de synthèse de glycosphingolipides (GSE) observés au cours du développement neuronal et, plus récemment, il a été démontré qu'il est régulé de manière interne par les GSL elles-mêmes, par lequel le globoside Le Gb3 régule négativement l'expression de l'enzyme de synthèse des gangliosides GM3S via un facteur de transcription neuronal AUTS2. Dans cette thèse, je montre qu'il existe une couche supplémentaire de régulation post-traductionnelle active sur le développement neuronal qui déstabilise l'enzyme de synthèse du Gb3, Gb3S, d'une part, tout en stabilisant le GM3S d'autre part. Le mécanisme de régulation atteint cet effet en doublant le taux de dégradation du Gb3S dans les cellules neuronales, probablement via des événements de trafic membranaire. Les détails exacts de l'effet de stabilisation du GM3S restent à déterminer car les résultats n'ont pas pu déterminer s'il s'agissait du même mécanisme ou d'un mécanisme complètement différent. Mon étude montre ensuite que ce mécanisme de régulation est activé tôt au cours du développement, précédant les changements de la tige canonique et des marqueurs neuronaux. Morphologiquement, l'étude pointe vers un point d'activation post-compaction mais pré-cavitation (E2.5-E3.5) pour le mécanisme de déstabilisation du Gb3S, par rapport au développement embryologique précoce de la souris. De plus, j'ai découvert que l'interacteur Gb3S et la cible transcriptionnelle AUTS2 UCHL1 sont une unité régulatrice clé de la machinerie, de sorte que l'inhibition de son activité entraîne un sauvetage spécifique de l'enzyme Gb3S.

Contents

List of Figures

Introduction

1 GSL Synthesis:

The full GSL synthetic, functional and pathological complexity has been exhaustively reviewed in multiple publications by our lab and others (Merrill 2011; D'Angelo et al. 2013; Russo, Capolupo, et al. 2018; Inokuchi et al. 2018) so to state briefly, GSL synthesis is embedded in the endomembrane system and begins in the Endoplasmic Reticulum (ER) where the common precursor to all GSLs, Ceramide (Cer), is first synthesized by the condensation of a sphingoid base with an acyl-CoA. The reaction is catalysed by a group 6 Ceramide Synthesizing enzymes (CerS) and the preference of these enzymes for acyl-CoA of different chain lengths adds another dimension to the complexity of these lipids. Ceramide can either get galactosylated (GalCer) in the ER or be transported to the Golgi via different routes resulting in separate pools compartmentalized by the Golgi. The pool that is transported to the Trans Golgi Network (TGN) by the Ceramide Transfer protein (CERT) is used for making Sphingomyelin whereas Cer reaching the cis-Golgi is glucosylated to form Glucosylceramide (GlcCer). GlcCer is further galactosylated by B4GALT5-6/LacCerSynthase(LCS) to form Lactosylceramide(LacCer) once it is translocated to the luminal membrane of the Golgi upon which, it is unable to flip back to the cytosolic leaflet thereby resulting in the exclusive expression of GSLs on the outer leaflet of the PM. LacCer is the common precursor used for the synthesis

1. GSL Synthesis:

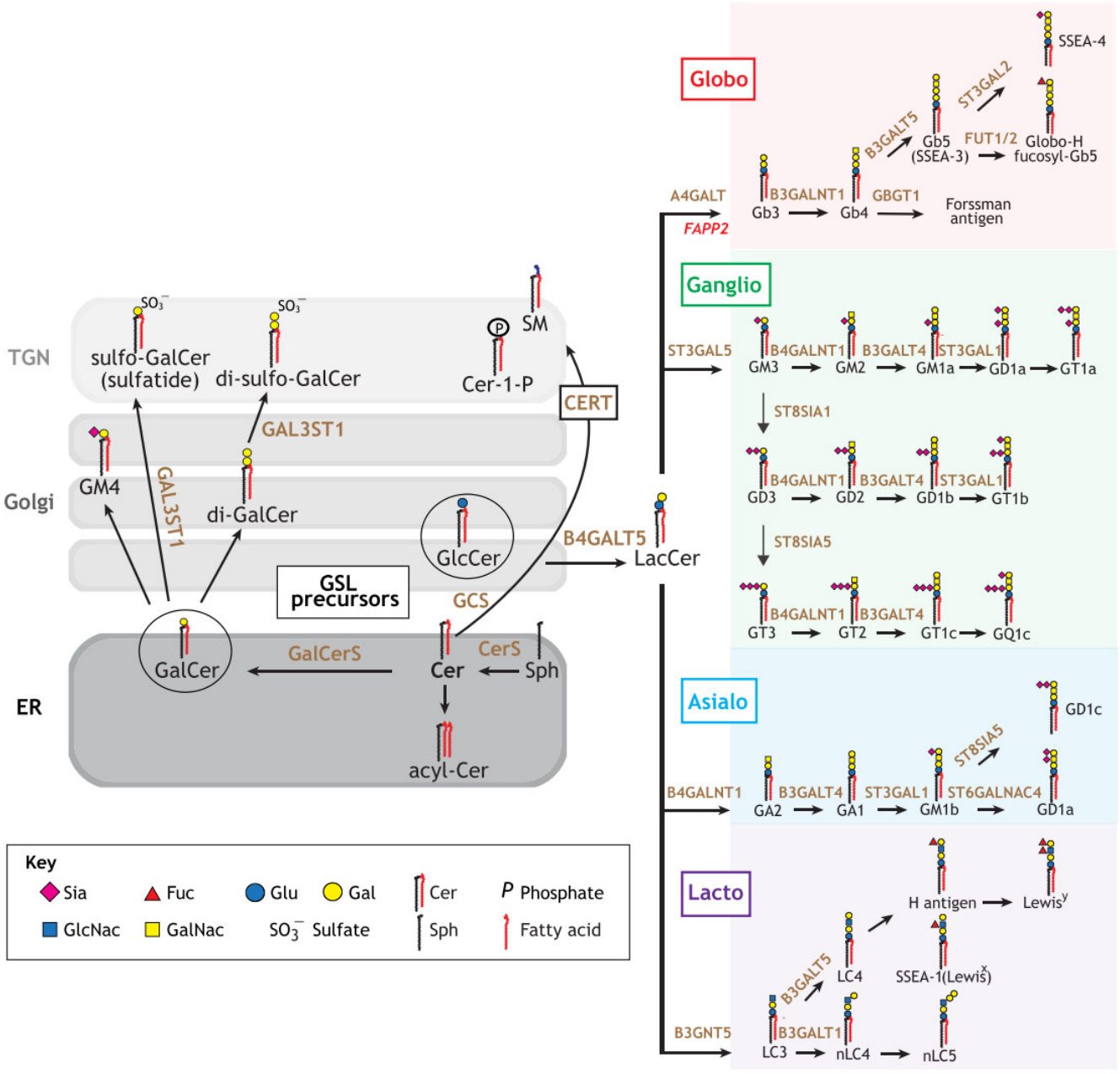

Figure 1.1: Schematic Representation of Glycosphingolipid Synthesis and diversity as illustrated in review 3.

of all complex GSLs (apart from sulfatides which are made by GalCer) by a series of sequential template-independent glycosylation events catalysed by specific glycosyltransferases (GTs) commonly termed for GSLs here as Glycosphingolipid Synthesizing Enzymes(GSEs)(Figure-1.1).

1. GSL Synthesis:

We now understand that the actual expression of a particular GSL is not only directly dependent upon the expression of the involved GSEs but also significantly impacted upon by their localization(Pothukuchi et al. 2020; Rizzo et al. 2021). In fact, the compartmentalized location of GTs has been proposed to be the dominant factor influencing the expression of a specific glycan such that when two or more enzymes compete for a single substrate, like LacCer, the order in which they get access to it determines the glycan profile of the cell(Fisher et al. 2019). For the purposes of this project, we shall focus on 2 such competing enzymes, globoside Gb3 Synthesizing enzyme (Gb3S) or A4GALT and ganglioside GM3 Synthesizing enzyme (GM3S) or ST3GAL5, that use LacCer as a precursor to produce the core structures for all globosides and gangliosides, respectively. Both are type II transmembrane proteins with a catalytic domain facing the lumen of the golgi, a transmembrane region and "cytosolic-tail" unit.

2

Gb3 Synthesizing Enzyme (Gb3S) or A4GALT

Gb3S catalyses the formation of Globoside, Gb3, by adding another galactose to the growing end of the sugar chain on LacCer with a α-1-4-linkage, hence the name A4GALT (Merrill 2011). Gb3 has been a topic of much discussion due to its role in pathologic conditions like Fabry's disease, as well as a receptor for Shiga toxin, verotoxin and HIV adhesin gp120(Merrill 2011), but the synthesizing enzyme itself, Gb3S, is poorly understood. Even though the enzyme has been effectively cloned since the early 90's, the actual expression states of the enzyme was never fully understood and only commented upon in a publication in 2010 which also showed that the the Gb3S enzyme can be post-translationally regulated to produce Shiga-Toxin (ShTx) resistant cell lines(Yamaji, Nishikawa, et al. 2010). In the study Yamaji et. al, revealed that the enzyme in present in 2 forms at steady state in HeLa which they characterized as; *Band1*- Endo-H resistant mature form with complex glycans, appearing as a glycosylated smear at ~45-50kd and; *Band2*- Endo-H sensitive high-mannose immature band, appearing as a sharp band ~37kd (Yamaji, Nishikawa, et al. 2010, (Supplementary FigS4A)). In fact, the study showed that the only other enzyme that conferred the same level of ShTx resistance upon overexpression was GM3S which would divert the flow of the common precursor,

LacCer, towards producing more GM3 thereby inhibiting ShTx binding. The study goes one to show that FAIM2 and GRINA, 2 members of the TMBIM family of proteins localized to the Golgi, both post-translationally regulated Gb3S by affecting its localization along with TGN46. Apart from this study, another description of the different forms of Gb3S is not yet available although overexpressing this enzyme to produce more Gb3 has been a common method for studying GSL mediated changes(Pothukuchi et al. 2020; Rizzo et al. 2021).

The idea that post-translational regulation of Gb3S might be more or at least just as critical as the actual expression of Gb3S mRNA has been steadily growing traction since its discovery as the same authors(and another individual screen(Pacheco et al. 2018)) have since identified 2 other proteins, LAPTM4a and TM9SF2, that had never been previously implicated in the GSL biosynthetic pathway nevertheless, confer ShTx resistance in whole genome CRISPR KO screens. LAPTM4a, a lysosome associated trans-membrane protein with unknown function, reduces Gb3S activity but not total levels whereas TM9SF2 KO cells seemed to mis-localize Gb3S, along with TGN46 and some other GSEs(Yamaji, Sekizuka, et al. 2019). The actual interaction of both of these proteins seemed to be specific for Gb3S although decreased interaction and perturbations in localization of the other GSEs was also seen(Yamaji, Sekizuka, et al. 2019). All of these examples point towards the post-translational regulation of GSEs controlling GSL expression.

3

GM3 Synthesizing Enzyme (GM3S) or ST3GAL5:

Most of our understanding about GM3S comes from substantial efforts by Inokuchi et.al and here I provide a brief summary of their efforts and others as reviewed as recently(Inokuchi et al. 2018). We now understand that *human* GM3S has 5 transcript variants(type- a1, a2, b1, b2 and c) that, upon leaky translation, give rise to 4 isoforms (M1, M2, M2' and M3) of the protein with variable cytoplasmic-tail lengths (69, 42, 47 and 14aa, respectively). The tail lengths are critical for these enzymes as it has been observed that isoforms of different tail lengths have different subcellular localization and half-life and, in fact, an "R/K-based motif" has been proposed by Inokuchi et.al as a novel ER export signal whereby two lysine residues located downstream of the canonical RR ER export sequence [$^{2}R^{3}R(X)_{5}{}^{9}K(X)_{3}{}^{13}K$] were seen to be critical for the export of the M3 isoform. M3 isoform seems to be capable of being expressed by all types of transcripts whereas M1 isoform is the only one bearing a retrograde transport signal, resulting in a mostly ER localization of the isoform. M2 is localized correctly in the Golgi but has a much shorter half life time than M3. Finally M2' isoform is only found in cells expressing type c transcript variant which is a special liver specific transcript that is currently being characterized. All together, it would seem that M3 and M2 transcripts

3. GM3 Synthesizing Enzyme (GM3S) or ST3GAL5:

make the bulk of the GM3 with M3 being the dominant form although Inokuchi et. al, also propose specific roles for other transcripts such that M1 transcript may regulate the expression levels of the other transcripts as observed by them in upublished data(Inokuchi et al. 2018).

4

Globo-to-Ganglio Switch and the AUTS2 axis over neuronal differentiation from stem cells:

The complete GSL remodelling events observed over embryonic development have been critically reviewed by us in the sub chapter titled "GSL changes during embryonic development and cellular differentiation" in a recent article (Russo, Capolupo, et al. 2018) so for the purposes of this project, I would direct the reader's attention to a specific regulatory event i.e. Gb3-AUTS2-GM3S circuit which is the cornerstone of this project.

The project stems from a previous published work from the lab which disclosed an intricate circuit whereby GSLs are able to self-regulate their expression (Russo, Della Ragione, et al. 2018). The study showed that the Globoside Gb3 had an inhibitory effect on the expression level of a neuronal transcription factor called AUTS2 which, in turn, promotes the expression of the enzyme that initiates the synthesis of ganglio series GSLs, i.e. GM3 synthase (GM3S)(Figure-4.1-A). The study achieved this understanding by a key experiment whereby differentiating stem cells supplemented with exogenous Gb3 do not progress towards their neuronal fate(Figure-4.1-B). When I joined the lab, I was captivated by the study and at least 2 questions particularly appealed to me; how do lipids on the plasma membrane

4. Globo-to-Ganglio Switch and the AUTS2 axis over neuronal differentiation from stem cells:

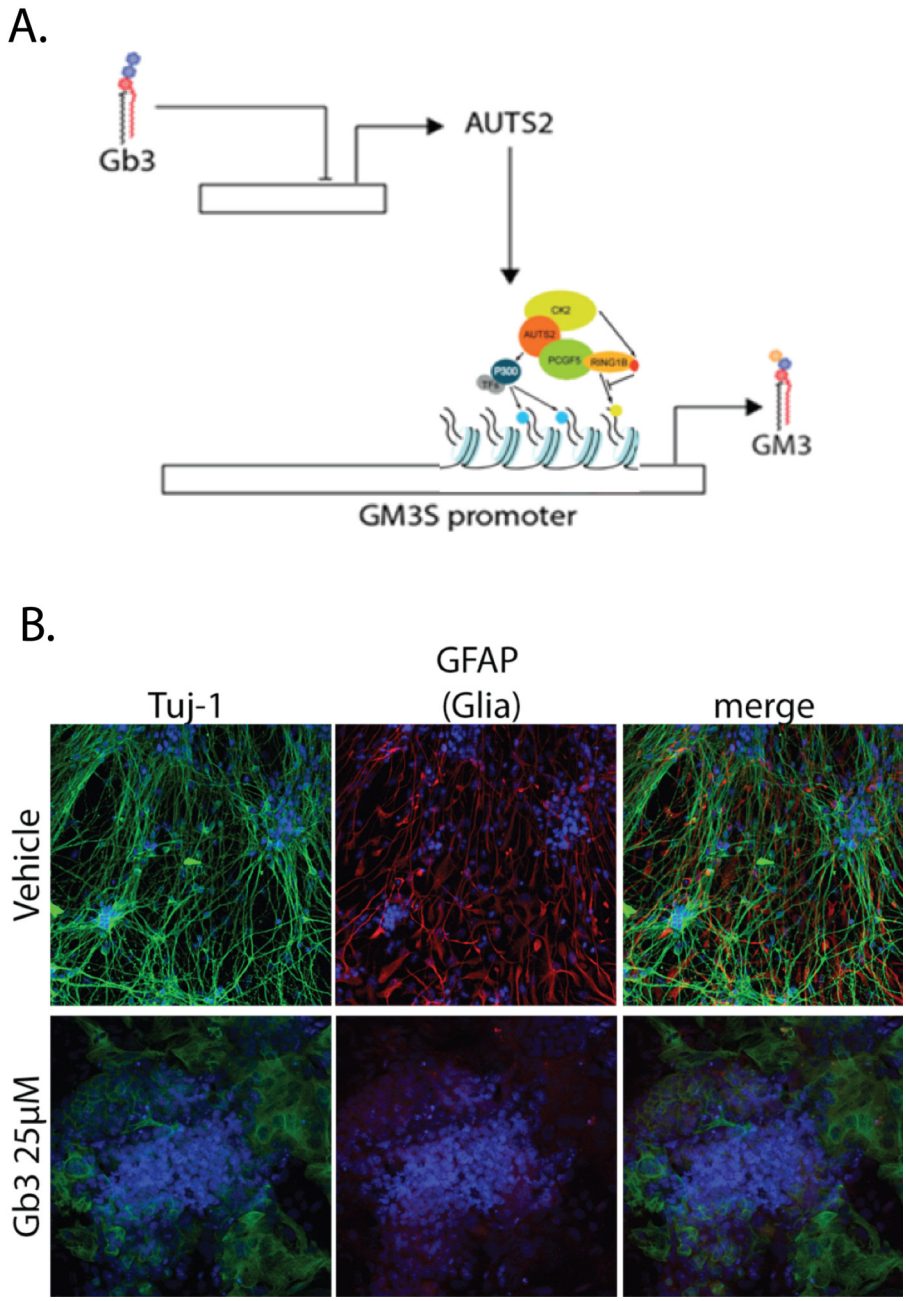

Figure 4.1: A. Schematic Representation Gb3-AUTS2-GM3S cirvuit and; B. Representative confocal image of effect of Gb3 on differentiating stem cell. Images courtesy Domenico Russo.

exert such direct control over a transcription factor? And, can cell fate decisions be directed by regulating the expression levels of GSL synthesizing enzymes (GSEs)?

Results

5

Glycosphingolipid metabolic reprogramming circuit is regulated by NF-kB pathway:

To answer the first query, the lab had already decided to look at the transcriptional regulation of genes that, like AUTS2, were induced upon globo series GSL depletion in HeLa cells for which they mined data previously obtained (Russo, Della Ragione, et al. 2018) on transcriptional changes induced by silencing GSEs in HeLa cells where their effect converges towards a reduction of cellular globo series GSL levels. Upon imposing stringent significativity thresholds we found 5 genes that have a similar transcriptional response as AUTS2 (i.e. they are induced by a decrease in Gb3 levels), these are CTDSP2, HOXA5, NLGN4X, PGCP and SLC48A1 (Zhao et al. 2018). We looked at the promoters of these genes to find shared regulatory elements and noticed that they were enriched in binding sites for NF-kB in proximity to their transcriptional start sites (TSS). Specifically AUTS2, NLGN4X, PGCP and SLC48A1 had NF-kB binding elements at their TSS while CTDSP2 and HOXA5 did not (Figure-5.1). Incidentally our previous data show that both CTDSP2 and HOXA5 are AUTS2 targets suggesting that their regulation upon globo series GSL depletion is downstream AUTS2 activation.

5. Glycosphingolipid metabolic reprogramming circuit is regulated by NF-kB pathway:

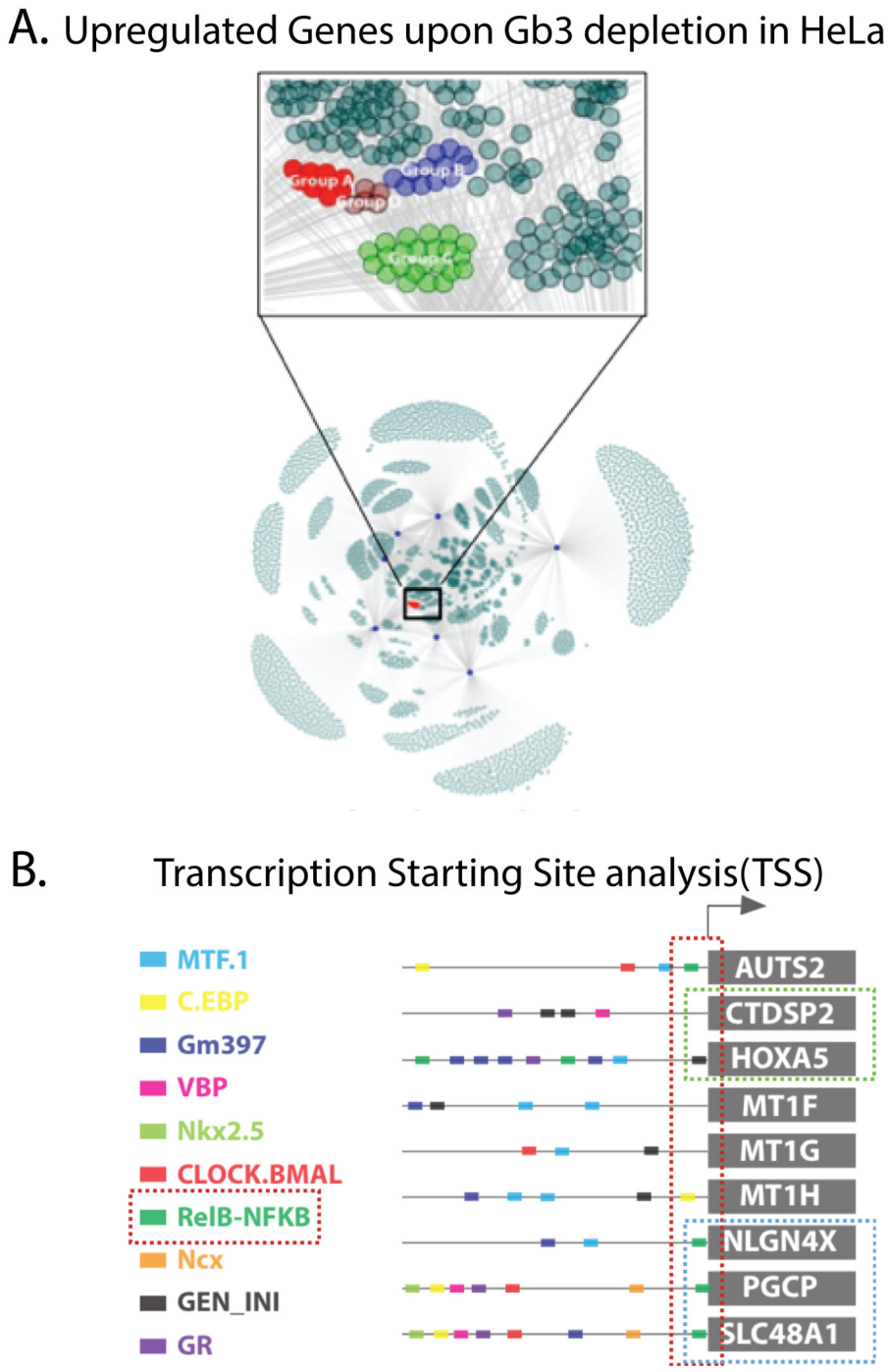

Figure 5.1: Schematic representation of A. Data mining of Commonly upregulated genes upon globo series GSL depletion in HeLa cells and; B. Transcription Starting Site (TSS) analysis on the promotor regions of commonly upregulated genes.

5. Glycosphingolipid metabolic reprogramming circuit is regulated by NF-kB pathway:

We thus tested the possible involvement of the NF-kB pathway in the GSL dependent AUTS2 modulation. First we silenced HeLa cells for the expression of Gb3S and looked at IkBa and p65 phosphorylation (two readouts of NF-kB pathway activation). As shown in Figure-5.2-A we noticed that Gb3S KD results in increased phosphorylation of both p65(Rel-A) and IkBa. We also noticed that the overall protein levels of IkBa were increased in Gb3S-KD HeLa cells . In fact, IkBa is a transcriptional target of NF-kB (Vu et al. 2013) and accordingly IkBa mRNA levels were increased in Gb3S-KD HeLa cells where this increase could be reverted by concomitant p65 silencing (Figure-5.2-B). Importantly, similar results were obtained when looking at AUTS2 and GM3S expression whereby silencing of Gb3S induces an increase in their mRNA levels that could be reverted by concomitant silencing of p65 or by pharmacological inhibition of the NF-kB pathway by BMS-345541 a highly selective inhibitor of I kappa B kinase(Burke et al. 2003) (Figure-5.3). Altogether these data suggest that globo series GSLs repress NF-kB pathway activation that is responsible for the induction of AUTS2 and of its downstream targets (including GM3S).

5. Glycosphingolipid metabolic reprogramming circuit is regulated by NF-kB pathway:

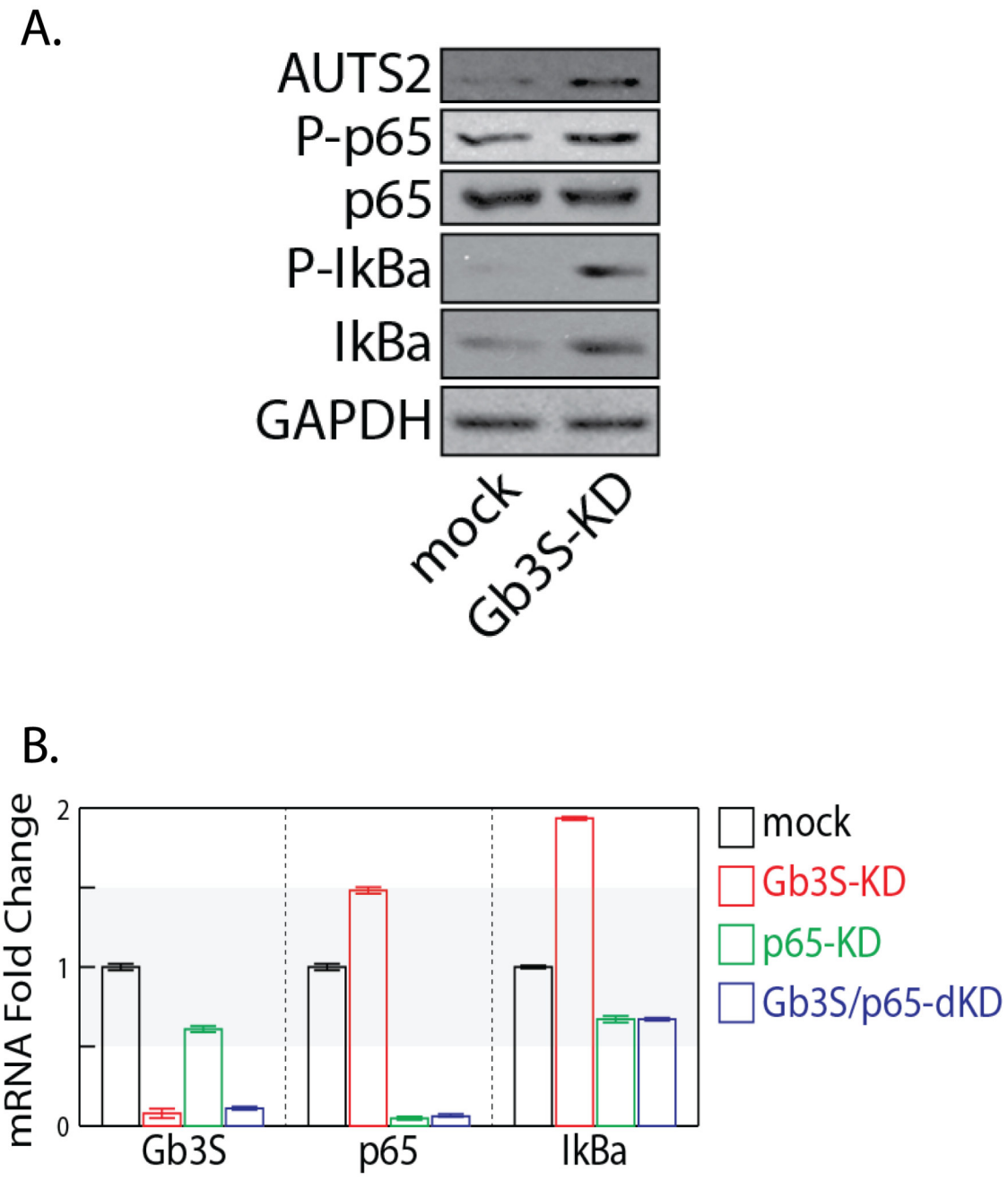

Figure 5.2: A. Representative western blot image of NFKB pathway activation upon Gb3SKnock-Down(KD) and; B. mRNA expression levels of IKBa upon Gb3SKD, p65(Rel-A)KD and double KD. Data are shown as the mean ± SD of 3 individual experiments

5. Glycosphingolipid metabolic reprogramming circuit is regulated by NF-kB pathway:

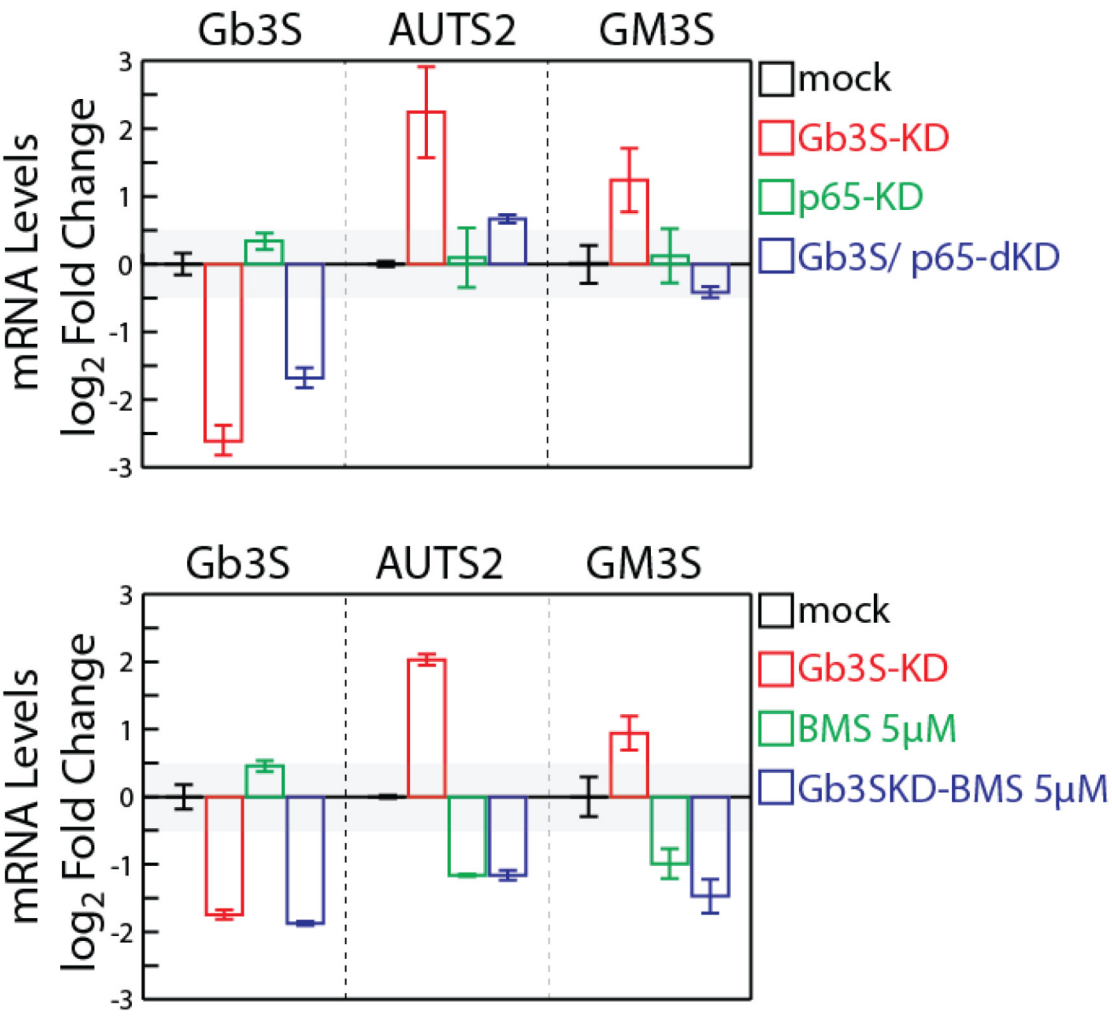

Figure 5.3: mRNA expression levels of AUTS2 and GM3S upon Gb3SKD with p65KD or BMS-345541. Data are shown as the mean ± SD of 3 individual experiments

5. Glycosphingolipid metabolic reprogramming circuit is regulated by NF-kB pathway:

NFkB signalling cascade is triggered by the engagement of a host of different receptor types as well as internal regulations and feedback loops but one of the largest and most ubiquitously expressed NFkB activating receptor families is the TNF Superfamily of receptors (Cheung and Ware 2013). The TNF family specifically interested me because of its history with other GSLs and for the fact that a study published back in 2008 bluntly pointed a finger towards the FasR(CD95)(Chakrabandhu et al. 2008), a member of the TNF Superfamily exhibiting a putative Glycosphingolipid Binding Domain (GBD). The GBD had been theorized in the early 2000's as these structurally related motifs in transmembrane proteins (mostly receptors) that are close to the membrane and have been shown to affect receptor internalization cycles. In fact, the study specifically mentions FasR to possess such a domain that docks with Gb3 and LacCer and, that disrupting this interaction by mutating the GBD in FasR results in a switch in the internalization route of the receptor whereby the "death" receptor starts activating the pro-survival signalling cascade. By probing the response of parental and Gb3S-KD HeLa cells to increasing levels of TNFa or FASL we found that Gb3S-KD HeLa cells were specifically sensitive to FASL induced NFkB activation(Figure-5.4). Moreover, immunofluorescence assays on Gb3S-KD HeLa cell overexpressing HA-tagged FasR did support the hypothesis that in the absence of Gb3, FasR is constitutively activated and incessantly internalized (Figure-5.5).

Overall, from these experiments we can conclude that globo series GSLs (and specifically Gb3) repress the expression of the neural transcription factor AUTS2 by counterting FAS mediated activation of the NF-kB pathway. NF-kB activation is indeed required for the induction of AUTS2 resulting from Gb3S silencing. When translated into the physiological contest of neural differentiation these data agree with published reports where NF-kB activation has been shown to be required in the initial steps of this process(Zhang and HU 2012) and pose the fundamental question of how the levels of inhibitory globo series GSLs are regulated in this crucial step.

5. Glycosphingolipid metabolic reprogramming circuit is regulated by NF-kB pathway:

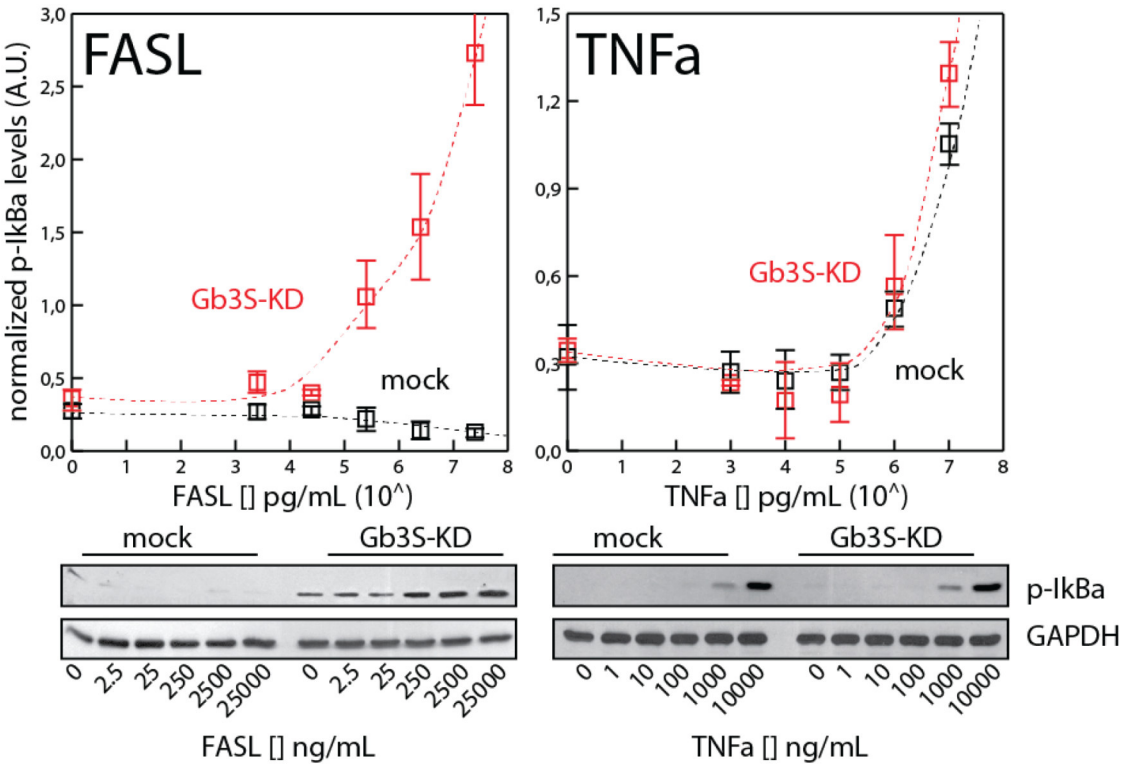

Figure 5.4: Control(mock) and Gb3SKD cells were treated with increaseing concentrations of FAS-Ligand (FASL) and TNFa. Data are shown as the mean ± SD of 3 individual experiments

5. Glycosphingolipid metabolic reprogramming circuit is regulated by NF-kB pathway:

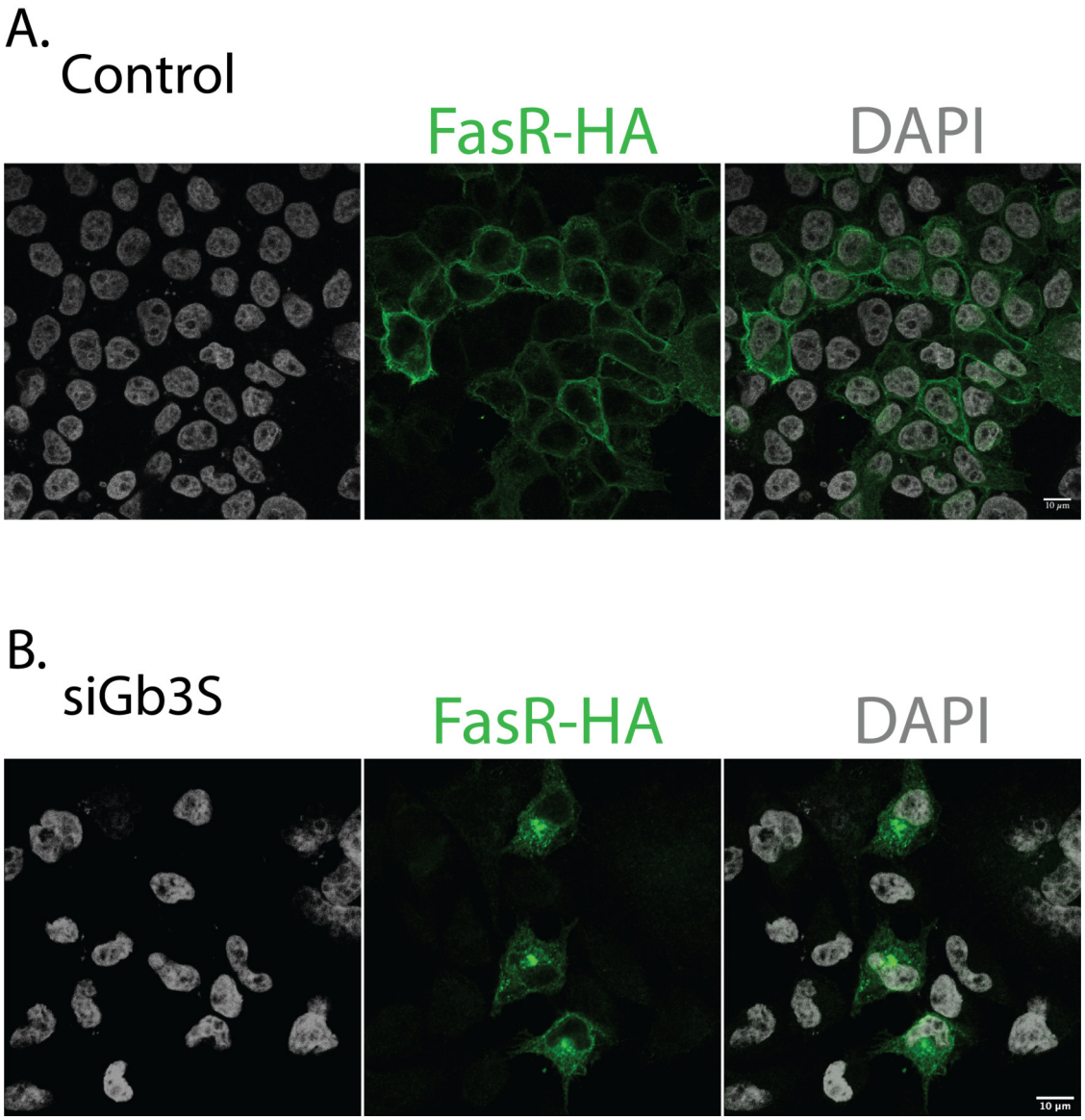

Figure 5.5: Representative confocal image of Control and Gb3SKD cells OverExpressing (OE) FAS-Receptor (FasR).

6

GSEs are post-transcriptionally regulated during neural differentiation.

Contents

6.1 Establishing human Gb3S-HA OE E14 mESC lines

The established system of adding exogenous lipids to the cell growth media had proved cumbersome when discerning complex signaling pathways in the neuronal differentiation model. The system had also been previously critiqued regarding the amount of exogenous lipid used even though the amount of uptake has been estimated to be only about 0.1%, still this was a concern. This prompted us to explore the idea of establishing mESc lines endogenously over-producing globo series GSLs over the course of the 13-day neuronal differentiation protocol. To

increase the possibility of evading any unbeknownst molecular regulation while at the same time be able to effectively monitor the enzyme to isolate pure Gb3S OE clones, we decided to randomly integrate HA-tagged human Gb3S under a constitutively active chicken B-actin promoter into the mouse E14 Embryonic stem cell genome using a PINCO derived vector called PALLINO, donated to us by Maurizio D'Esposito(Figure-6.1). Our strategy allowed for a large assortment of clonal cell lines with varied expression profiles by sacrificing control over the location of the integrate. This would also mean that genome integration would not guarantee protein expression. The construct was linearized, dephosphorylated and electroporated into mESc whereupon the puromycin resistant cells were isolated and expanded as described in materials and methods. Genomic integration and protein expression and localization were validated in the surviving clones(Figure-6.2).

6. GSEs are post-transcriptionally regulated during neural differentiation.

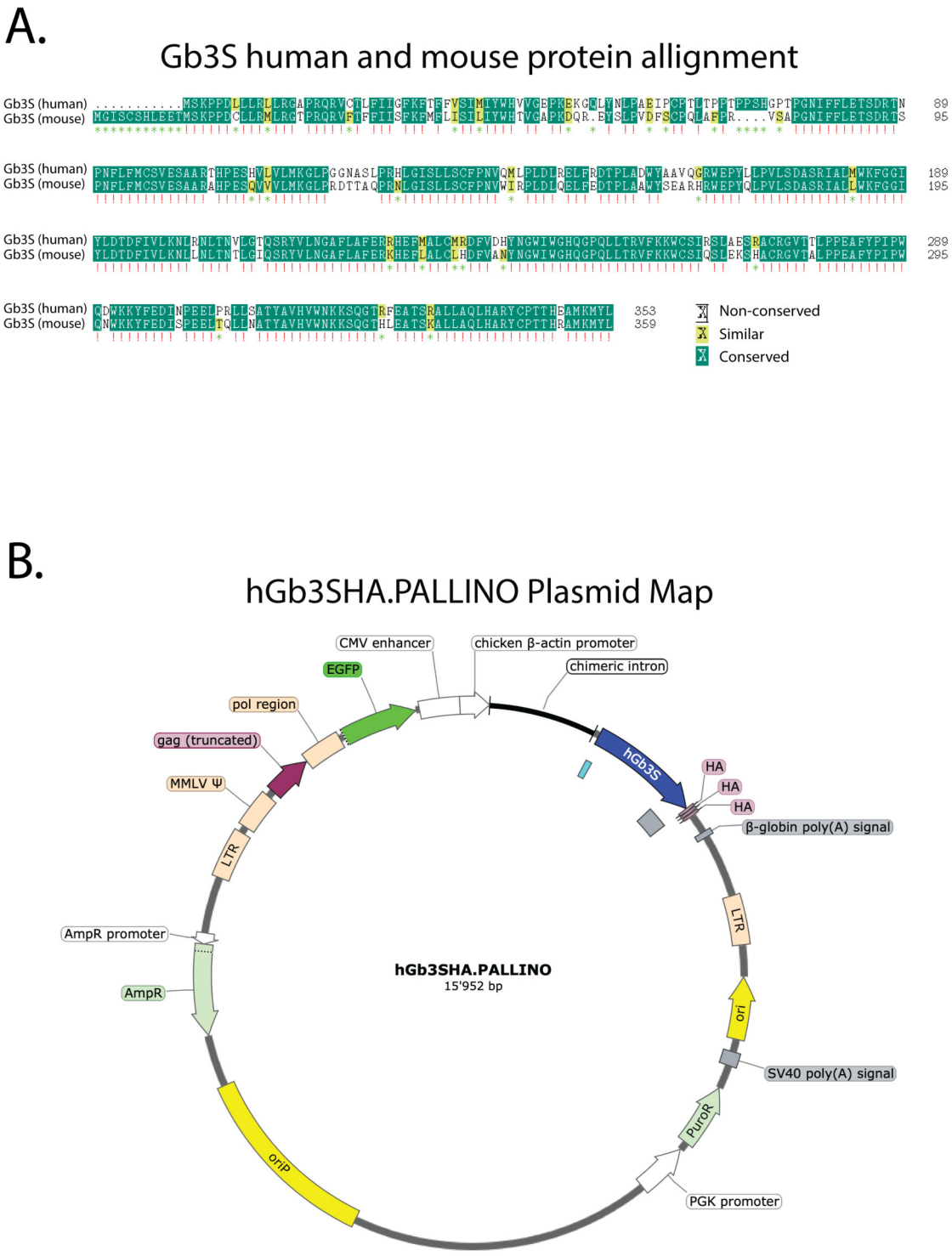

Figure 6.1: A. Human Gb3S and Mouse Gb3S protein allignment; B. Schematic representation of the final construct i.e. Human Gb3S X3HA in PALLINO

6. GSEs are post-transcriptionally regulated during neural differentiation.

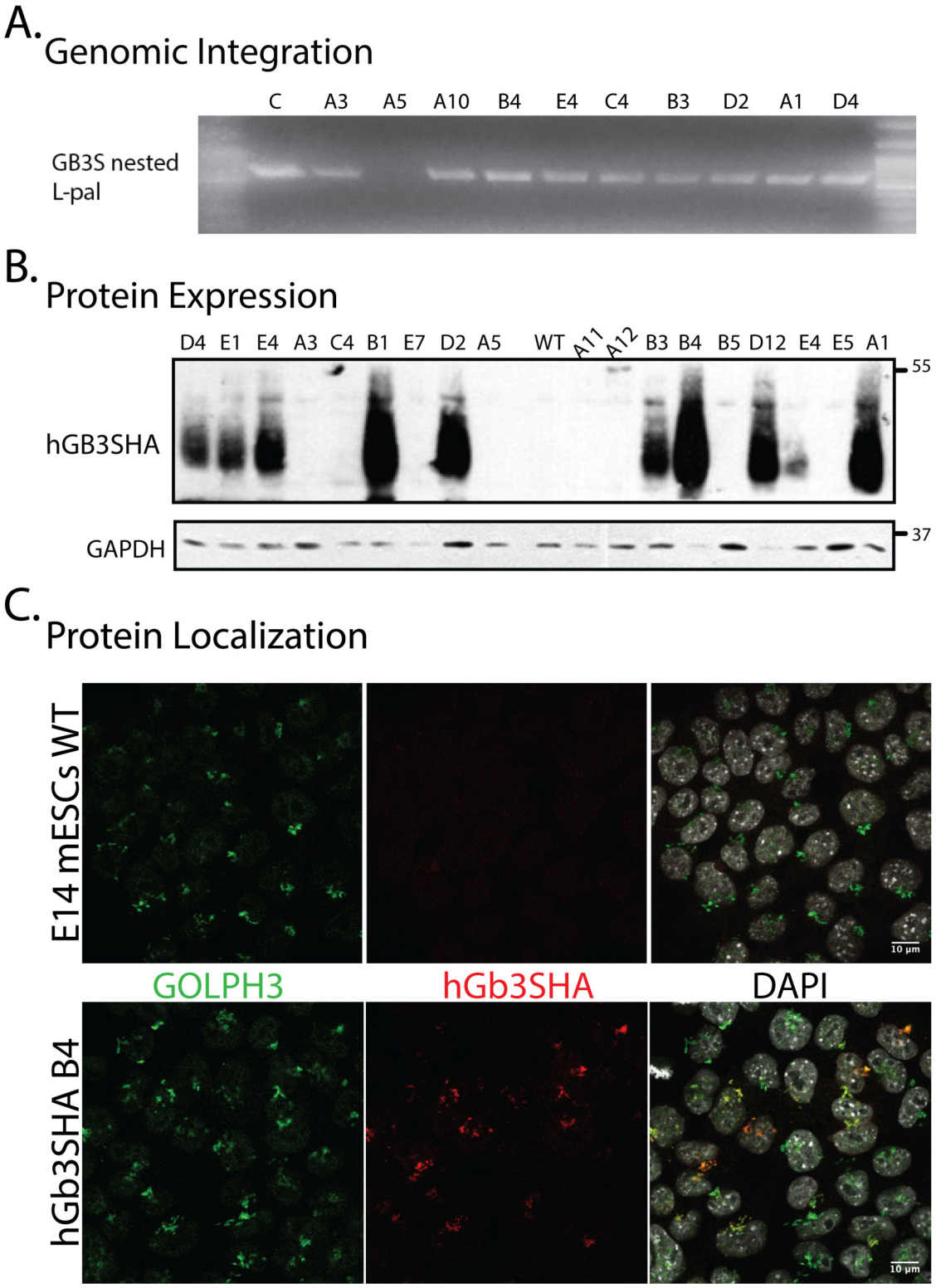

Figure 6.2: A. Representative image of Genetic Integration in hGb3SHA positive clones tested contruct specific primers; B. Protein expression levels of isolated hGb3SHA positive clones and; C. Representative confocal image of the protein localization in one hGb3SHA Clone B4. *All other positive clones show similar colcalization with Golgi marker GOLPH3

6. GSEs are post-transcriptionally regulated during neural differentiation.

6.2 Differentiation of hGb3SHA clones and an unexpected development:

We proceeded with our scheme of differentiating the OE cell lines and expected to recapitulate the same kind of phenotypic behavior as observed when neuronal differentiation is carried out in the presence of exogenous Gb3(Figure-4.1-B). Over the course of the 13-day neuronal differentiation protocol, major morphological transformations can already be observed by day 6-7 when the neuronal precursors start sprouting delicate fibrils which later establish into strong axons sometime spanning the diameter of the culture dish. The severity of the phenotype observed upon exogenous lipid substitution brought about a complete halt to such transformation and the cells remained in amorphous shapes throughout the protocol. For our first differentiation experiment we decided to use a high expressing (B4) and a low expressing (D4) clone although neither directly contributed to any significant difference in the globoside levels at stem cell stage. It soon became apparent that we would not be witnessing the catastrophic phenotype as observed by exogenous Gb3 substitution in the media as all 3 cell lines looked very similar morphologically. Transcription profiling also confirmed that the clonal cell lines differentiation mirrored the WT differentiation with little to no differences in the hGb3SHA mRNA levels post differentiation(Figure-6.3). The immunofluorescence, on the other hand, revealed something unexpected(Figure-6.4).

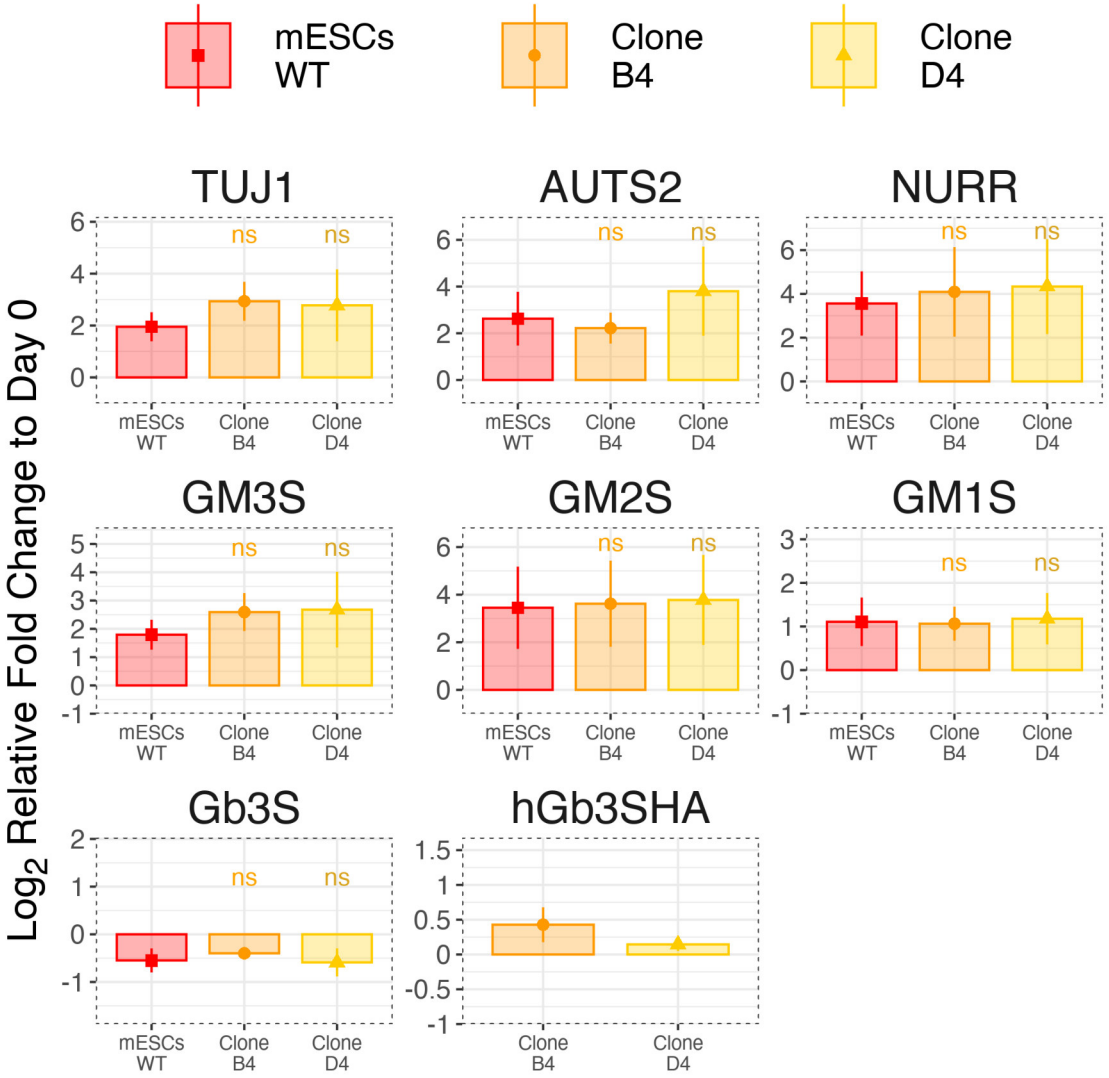

Figure 6.3: mRNA expression levels plotted as Relative Fold Change (RFC) to Day 0 for each individual cell line Post-Differentiation. There were no significant differences in the expression of Neuronal markers (TUJ1, AUTS2, NURR), Endogenous Gb3S or GSEs(GM3S, GM2S, GM1S) between the mESC WT and the hGb3SHA clones. mRNA expression level of our integrate, hGb3SHA, remains mostly unchanged in the both the clones (B4 and D4). Data are shown as the mean ± SD of 3 individual experiments

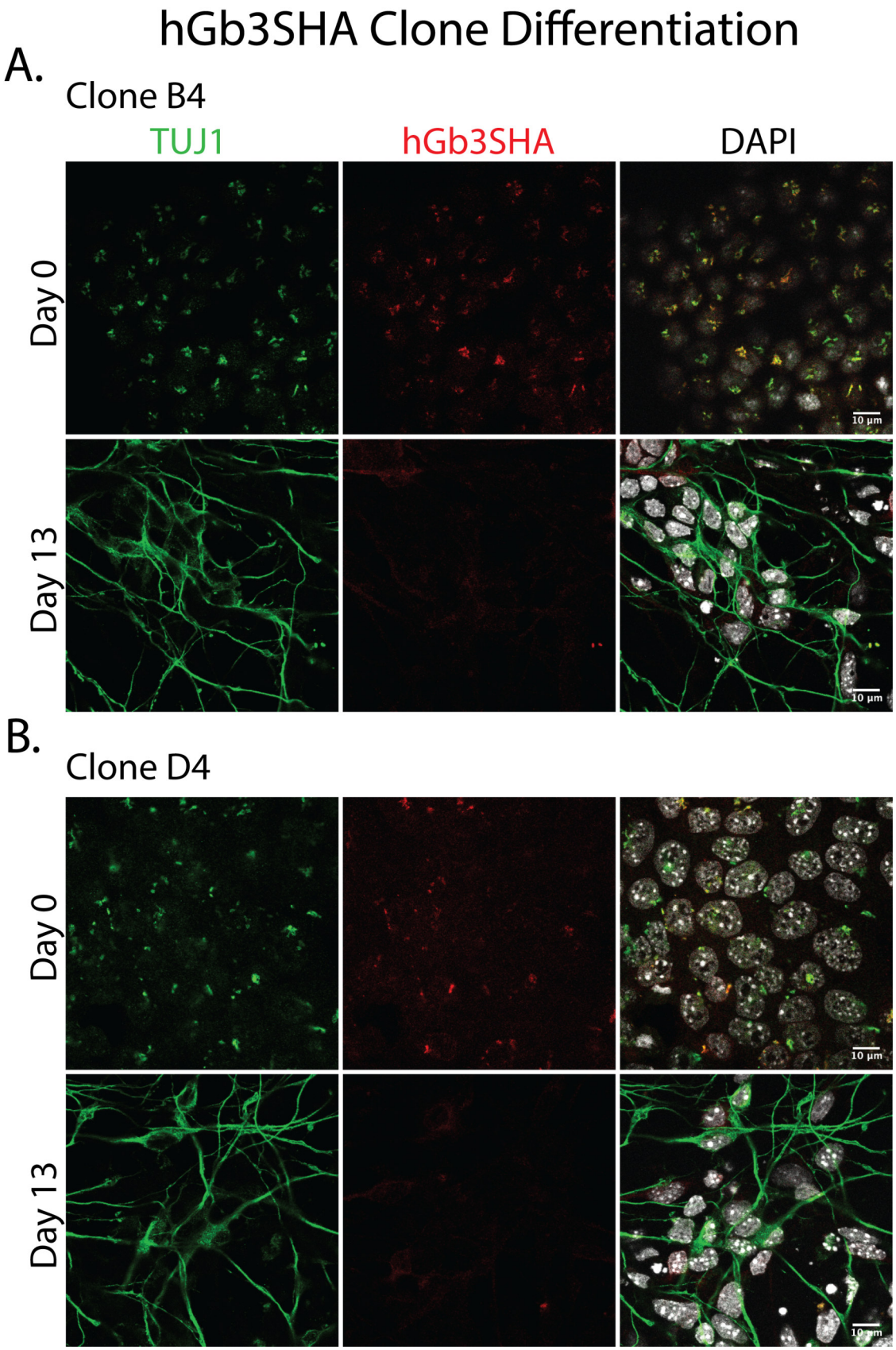

Figure 6.4: A. and B. Representative confocal images of hGb3SHA clones B4 and D4 at Stem (Day0) and Neuronal(Day13) stages. hGB3SHA is clearly visible at the Golgi (GOLPH3 as marker) as Stem cells whereas as Neurons (TUJ1 as marker) hGb3SHA staining is barely visible.

6. GSEs are post-transcriptionally regulated during neural differentiation.

The 13-day neuronal differentiation protocol is optimized to drive the stem cells to neuronal fate still, it does not entirely ensure a pure population of neurons. In fact, in a well-controlled differentiation experiment one can expect 50-70% of the cells to undergo neuronal transformations while the rest either don't differentiate or go down some alternative differentiation paths. This realization was imperative for analyzing the immunofluorescence assay as we observed that hGb3SHA was almost completely invisible in the differentiated cells whereas the control stem cells for the same clones still showed a crisp localization of the enzyme in the Golgi(Figure-6.5). The effect was much more striking in the low expressing clone (D4) but the high expressing clone (B4) contributed more to our understanding of the observation as in differentiated B4 cells it could be observed that although most of the cells showed almost no staining with anti-HA antibody, some cells did retain the enzyme albeit the staining was highly scattered. When these differentiated cells were counter-stained with the neuronal marker TUJ1, a strange pattern appeared in the clonal cell lines where the staining of TUJ1 seemed to be mutually exclusive to the cells which retained the enzyme. Western blot analysis validated these observations and revealed >70% reduction in the total enzyme levels post-differentiation(Figure-6.6).

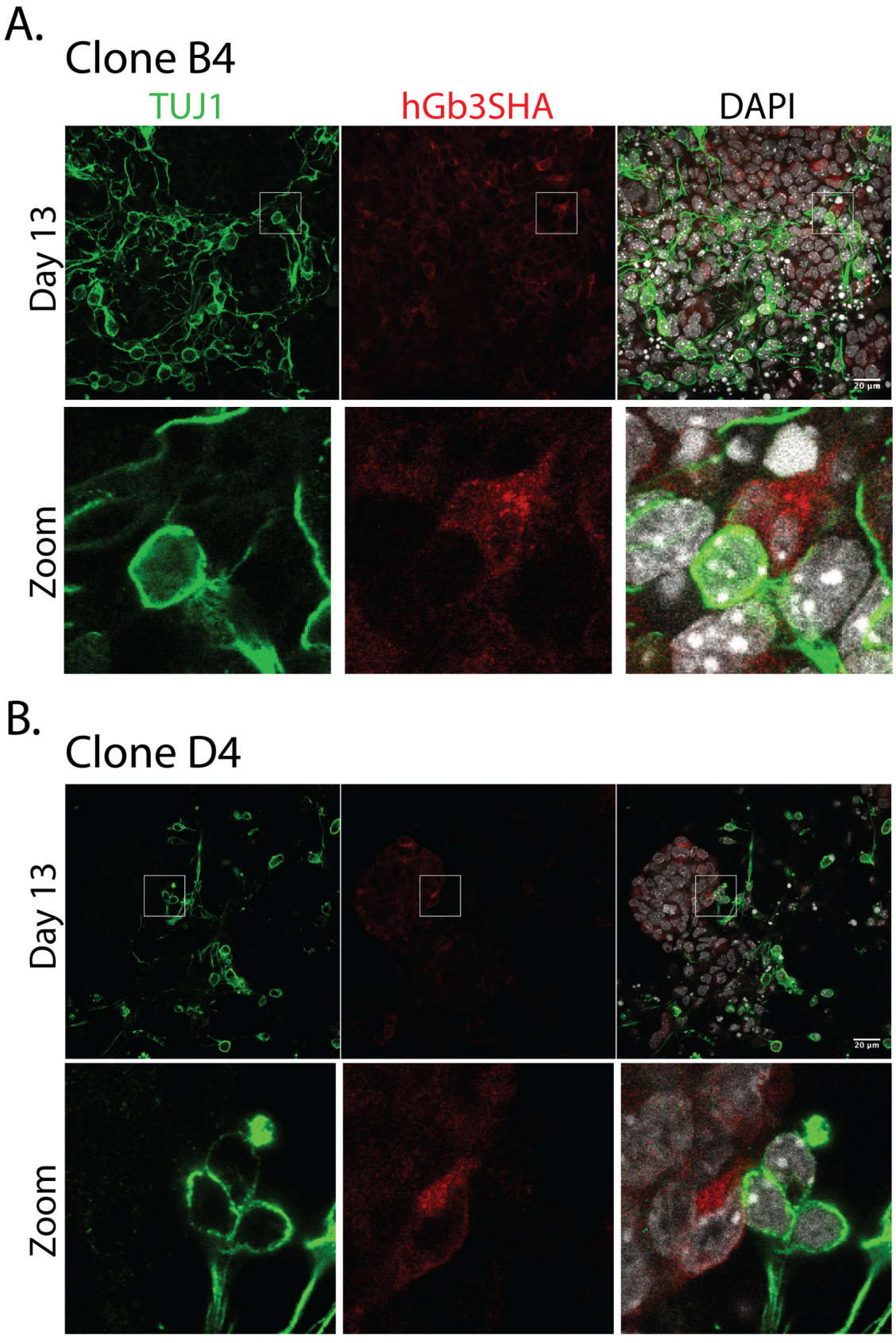

Figure 6.5: A. and B. Representative confocal images of hGb3SHA clones B4 and D4 at Neuronal(Day13) stage. hGB3SHA shows a mutually-exclusive expression behaviour with the Neuronal marker TUJ1.

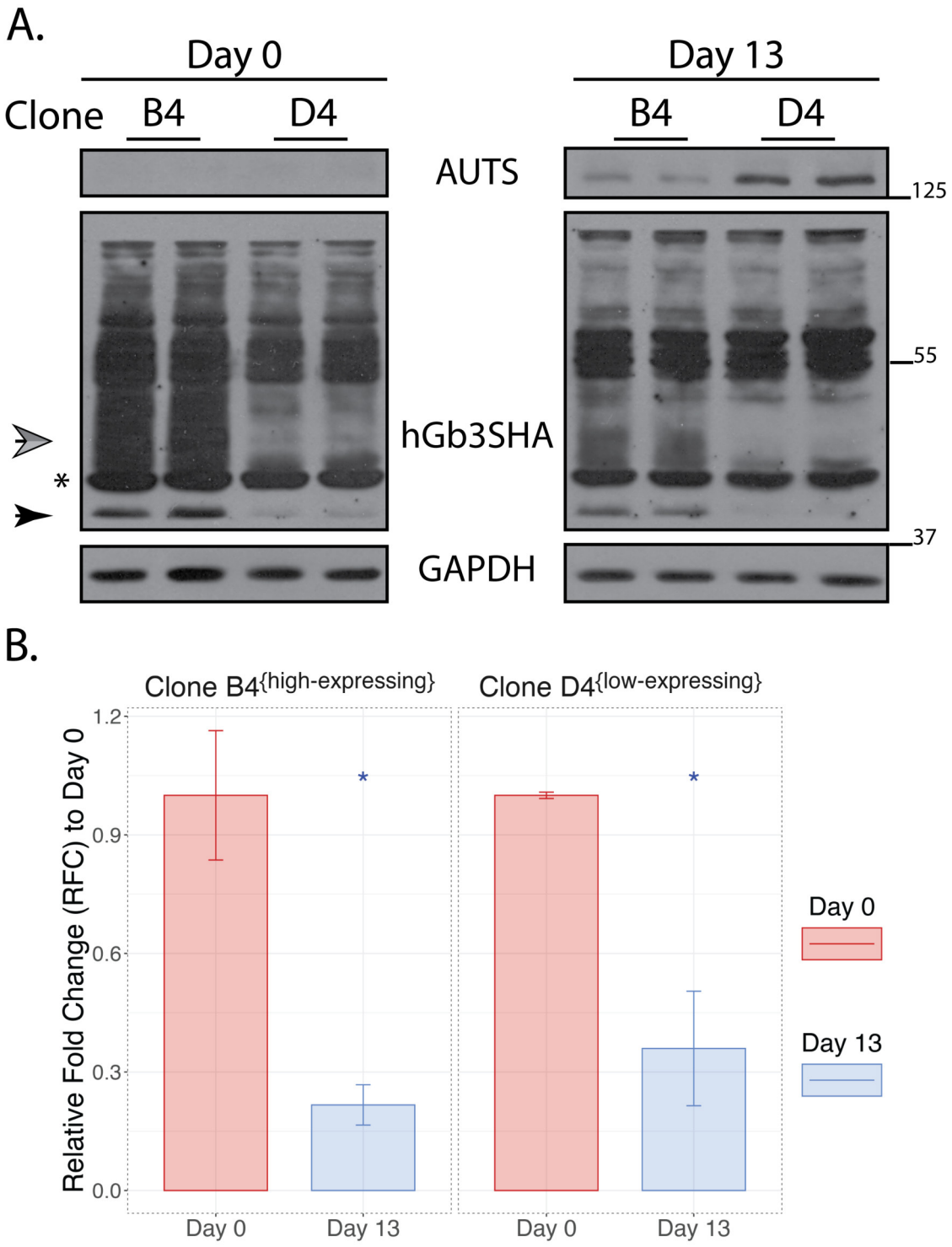

Figure 6.6: A. Representative image of western blot of hGB3SHA clones B4 and D4 at Stem (Day 0) and Neuronal (Day 13) stage. The 2 arrows point to the canonical forms of hGb3SHA (lower molecular weight->high-mannose band and higher molecular weight->complex glycan band) whereas * points to a contaminant band. AUTS2 is shown as a Neuronal marker.; B. Quantification of hGB3SHA expression levels in each individual clone relative to the expression level at Day 0. There is a significant decrease in hGb3SHA expression level in both clones. Data are shown as the mean ± SD of 3 individual experiments; *p < 0.05

6. GSEs are post-transcriptionally regulated during neural differentiation.

Concomitantly, one of our collaborators had also been successful in isolating other 9 hGb3SHA clones using identical protocols. We thus decided to carry out a bulky experiment and differentiated all 18 clonal cell lines for hGb3SHA mRNA and protein levels and were pleasantly surprised to see that all 18 clonal cell lines behaved identically i.e. in all clonal cell lines the hGb3SHA protein levels drastically dropped post differentiation while the mRNA levels remained unchanged for most clones or even if changed they do not explain resulting protein levels(Figure-6.7 and 6.8). The analysis elevated our suspicions from merely a 'strange behaviour' to a possible phenotype of Gb3S in neuronal development.

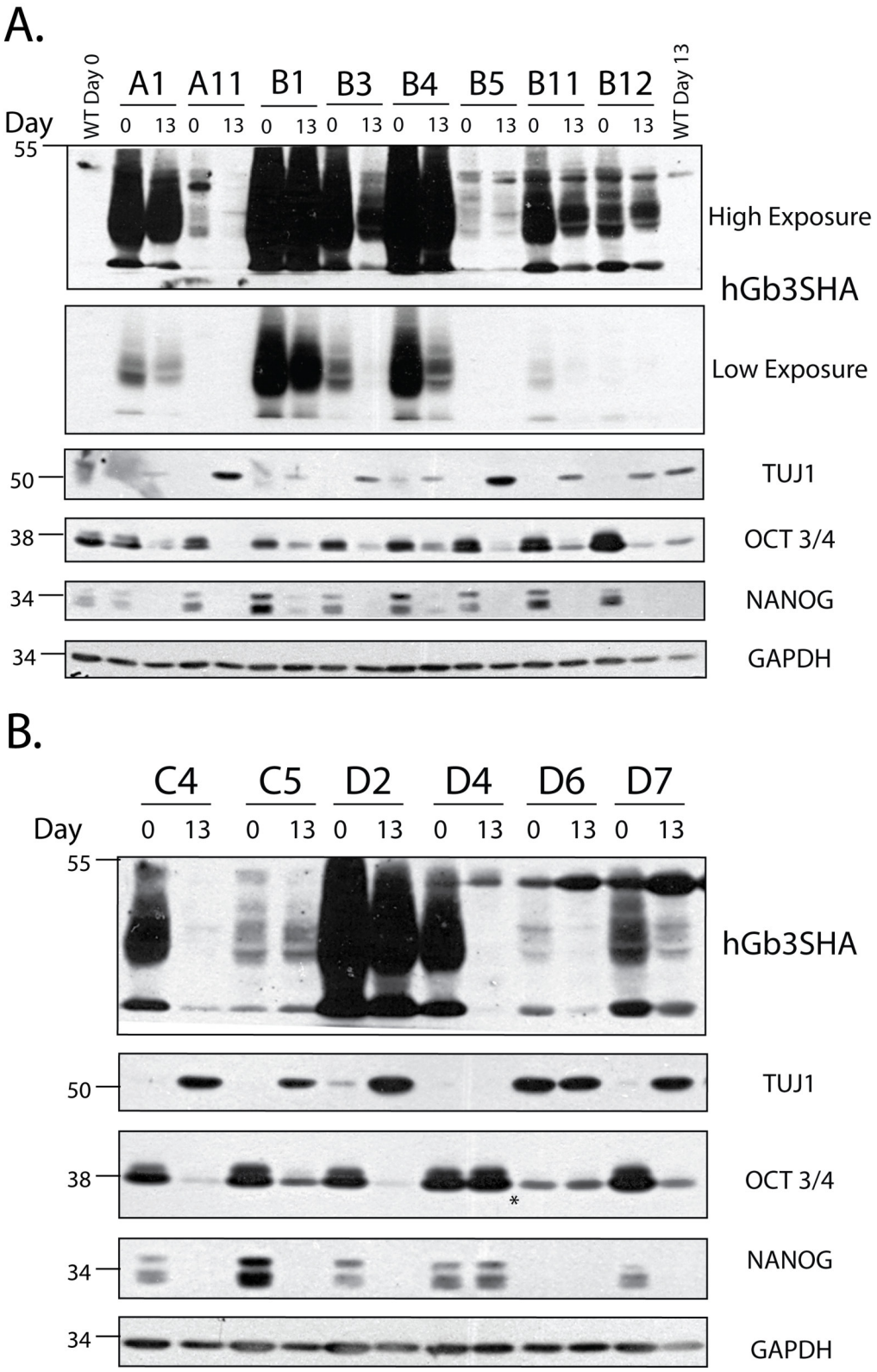

Figure 6.7: A. and B. Representative western blot images of hGb3SHA expression levels in 14 OE clones Post-Differentiation. Each sample was run in technical duplicates to avoid stripping. hGB3SHA and GAPDH were blotted from the same SDS PAGE whereas Neuronal Marker (TUJ1) and Stem Markers (NANOG and OCT3/4) were blotted on a technical duplicate. *Clone D4 and D6 samples were swapped in the technical duplicate SDS PAGE.

6. GSEs are post-transcriptionally regulated during neural differentiation.

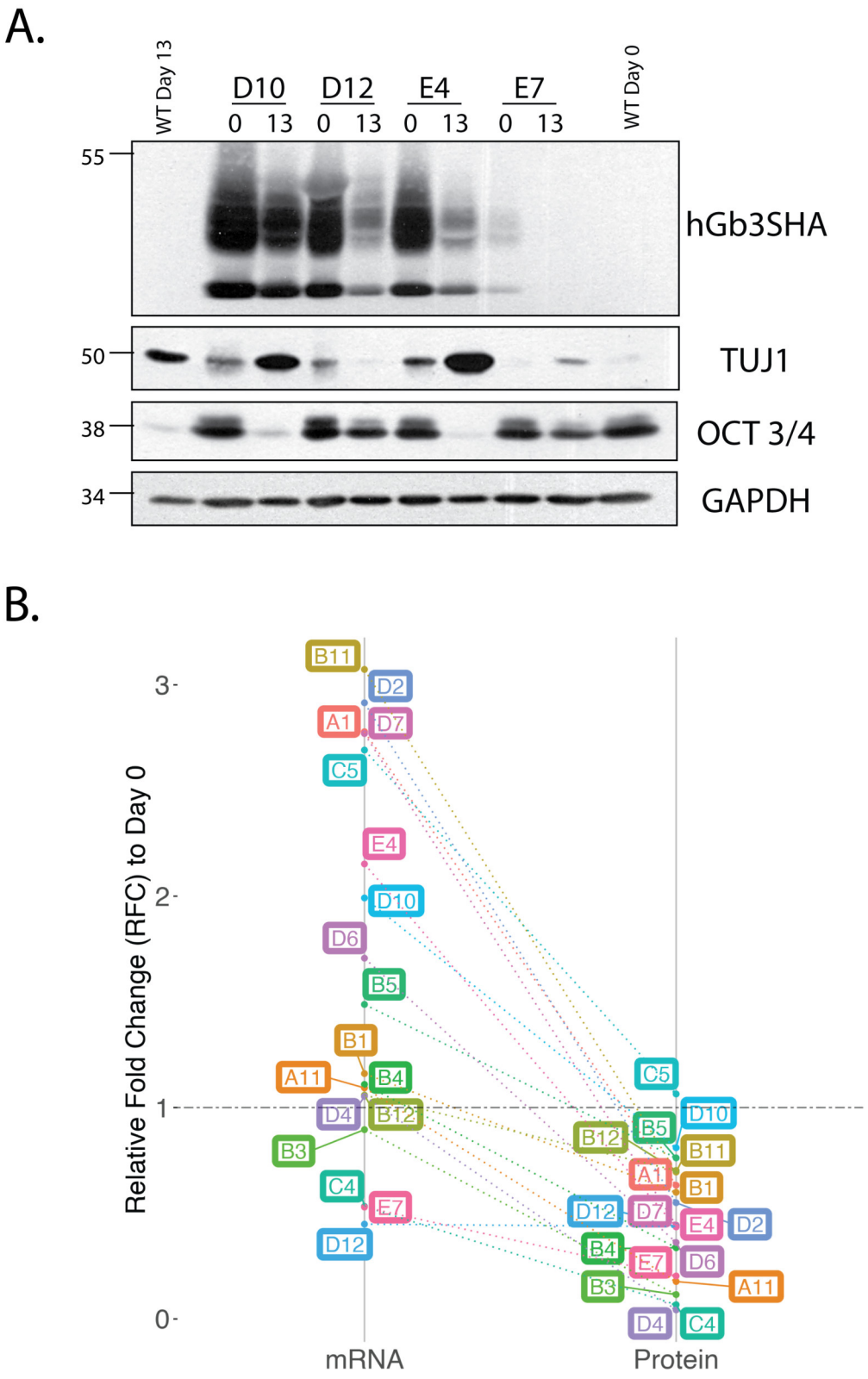

Figure 6.8: A. Representative western blot images of hGb3SHA expression levels in 4 OE clones Post-Differentiation; B. Parallel representation of mRNA and Protein expression levels of hGb3SHA in all 18 OE clonal cell lines plotted as Relative Fold Change (RFC) to Day 0, individually

6. GSEs are post-transcriptionally regulated during neural differentiation.

6.3 Establishing hGM3SHA clonal cell lines

After we established that the loss of hGb3SHA was not a clonal variation rather it seemed to be a post-transcriptional regulatory mechanism active over neuronal differentiation; we wanted to find out if this phenomenon was specific to Gb3S or if it was an artifact of the cloning process. To resolve this concern, we decided to establish a second clonal cell line this time overexpressing the human GM3SHA using the same protocol. Gb3S and GM3S are structurally very similar enzymes, both being type II transmembrane proteins localized to the Golgi but their transcriptional expression over neuronal differentiation is in stark contrast to each other so if this phenotype is actually pointing towards something physiological and not a relic of the cloning process, one would not expect the same regulatory control over the hGM3SHA.

The GM3S gene has been much better studied than Gb3S and due to substantial contributions by Inokuchi et.al (Inokuchi et al. 2018), we understand that out of the 3 existing isoforms of the GM3S transcripts in humans, most of isoform 1 and some of isoform 3 are translocated back to the ER where they are unable to synthesize GM3, while a remaining part of isoform 3 is also readily degraded in the lysosomes. Only Isoform 2 (SAT-I-M3) truly localized to the Golgi and probably is the dominant isoform for most of the GM3 synthesis. We electroporated this isoform in the mESC's and after selection we were successful in isolating 6 hGM3SHA OE clones which showed genomic integration, mRNA and protein expression and, proper protein localization at stem cell stage(Figure-6.9).

6. GSEs are post-transcriptionally regulated during neural differentiation.

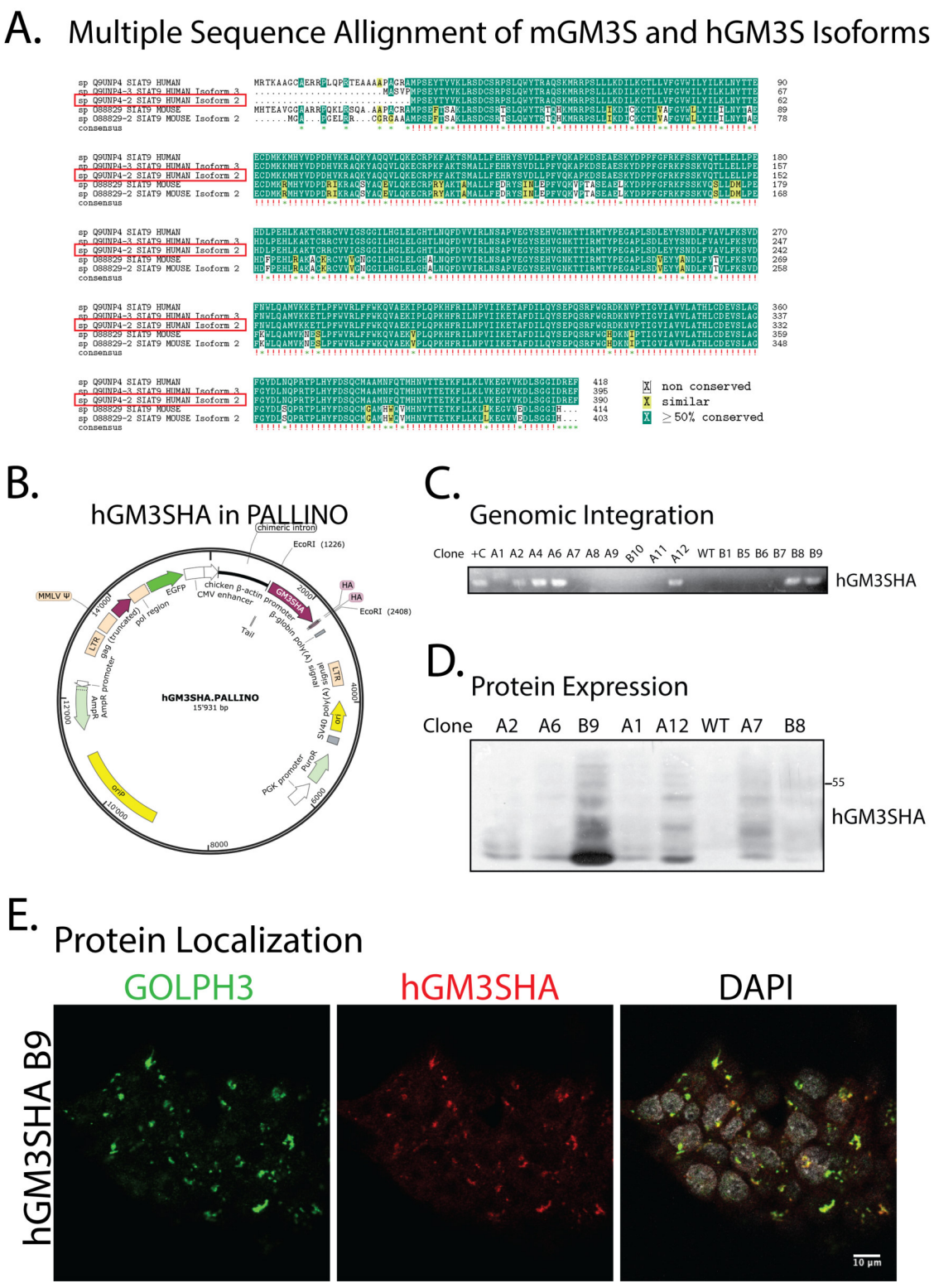

Figure 6.9: Establishing hGM3SHA OE clonal cell lines. A., B., C., D. and E. are all validation steps similar to hGb3SHA clones.

6. GSEs are post-transcriptionally regulated during neural differentiation.

6.4 Simultaneous Differentiation of OE clonal cell lines; the gift that keeps on giving.

Immunofluorescence analysis of differentiated WT, hGb3SHA clone B4 and hGM3SHA clone B9 cells confirmed our suspicion that the loss of hGb3SHA in differentiated neurons was a specific event as hGM3SHA was clearly visible post differentiation(Figure-6.10). mRNA expression profile revealed other hidden features of the clones in that it seemed that although expression of neuronal marker (TUJ1) was not altered in either of the clonal cell lines, SOX2 mRNA expression in hGb3SHA OE clone (B4) does not exactly replicate the canonical drop observed in the WT and hGM3SHA clone (B9). Second, the post-differentiation increase of endogenous GM3S mRNA expression is significantly weakened in hGM3SHA OE clone B9. Apart from this, both clonal cell lines did show almost unchanged levels of mRNA expression of their respective integrates. The western blot analysis, on the other hand, took us by surprise for a second time(Figure-6.11).

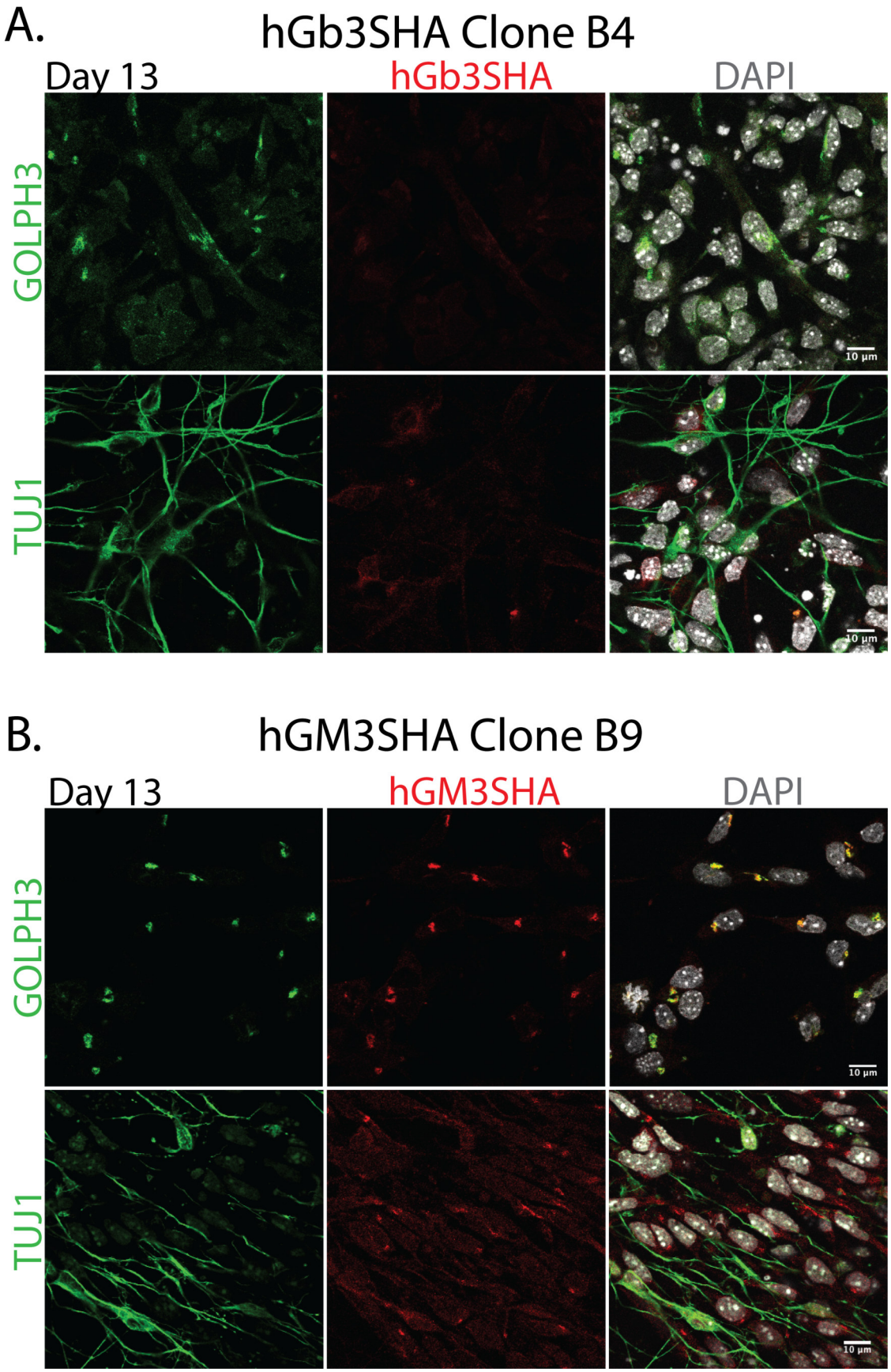

Figure 6.10: Immunofluorescence images of Differentiated A. hGb3SHA Clone B4 and; B. hGM3SHA Clone B9. hGM3SHA is clearly visible in the Golgi (GOLPH3 as marker) in differentiated cells.

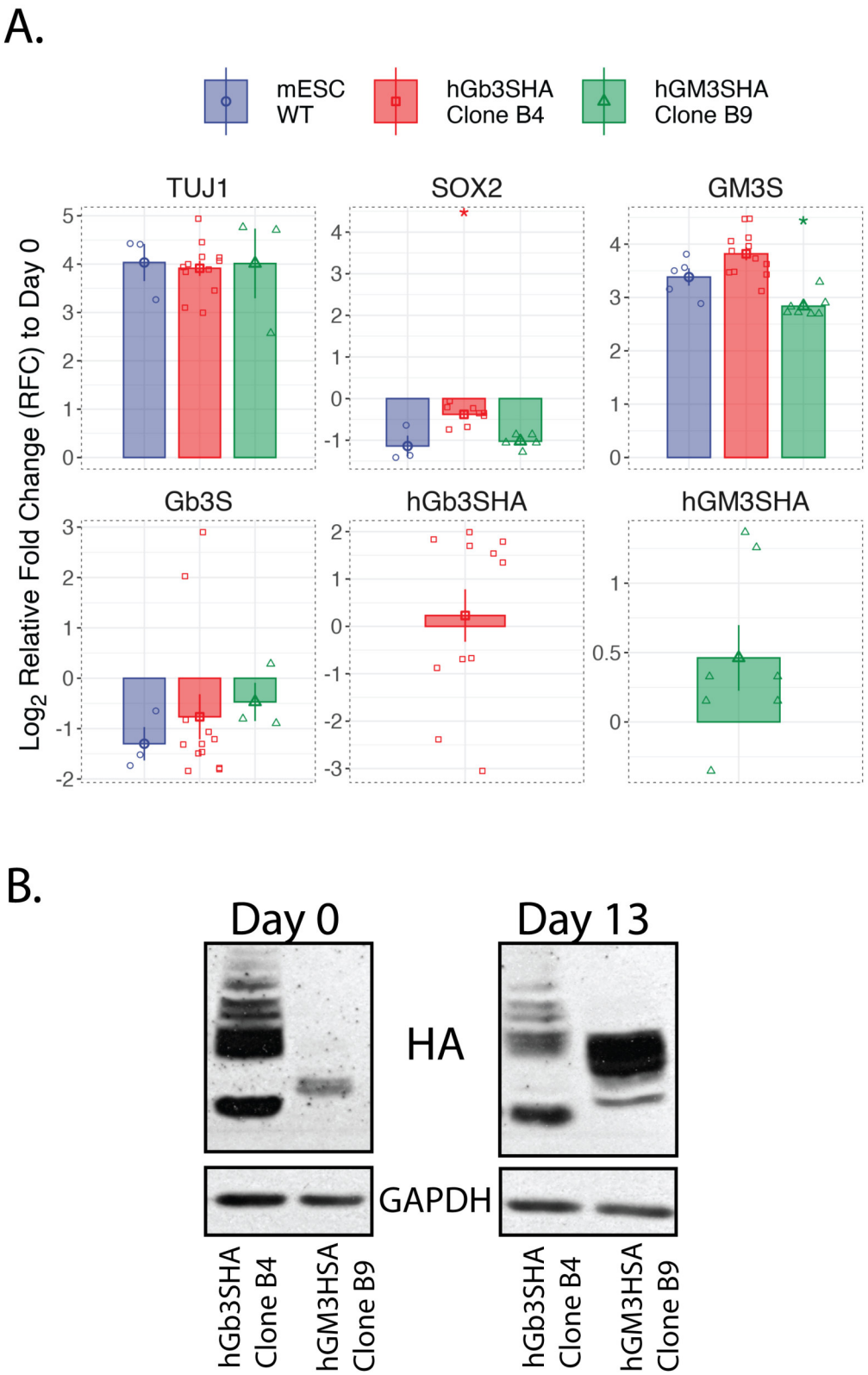

Figure 6.11: A. Relative Fold Change in mRNA expression levels of Neuronal marker (TUJ1), Stem Cell marker (SOX2), Endogenous GSEs (Gb3S and GM3S) and Integrates (hGb3SHA and hGM3SHA) in WT, hGb3SHA Clone B4 and hGM3SHA clone B9 cells Post-Differentiation; B. Representative western blot image of hGb3SHA Clone B4 and hGM3SHA Clone B9 Post-Differentiation. Data are shown as the mean ± SD of at least 3 individual experiments with multiple technical duplicates where indicated; *p < 0.05

6. GSEs are post-transcriptionally regulated during neural differentiation.

In the western blot, it was quite evident that the hGM3SHA cell line was not completely innocent and, in fact, mirrored the post translational regulation of hGb3SHA. There was a drastic increase in the protein level of hGM3SHA with no supporting increase in mRNA expression(Figure-6.11) and a hasty differentiation experiment of all the other isolated hGM3SHA clones resulted in a unanimous confirmation of the phenomenon(Figure-6.12). This led us to seriously contemplate the existence of a regulatory mechanism acting on top of the transcriptional program that is activated upon a neuronal differentiation favoring environment. Whether this represented some sort of checkpoint or more of a consequence of neuronal differentiation could only be hypotheticals at this point but, the most mechanistic questions that could be immediately experimentally addressed were; when does the system become active? And how do the cells actually achieve this effect?

6. GSEs are post-transcriptionally regulated during neural differentiation.

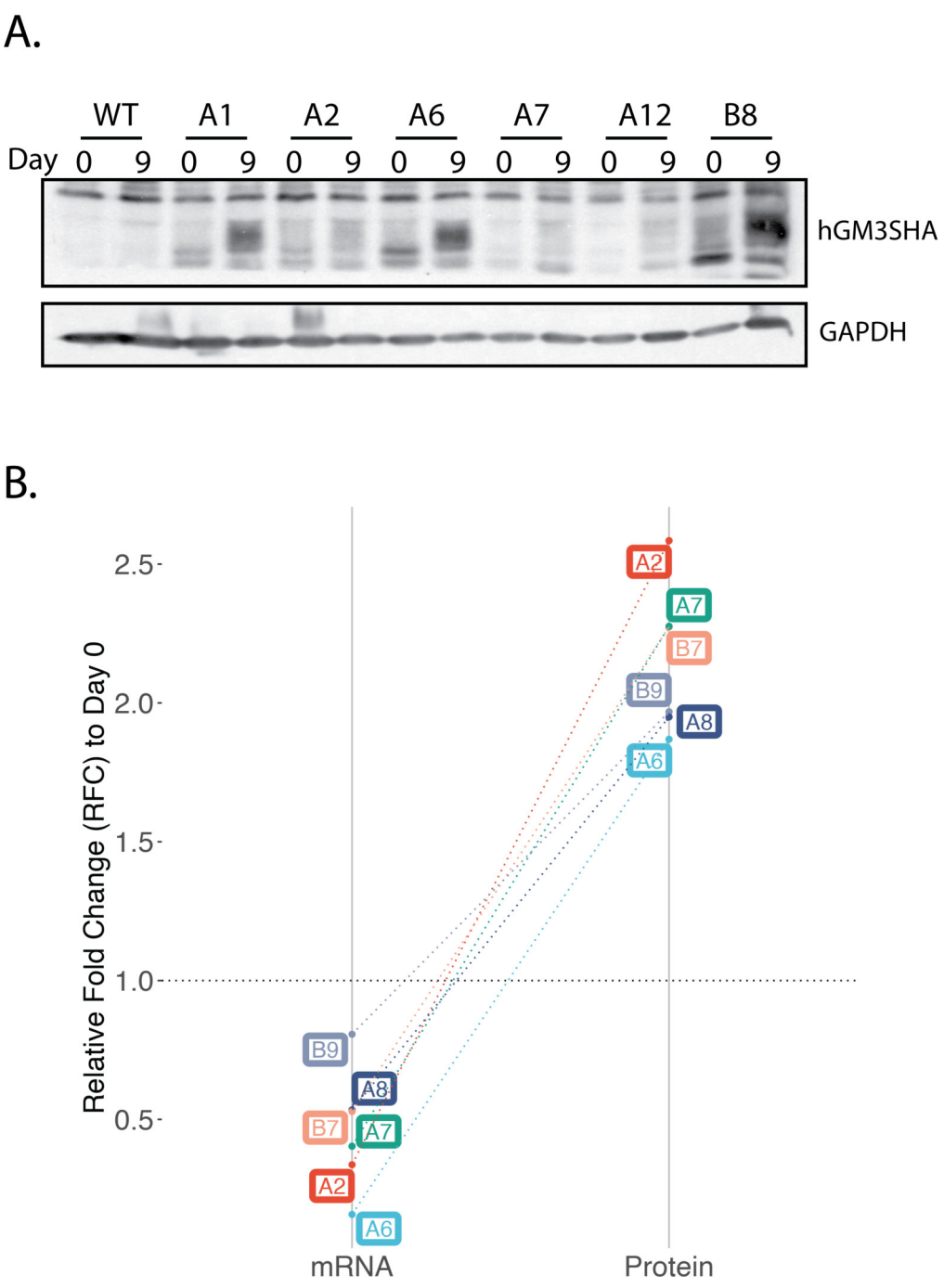

Figure 6.12: A. hGM3SHA protein expression level in 6 OE clones by Day 9 of differentiation; B. hGM3SHA protein and mRNA expression levels in all OE clonal cell lines Post-Differentiation.

7

Characterization of the regulation in Neurodevelopment

Contents

7.1 Characterization in '2d' Differentiation.

The sheer number of clonal cell lines mixed in with the inherent variability of the differentiation protocol was starting to become a hurdle in the effective dissection of mechanism so we decided to focus our future experiments using two high OE clones which had minimal variation in the mRNA levels post differentiation, hGb3SHA clone B4 and hGM3SHA clone B9. In both of these cell lines the respective change in enzyme levels was robust enough to be statistically significant when just the total protein levels relative to GAPDH are compared over multiple experiments(Figure-7.1-A and Figure-7.3-A). An intermittent mRNA(Figure-7.1-

B) and protein expression(Figure-7.2-B) analysis over 13 days revealed that the initiation of the loss of hGb3SHA was a very early event in the program, even preceding the drop in the canonical stem cell marker OCT3/4(Figure-7.2-A). Then the enzyme levels gradually decrease over the differentiation course, mimicking the OCT3/4(Figure-7.2-B). The increase in hGM3SHA is slightly different in that the hGM3SHA protein level initially drops for 3-5 days(Figure-7.2-A) and then sometime at Day 6(Figure-7.4-A) the protein 'stabilizes' and we start to see an increase in the amount. This initial drop in hGM3SHA protein level is replicated in the mRNA levels(Figure-7.3-B) so it could not be said if there was a similar regulation as hGb3SHA but the later increase seems pretty similar with an event at day 6 that stabilizes the protein and then a gradual increase till day 13(Figure-7.4-B).

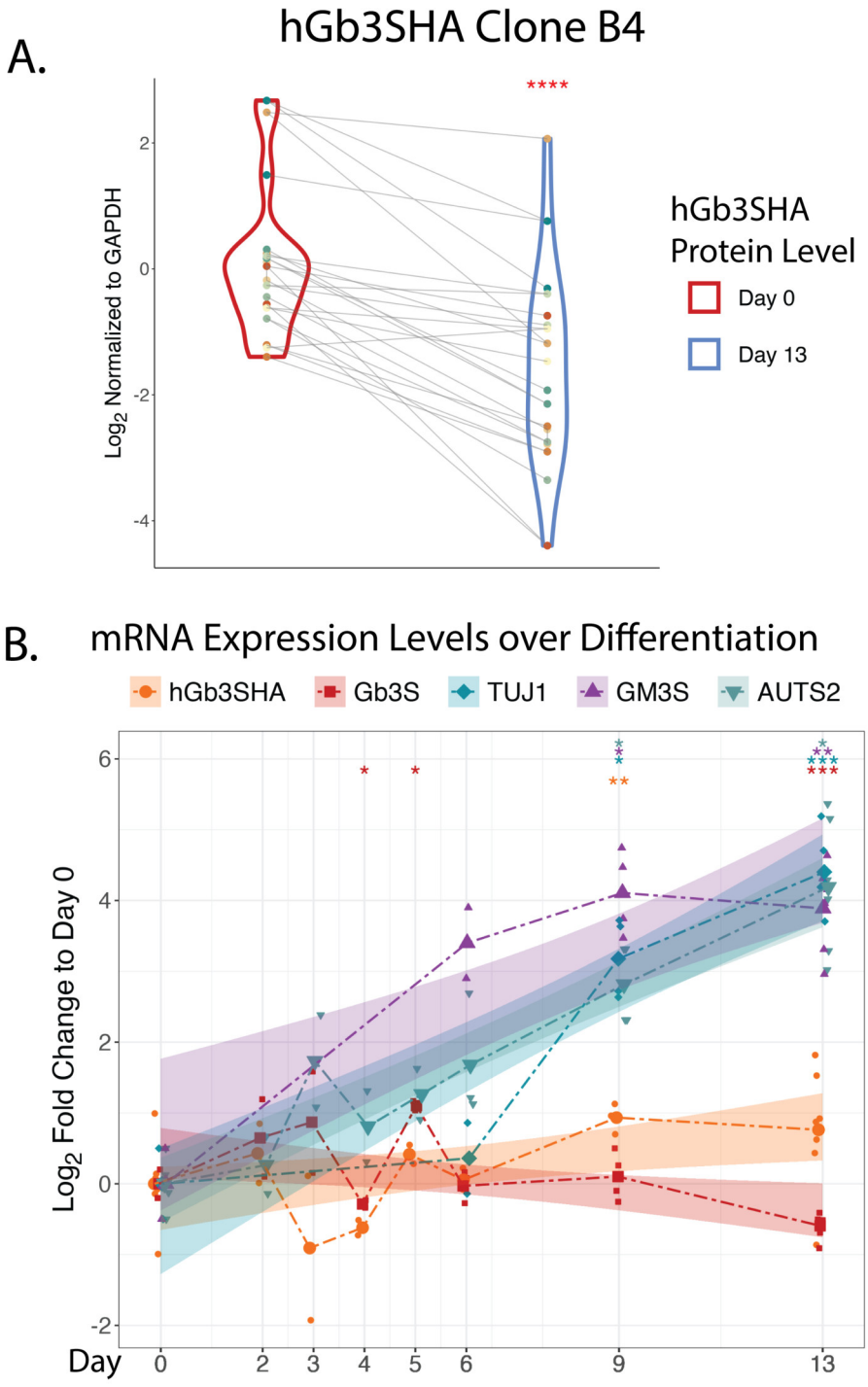

Figure 7.1: A. hGB3SHA expression levels at Day 0 and Day 13 normalized to GAPDH in 14 different experiments; B. mRNA expression levels of Neuronal Marker(TUJ1, AUTS2), GSEs(GM3S, Gb3S) and hGb3SHA over Differentiation. Data are shown as the mean ± SD of 3 individual experiments

A). hGb3SHA Clone B4 and hGM3SHA Clone B9 Protein expression levels at Day 0, 3 and 5.

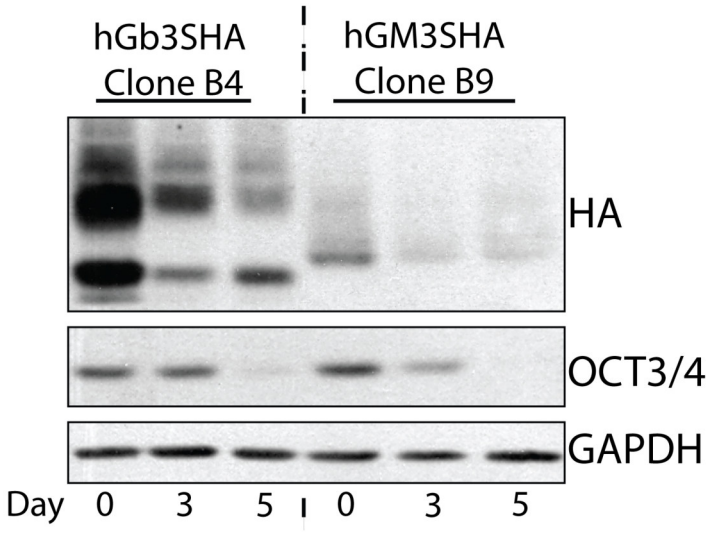

B). hGb3SHA Clone B4 Protein expression levels over Differentiation

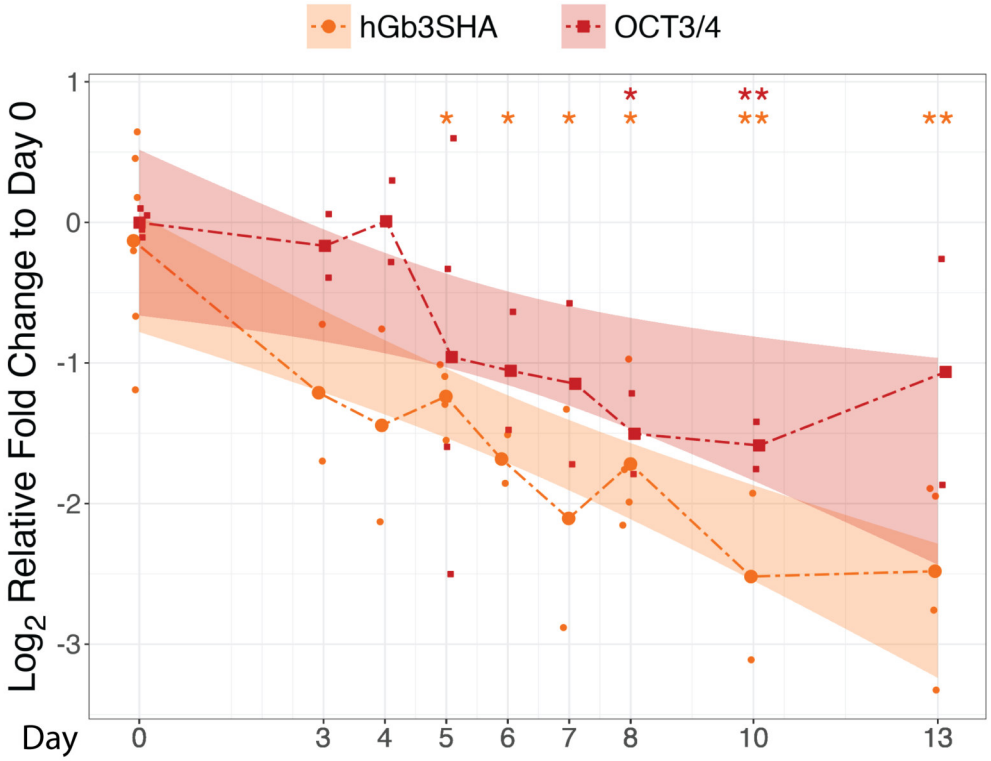

Figure 7.2: A. Representative western blot image of hGb3SHA and hGM3SHA expression at Day 0, 3 and 5 in hGb3SHA Clone B4 and hGM3SHA Clone B9, respectively; B. hGb3SHA and OCT3/4 protein expression levels over differentiation (as RFC to Day 0). Data are shown as the mean ± SD of 3 individual experiments.

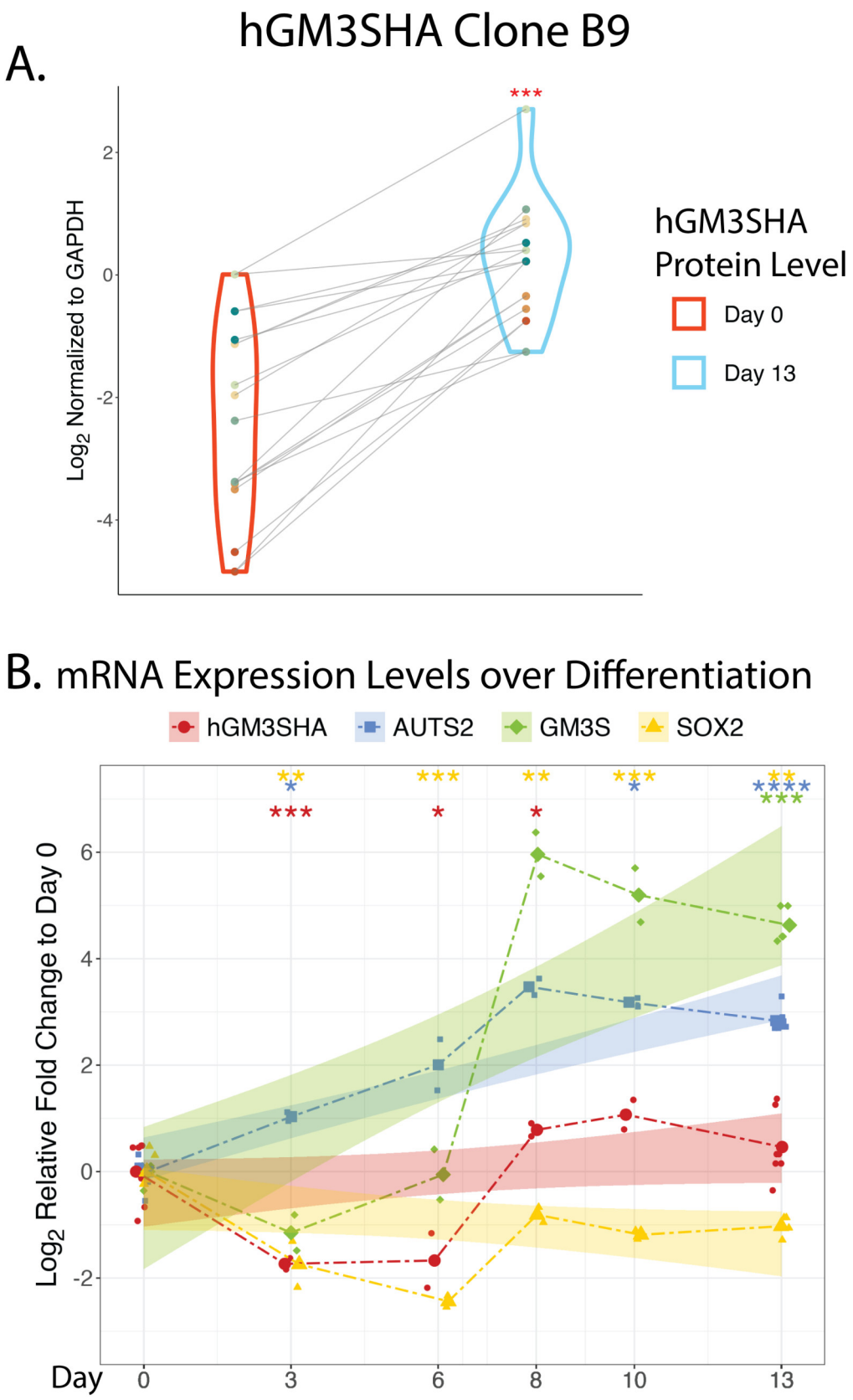

Figure 7.3: A. hGM3SHA expression levels at Day 0 and Day 13 normalized to GAPDH in 9 different experiments; B. mRNA expression levels of Neuronal Marker(AUTS2), Stem Marker(SOX2), GSEs(GM3S) and hGM3SHA over Differentiation. Data are shown as the mean ± SD of 3 individual experiments

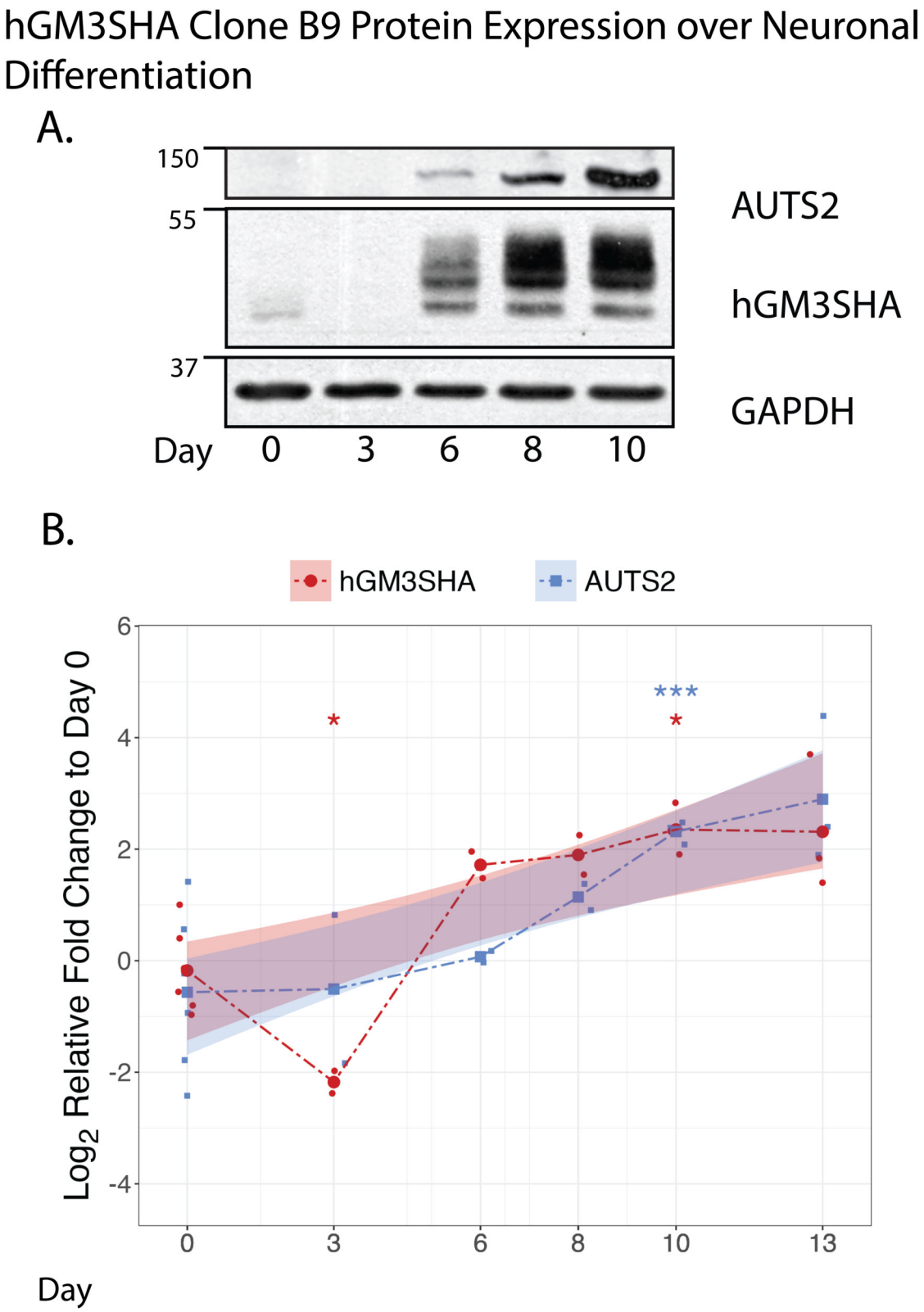

Figure 7.4: A. Representative western blot image of hGM3SHA expression levels over Differentiation in hGM3SHA Clone B9; B. hGM3SHA and AUTS2 protein expression levels over differentiation (as RFC to Day 0).

The variability of the differentiation protocol is truly captured by the close early time points in the experiment but whether it reflects the variation in population ratio (sample to sample) or an actual feature of the differentiation process was not a question that could be addressed by our current mixed bag approach to neurogenesis. We strongly suspected that at least the loss of the hGb3SHA protein was intimately linked with the neuronal differentiation process but a question I had while characterizing the clones was if the cells that retain the enzyme post differentiation were a cause or a consequence of the enzyme?

7.2 Characterization in '3d'-Differentiation: Neural Tube Organoids

A window of opportunity opened up when we moved to EPFL and were lucky to cohabit the lab space with a well-established organoid research lab. I was personally entranced by the system and its possibilities and so, during the initial months of setting up the lab we decided to try and differentiate our clonal cells into these homogenous neural tube organoids as characterized by (Meinhardt et al. 2014). Our rationale for the study was 2-pronged; first, previous established mice models knock-out for certain ganglioside synthesizing enzymes (some killing the complete family) had not reported any developmental defects and rather indicated a fairly 'aphenotypical' litter although many neurological defects materialized later(Allende and Proia 2014). Second is the study published by our own lab which illustrated a much more catastrophic role of globosides on neurological morphogenesis, so we wanted to see if there were any differences between organoids derived from our clones in this much more homogenous and physiological setting. Allowing that both of our clonal cell lines are able to replicate the single lumen hallmark of neuroepithelial cysts despite or because of their individual 'quirks', a second more desirable result would have been a clear demarcation of cells or cell types that retain/lose the enzymes reminiscent of the beautiful patterning behavior illustrated by lutolf et al. We envisioned a scenario for the hGb3SHA clone where, in the

post-patterned neuroepithelial cyst, some cells retained the enzyme and hopefully they correlate with some known cell type markers.

There were some fundamental differences in the cell lines used by the Lutolf Lab and our own. To begin with all of the cell lines used in their lab were at max E10 while ours were derived at E14. Our stem cell maintenance conditions were slightly different, with us using the more primitive maintenance medium (LIF only)(Tamm et al. 2013) and their lab using a non-adherent culture condition for maintenance where we used gelatin 0.1% to adhere the stem cells during culture(Meinhardt et al. 2014). After failing the first few times we decided to adjust some parameters in the protocol and this was an additional cause for concern but these adjustments finally pushed our cell lines towards forming these neuroepithelial cysts with the hallmark lumen. IF at Day 2 confirmed that our hGb3SHA cell line was capable of forming similar cysts and it seemed that cysts that are forming a lumen are already losing the enzyme(Figure-7.5) whereas hGM3SHA seems static(Figure-7.6), although there was a lot of 'bleeding' from flurophored phalloidin into the HA channel. By Day 5 hGb3SHA was almost completely lost from cysts that form a true lumen(Figure-7.7) (as confirmed by a different flurophored phalloidin) whereas hGM3SHA is still clearly visible(Figure-7.8), although a slight dip in fluorescence could be observed. Optical sectioning(fig) of cysts confirmed that hGb3SHA starts getting lost right after after the 'Moruloid' (8-16 cells) stage, placing the event somewhere between the 'compaction' and 'cavitation' stages of the development(E2.5-3.5) (Figure-7.9 to 7.14). We thus concluded that the loss of hGb3SHA protein is a point that corresponds or even precedes the lumen formation and decided to go back to the 2d differentiation model to probe the molecular mechanism further.

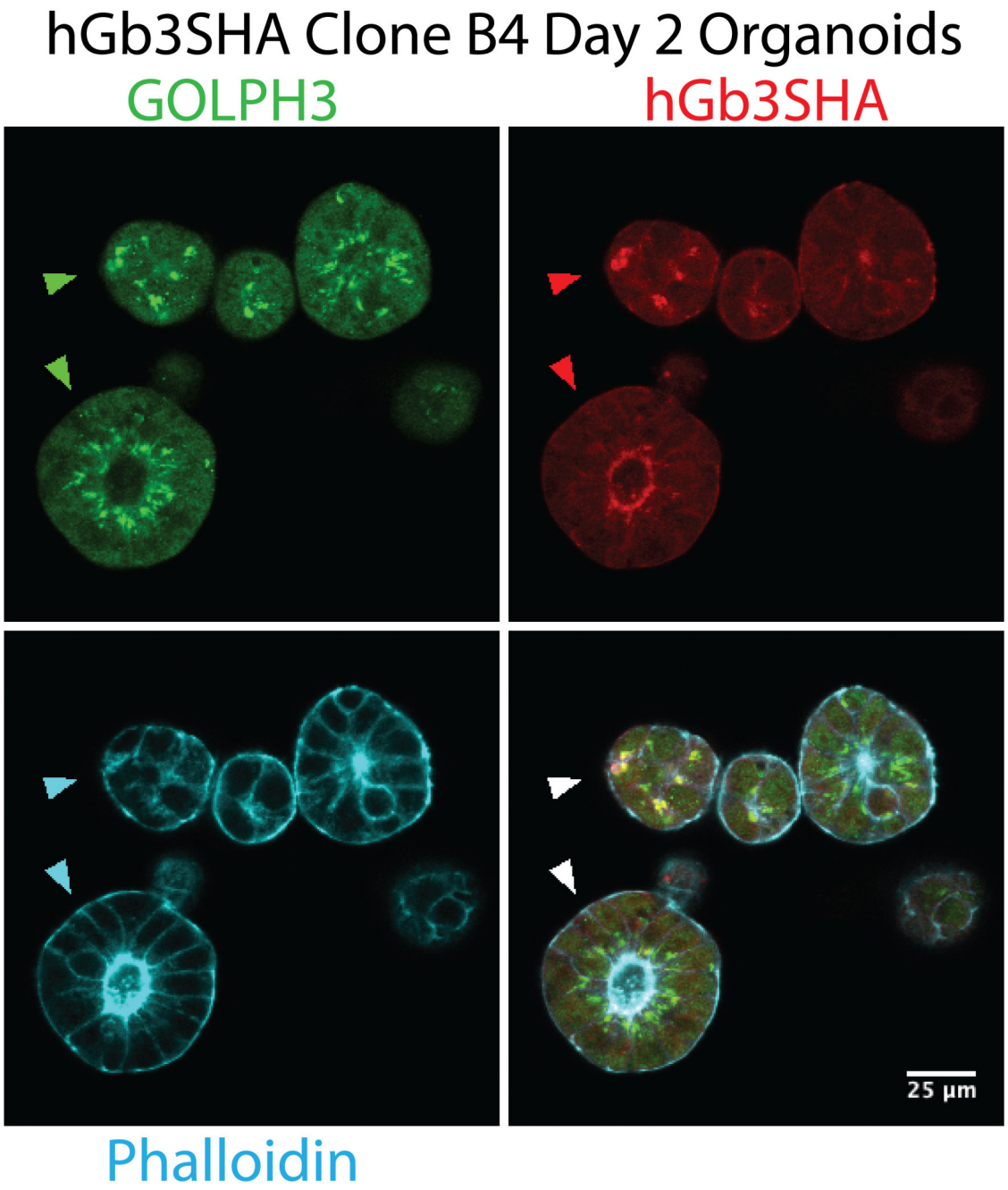

Figure 7.5: Representative confocal image of Day 2 organoids from hGB3SHA Clone B4. Multiple different phases of development can be seen in a a single image and arrows point to 2 such phases where organoids, with lumen and without lumen (as characterized by the Phalloidin staining), are losing or retaining the hGB3SHA protein, respectively. This particular Phalloidin-633 was showing unnantural cross-talk with the 568 channel.

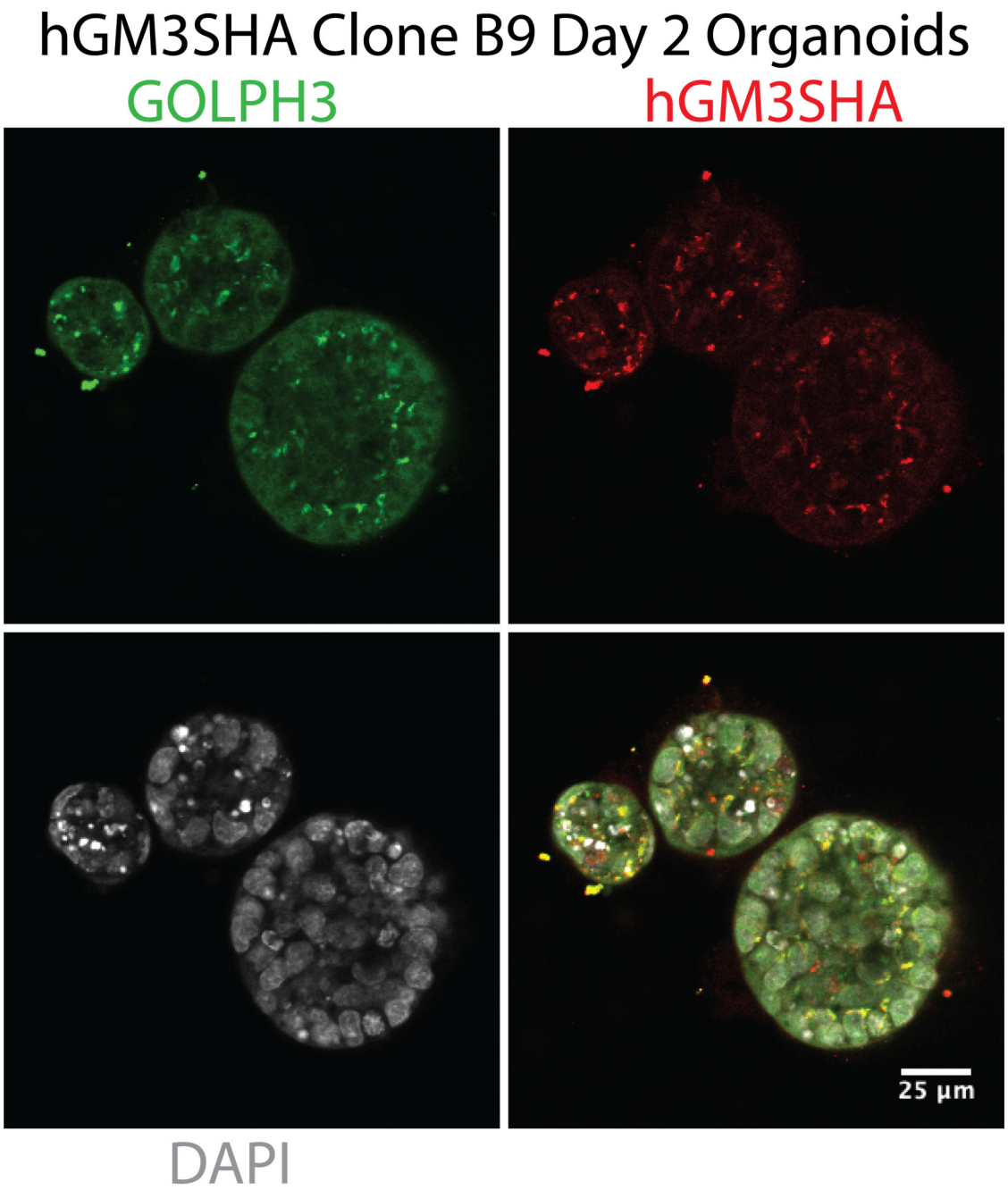

Figure 7.6: Representative confocal image of Day 2 organoids from hGM3SHA Clone B9. hGM3SHA was crisply seen in the golgi in all organoids. As the phalloidin staining at this time was quite disruptive, Golgi (GOLPH3) orientation towards the lumen can be utilized as a marker for lumen formation as seen elsewhere.

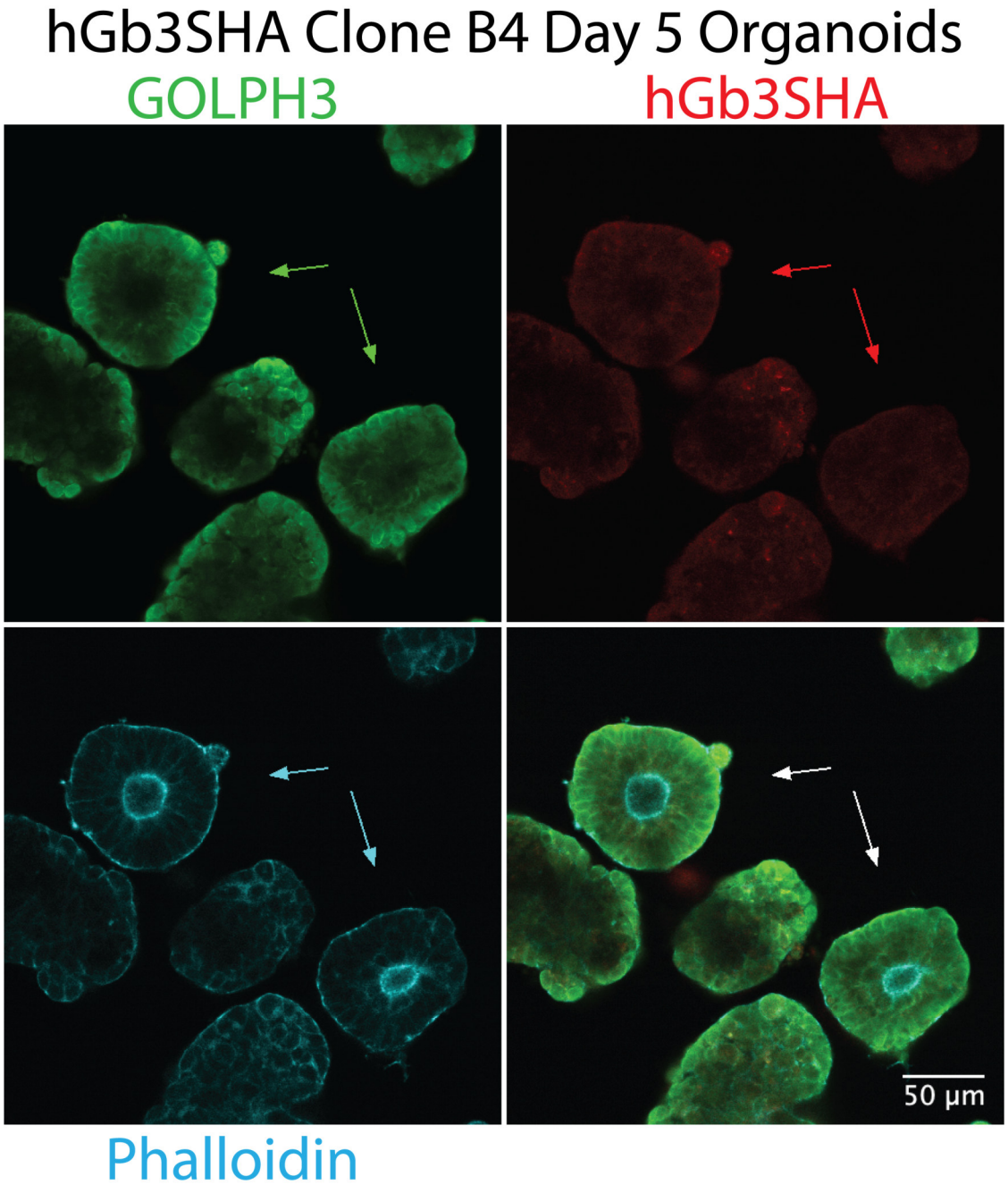

Figure 7.7: Representative confocal image of Day 5 organoids from hGb3SHA Clone B4. hGb3SHA is almost completely lost by Day 5 specifically in cysts that form a lumen. *Different phalloidin-647 was used here.

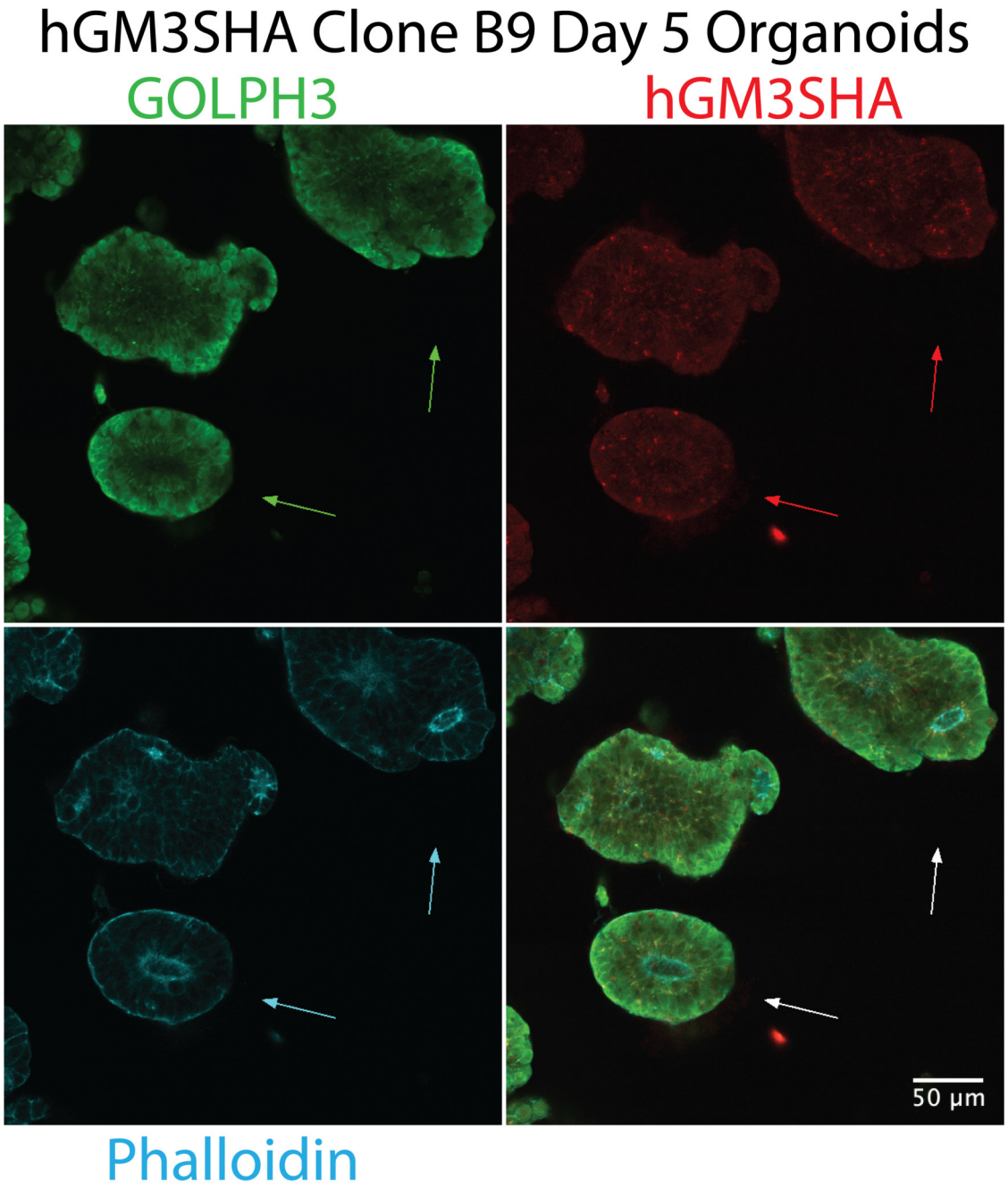

Figure 7.8: Representative confocal image of Day 5 organoids from hGM3SHA Clone B9. hGM3SHA is still clearly visible in cysts that form a lumen

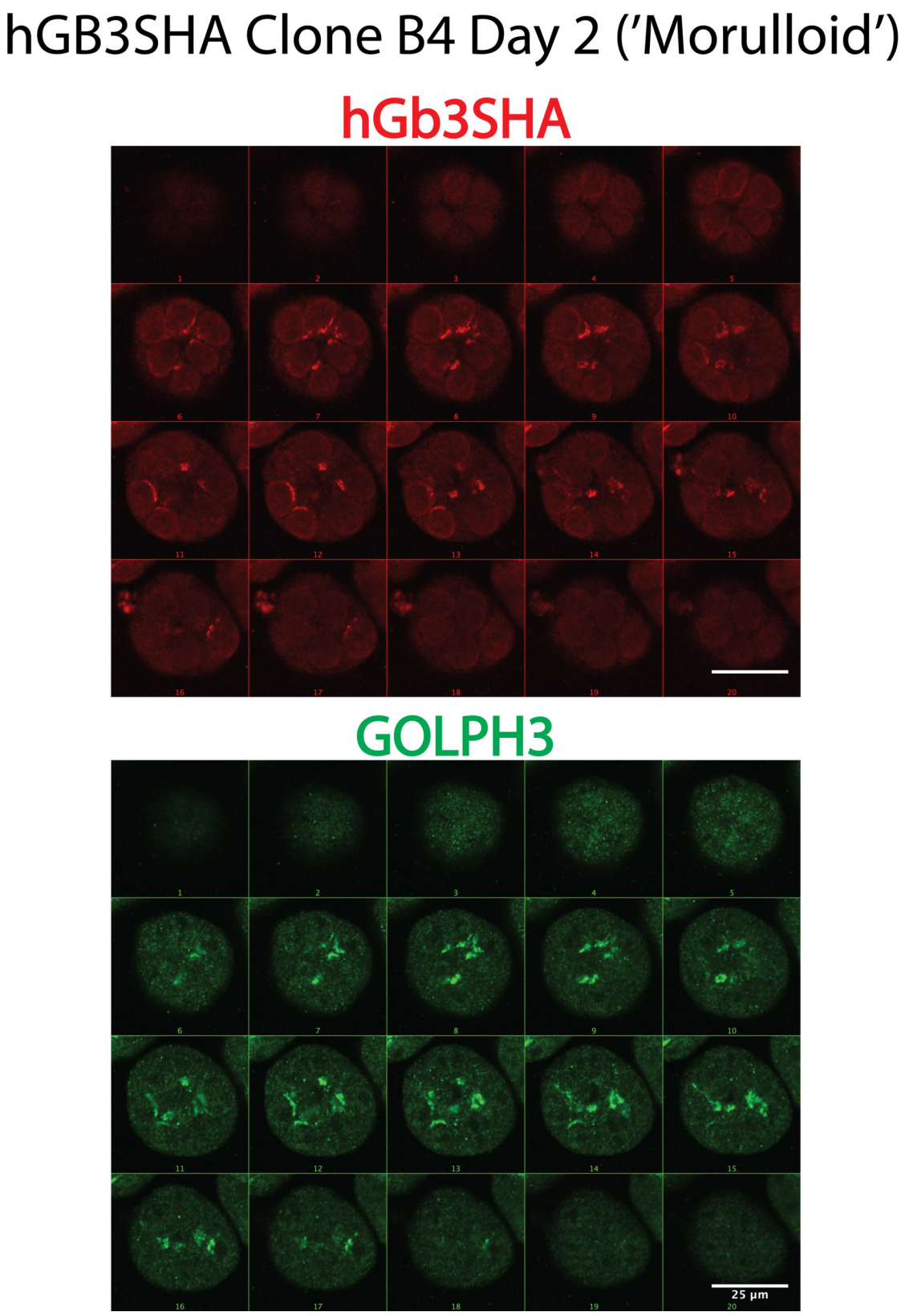

Figure 7.9: Representative confocal image of Day 2 organoids from hGB3SHA Clone B4. Z-projection of a single cyst with 16-32 cells ('morulloid'). hB3SHA (red) is clearly visible and colocalizing with Golgi (GOLPH3).

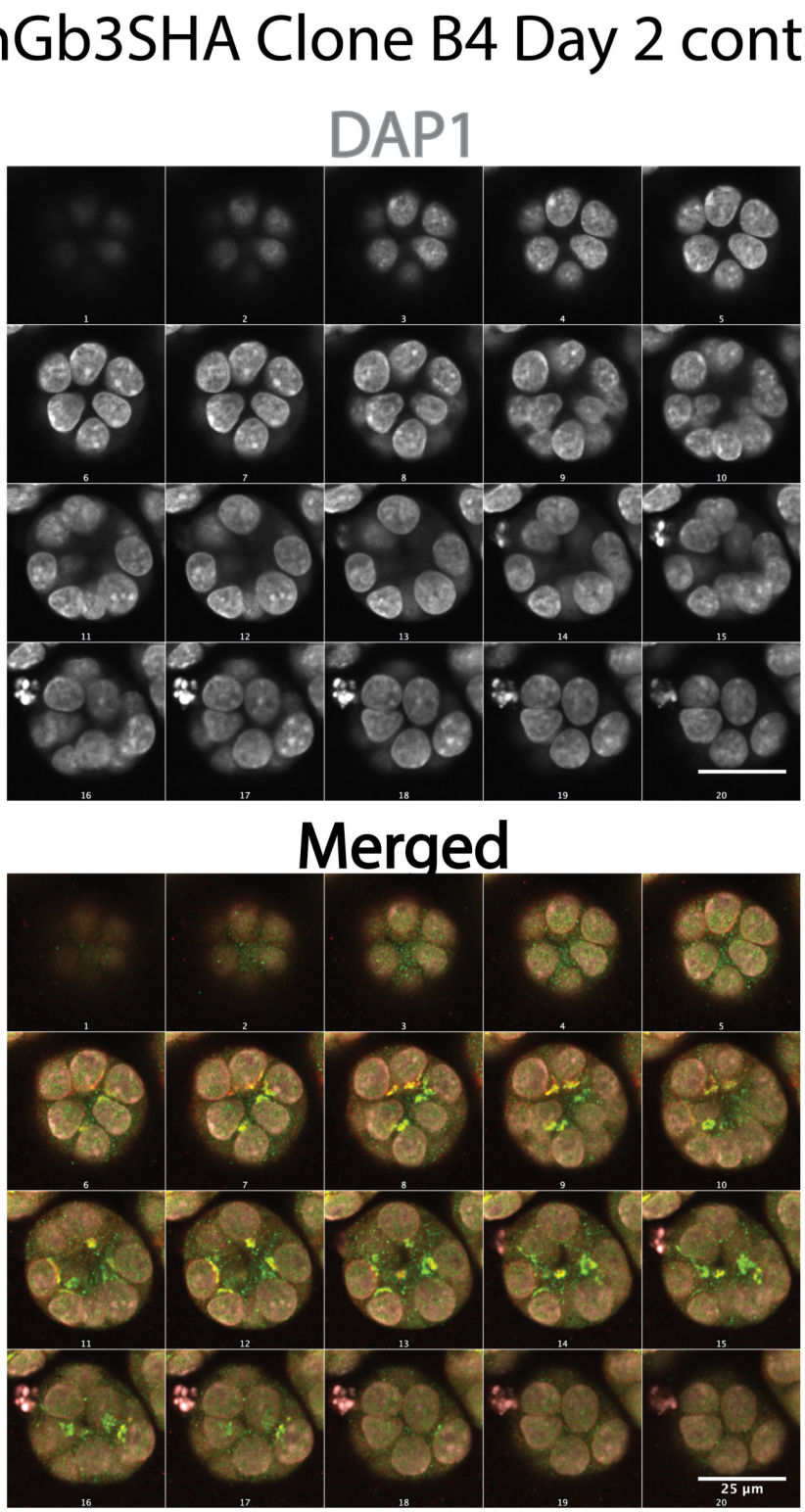

Figure 7.10: *contd.*. DAPI in grey and Merged.

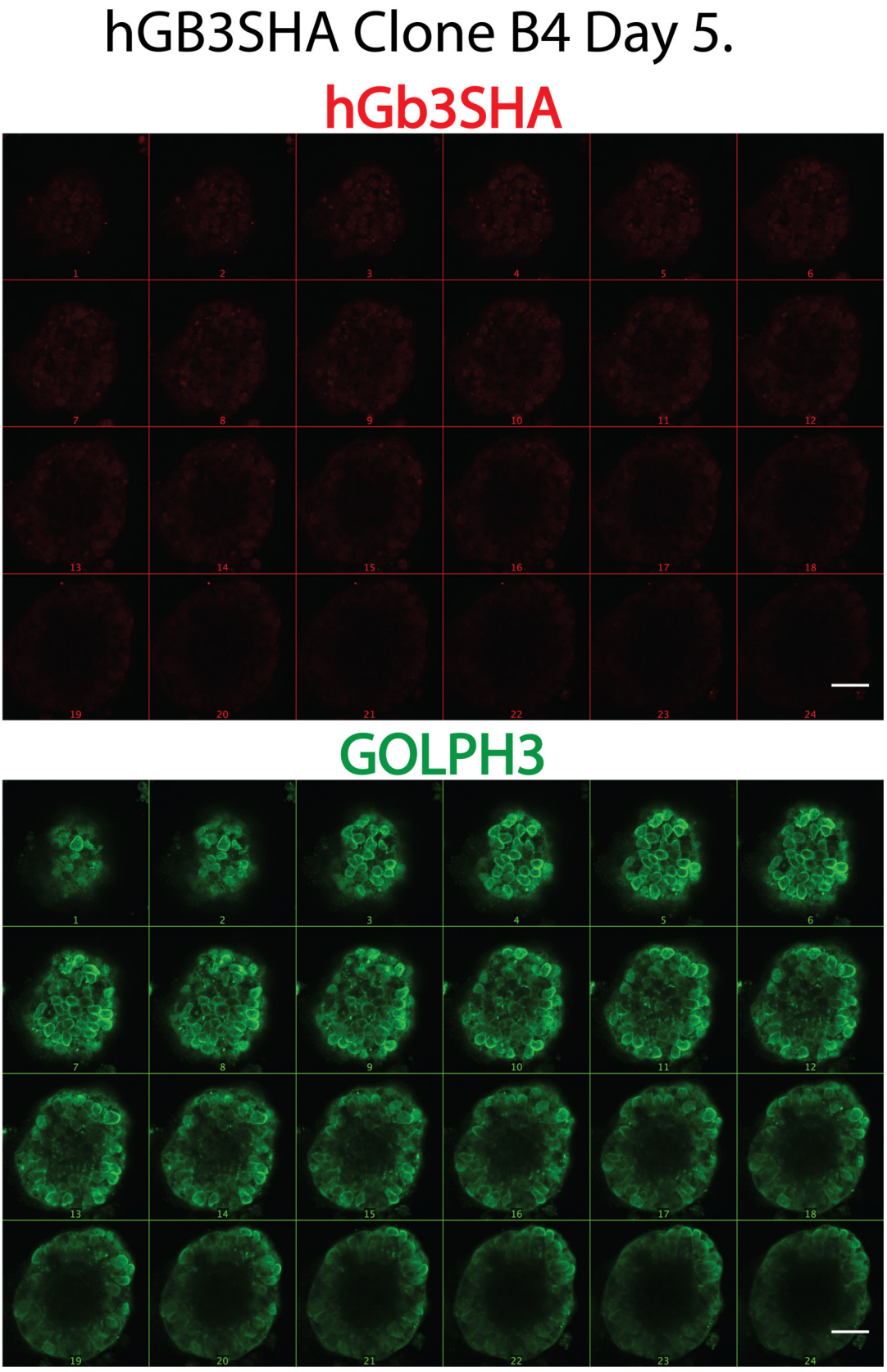

Figure 7.11: Representative confocal image of Day 5 organoid from hGB3SHA Clone B4. Z-projection of a single cyst. hB3SHA (red) is no more visible.

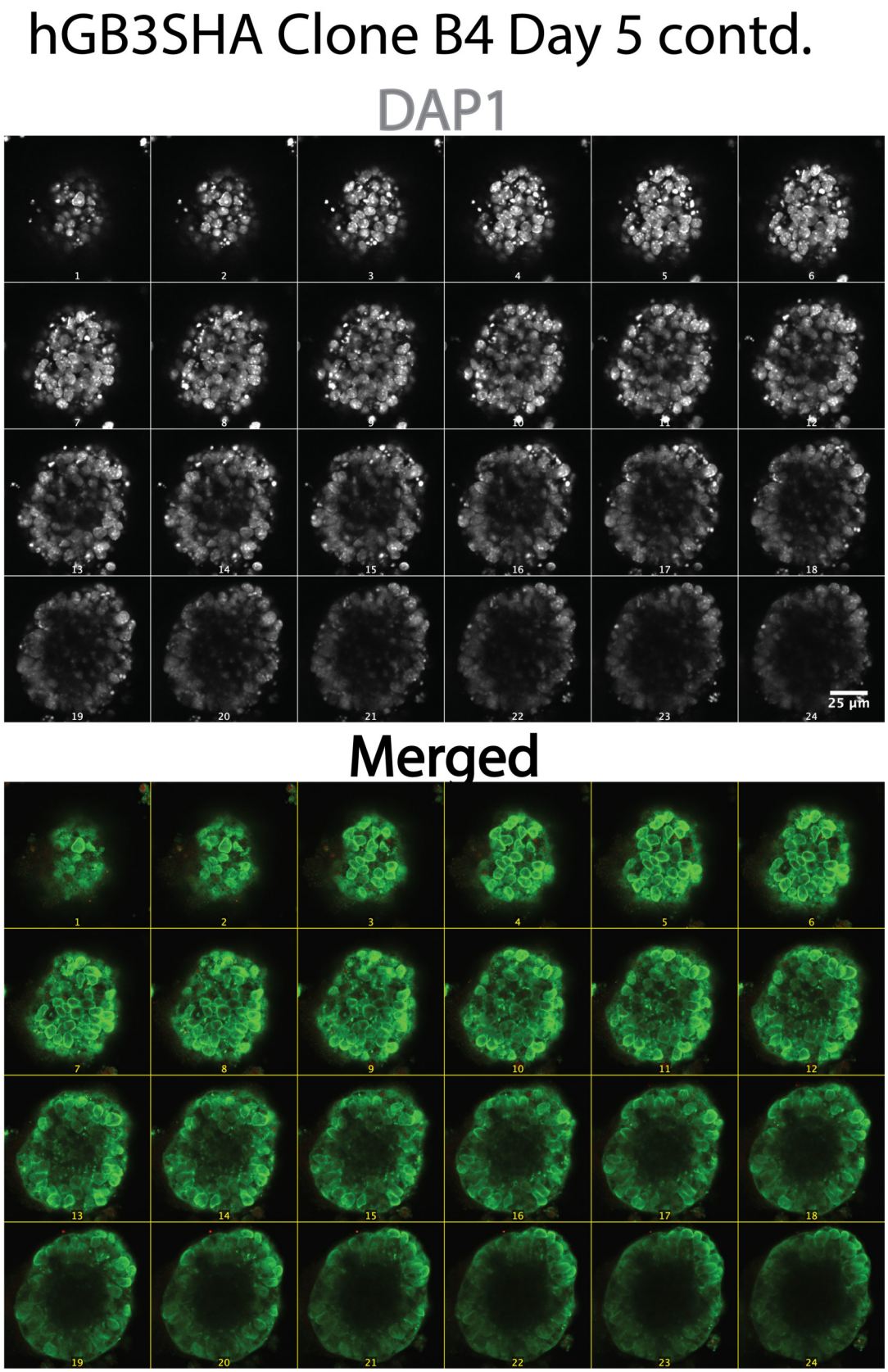

Figure 7.12: *contd*. DAPI in grey and Merged

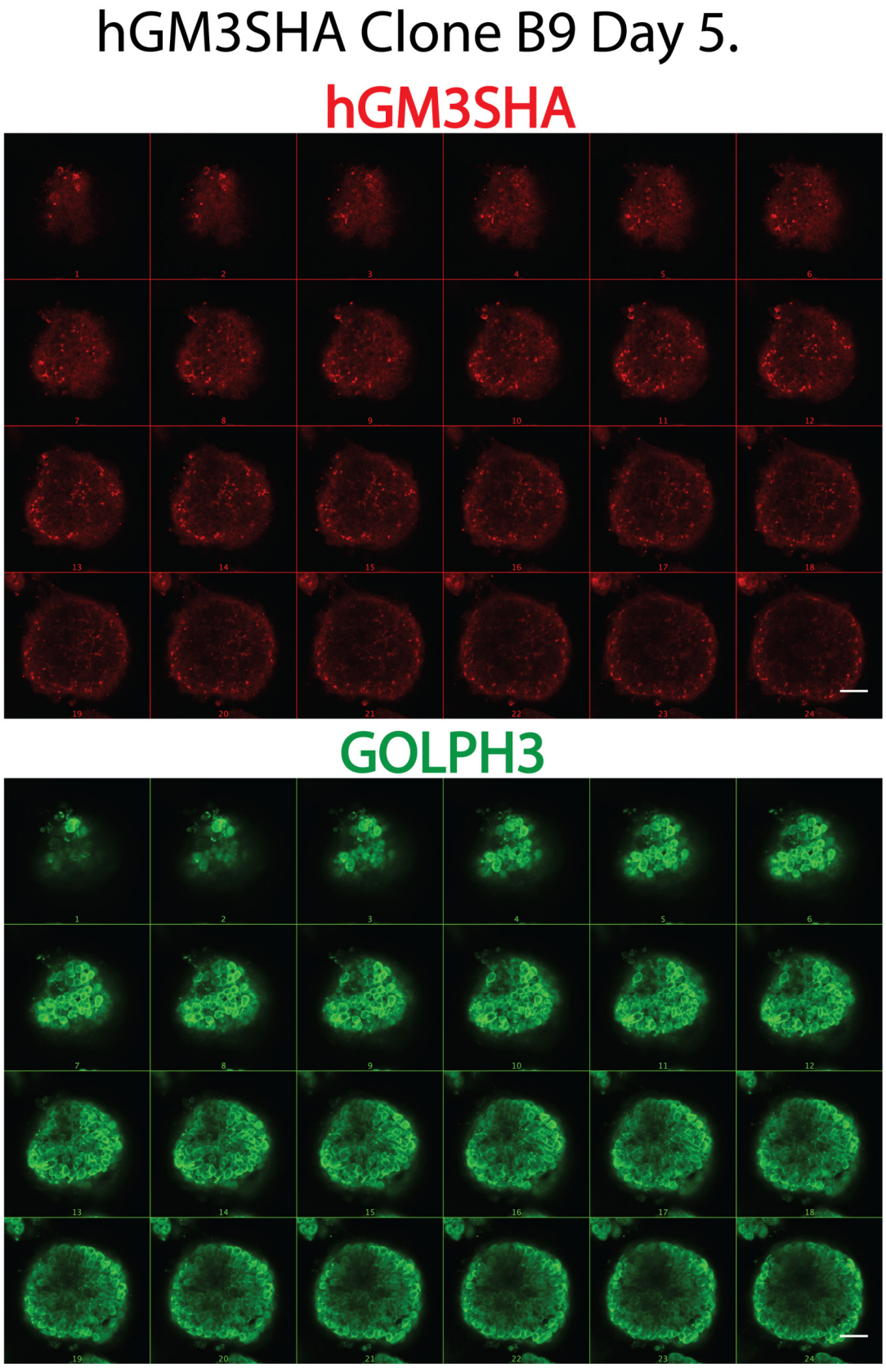

Figure 7.13: Representative confocal image of Day 5 organoid from hGM3SHA Clone B4. Z-projection of a single cyst. hM3SHA (red) is clearly visible and colocalizing with Golgi(GOLPH3).

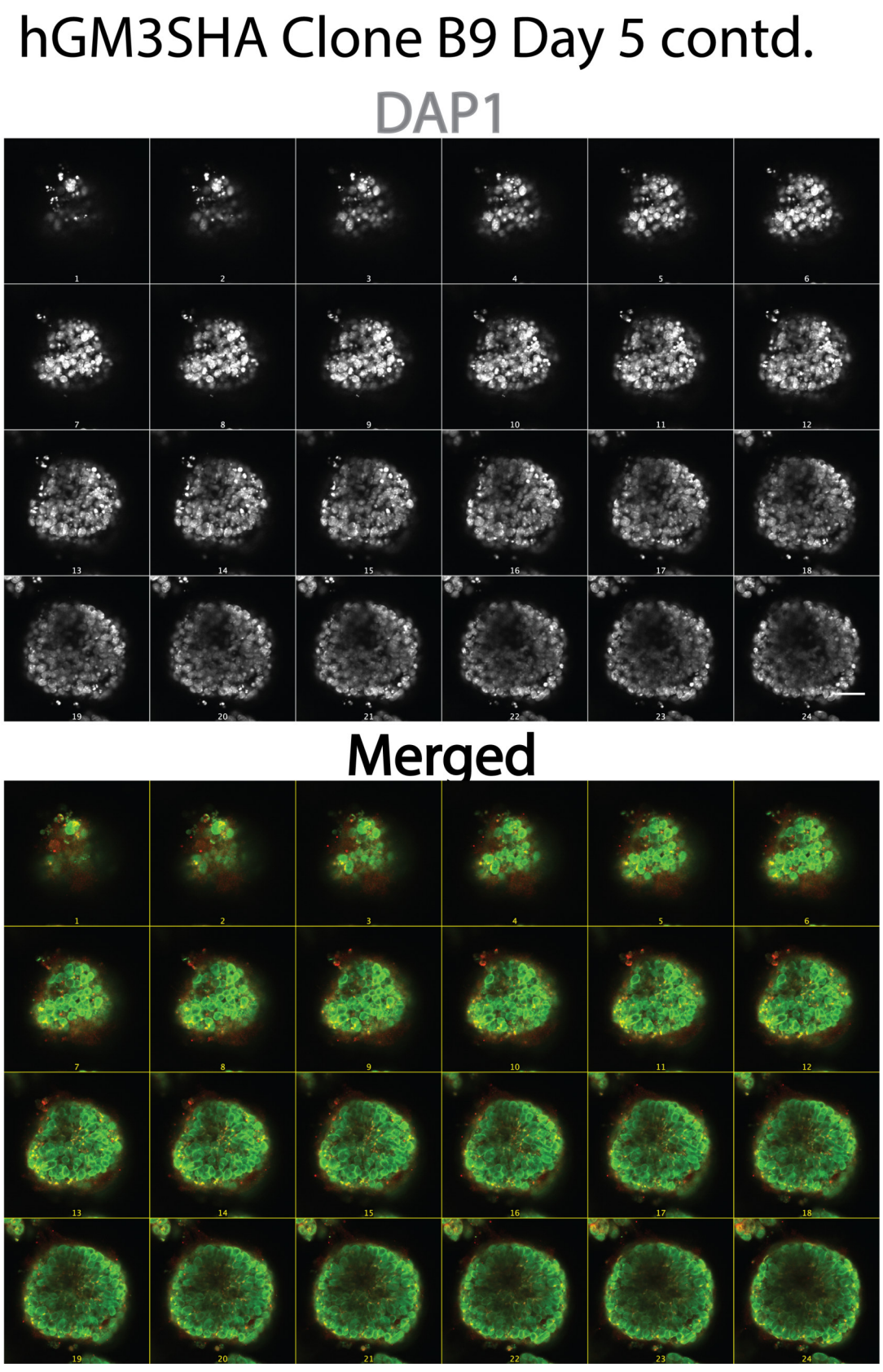

Figure 7.14: *contd*. DAPI in grey and Merged

7.3 Post-Translational regulation localizes hGb3SHA in lysosomes.

One major question that still remained was that although we had established that the regulation was at the level of the protein, we still did not yet know if it was translational stall or a post translational effect. We thus decided to use lysosomal and proteasomal inhibitors to see if we could rescue the hGb3SHA protein post-differentiation and possibly elicit some response for hGM3SHA.

Our own control experiments on with the plasmids transfected in HeLa (Cycloheximide treatment for 8hrs) (Figure-7.15-A. and B.) gave us a good idea that the half-life of these proteins is approximately 8 hrs, at least in HeLa cells. Using this as reference we performed a series of experiments on hGb3SHA clones using lysosomal inhibitor, Bafilomycin A1 (BAF) and proteasomal inhibitor Calpain Inhibitor I (ALLN)(Purich 2017), which revealed that the protein is still being synthesized post-differentiation but the initial pool of the protein that can be rescued is greatly diminished in differentiated cells(Figure-7.16). It seemed that both the inhibitors were able to rescue the protein at stem cell stage in 8 hrs but it required a significantly more amount of the proteasomal inhibitor to elicit a response (650X approx.)(Figure-7.16). At the neuronal stage the picture becomes much clearer as we see that protein at this stage is predominantly lost by lysosomal degradation but the most striking finding was that the rate of degradation was severely affected as post-differentiation, BAF is able to rescue almost twice the amount in 8hrs (Rate of degradation was calculated as

$$\delta^{(Day0)} = \frac{RFCDay0^{(BAF-Control)}}{RFCDay0^{(Control)}}$$

for Day 0 and Day 13, seperately). Immunofluorescence of cells treated with BAF further verified that most of the protein at stem cell stage is localized to the Golgi and upon treatment with BAF some of it can be seen colocalizing with the lysosomal marker LAMP1(not shown) but at the neuronal stage, almost all the protein is encapsulated in LAMP1 positive vesicles(Figure-7.15-B). Counterstaining

with TUJ1 confirmed that the protein was also rescued in terminally differentiated TUJ1 positive cells, which had previously been seen to be most adept at losing the enzyme(Figure-7.15-B).

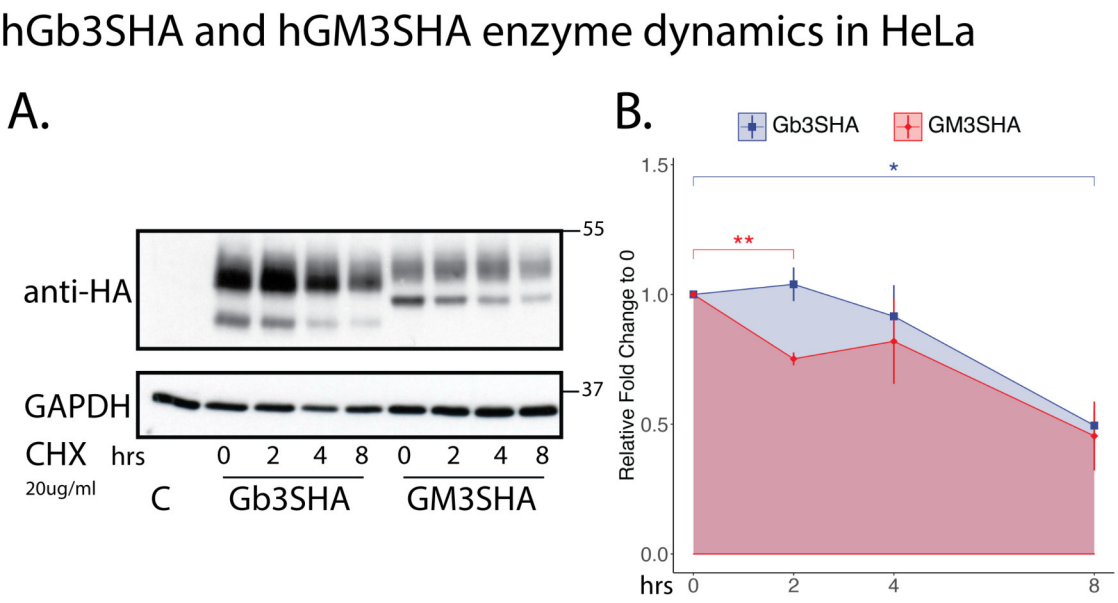

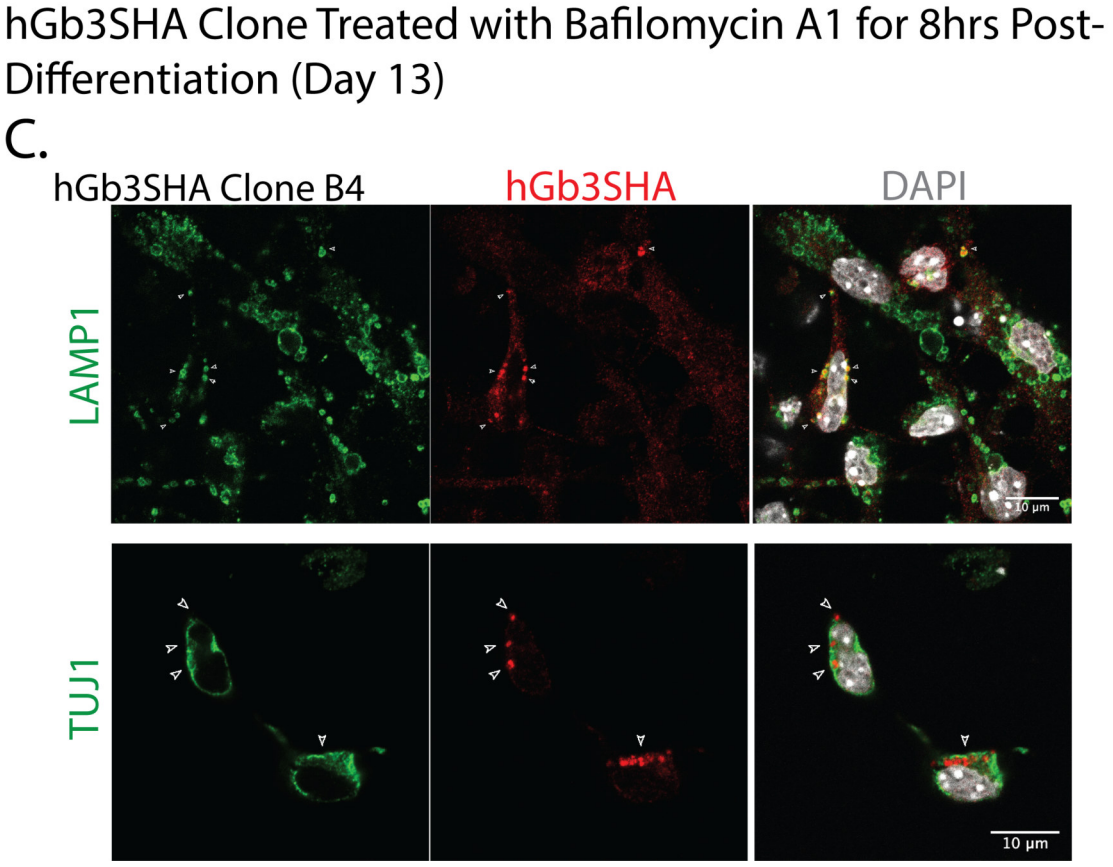

Figure 7.15: A. and B. Rpresentative western blot and quantification, respectively, of hGb3SHA and hGM3SHA enzymes transfected in HeLa and treated with CycloHeXimide (CHX) over a time-course of 2,4 and 8 hrs. CHX is a 'Translation Inhibitor' that inhibits the peptidyltransferase activity on the 60S subunit of the ribosome. Data are shown as the mean ± SD of 3 individual experiments; C. Representative confocal images of Differentiated hGb3SHA Clone B4 cells treated with lysosomal inhibitor, BAF, for 8hrs. hGb3SHA was seen to accumulate in lysosomes(LAMP1) upon BAF treatment, even in Neuronal cells (TUJ1)

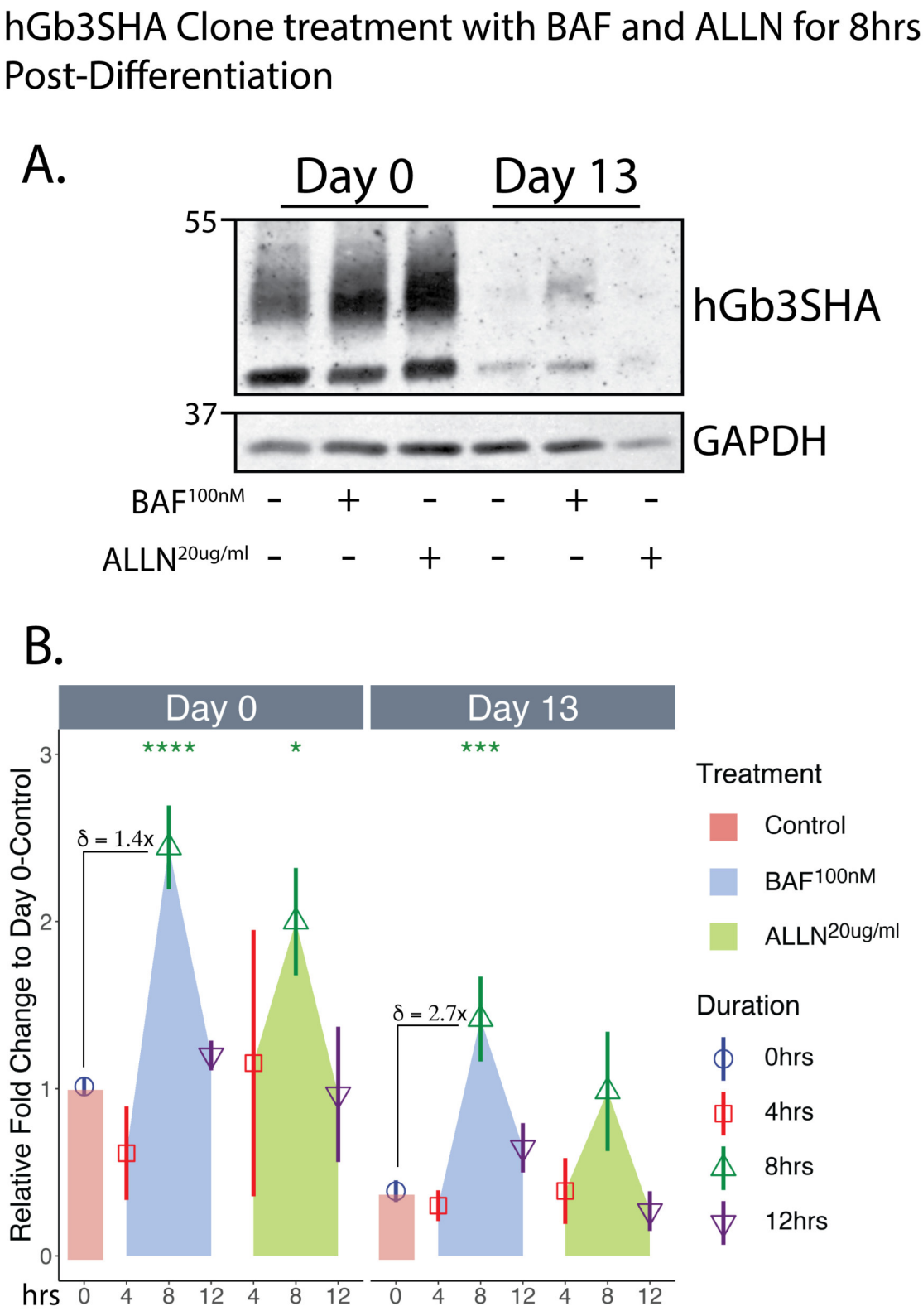

Figure 7.16: A. and B. Representative Western blot image and quantification of hGb3SHA Clone B4 upon treatment with lysosomal(BAF) and proteosomal(ALLN) inhibitors at Day 0 and Day 13. hGb3SHA seems to be mostly lysosomally degraded and the rate of degradation is doubled in neuronal cell. Data are shown as the mean ± SD of 3 individual experiments.

For hGM3SHA, this does not seem to be the case i.e. although it was observed in multiple experiments that we could increase protein levels is both cell stages by using BAF still, the increase is not significant in either of the cases (Day 0 and Day 13) and nowhere near the increase in levels observed post differentiation(Figure-7.17). As hGM3SHA had always been crisply visible at the Golgi pre and post differentiation, IF analysis of hGM3SHA clone B9 treated with BAF did not give any interesting insights on hGM3SHA and showed partial co-localization with LAMP1 at both cell stages (data not shown). It may very well be possible that the hGM3SHA, although part of the same circuit, is regulated by a completely different mechanism.

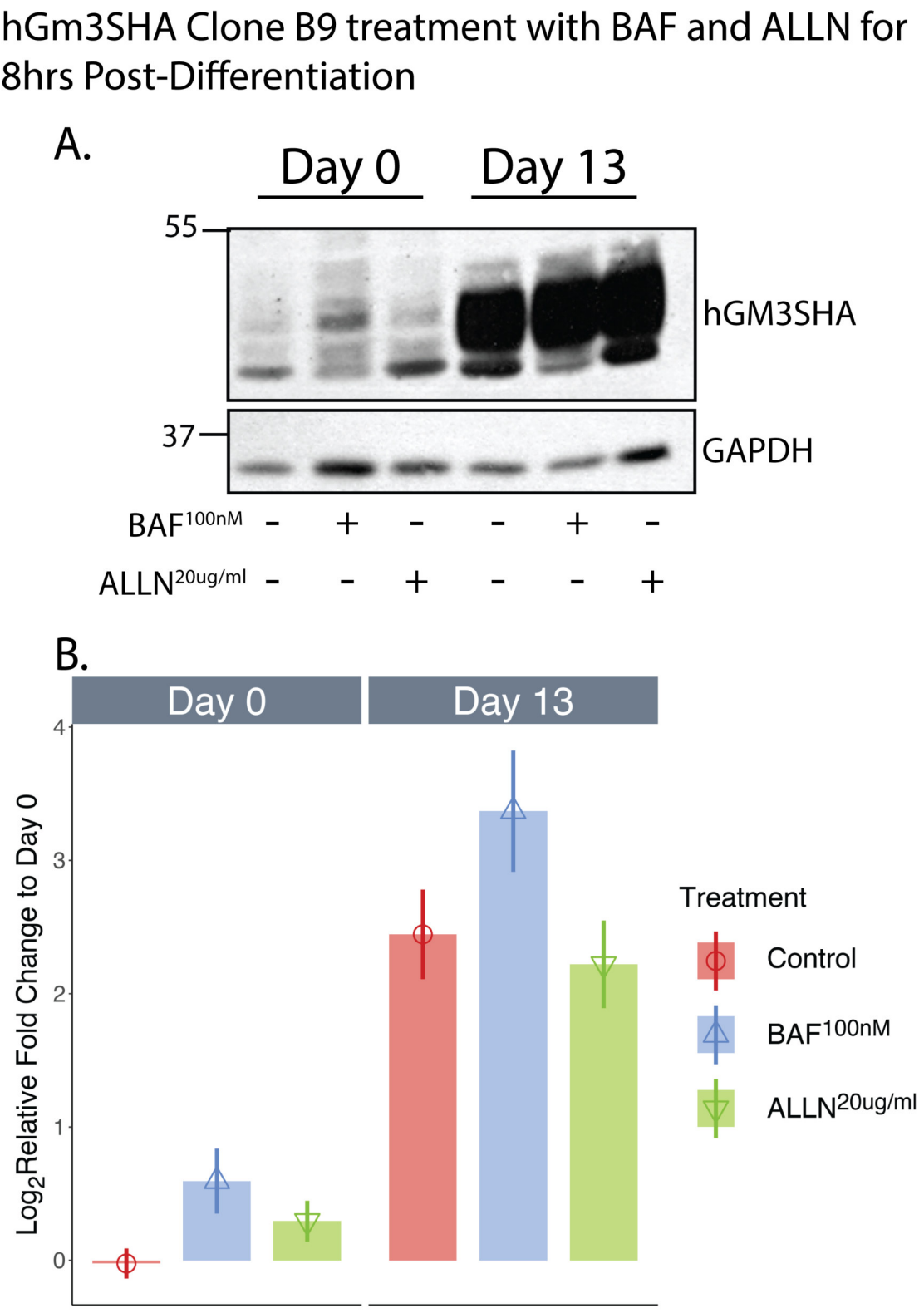

Figure 7.17: A. and B. Representative Western blot image and quantification of hGM3SHA Clone B9 upon treatment with lysosomal(BAF) and proteosomal(ALLN) inhibitors at Day 0 and Day 13 for 8hrs. Although some amount of hGM3SHA is also preferentially rescue by BAF, it was not a significant increaseand nowhere near the increase observed Post-Differentiation. Data are shown as the mean ± SD of 3 individual experiments.

8

Probing the molecular basis of the Regulation

Contents

8.1 Literature based search of molecular mechanism:

We decided to look for a molecular mechanism of the regulation and since we understood its post-translational nature, we confronted the matter in 2 ways. First, we went looking at the enzymes themselves to look for differences in post-translational modification and since most hGb3SHA is lost via the lysosomes, it was tempting to expect the mono-ubiquitination pathway that leads to lysosomal degradation (Hicke 2001) to be more active at day 13 than at day 0 so we looked for an increase in ubiquitination pattern in day 13 IP experiments. Although there was some increase in ubiquitinated bands, the increased bands appeared at a much

lower molecular weight (<50) and when blotted for HA we realized a technical flaw in the experiment(Figure-8.1-A). It would seem that both, anti-HA antibody and anti-HA dynabeads, used for the IP was not very efficient in pulling down the mature form of the protein(Figure-8.1-A-*in anti-HAblot) . The experiment also warned about future hurdles with such IP's for these enzymes because the heavy chain of the antibody completely masked the mature form of the enzyme. A second avenue to be investigated was the actual interacting partners of the enzymes and one staring us in the face was FAIM2.

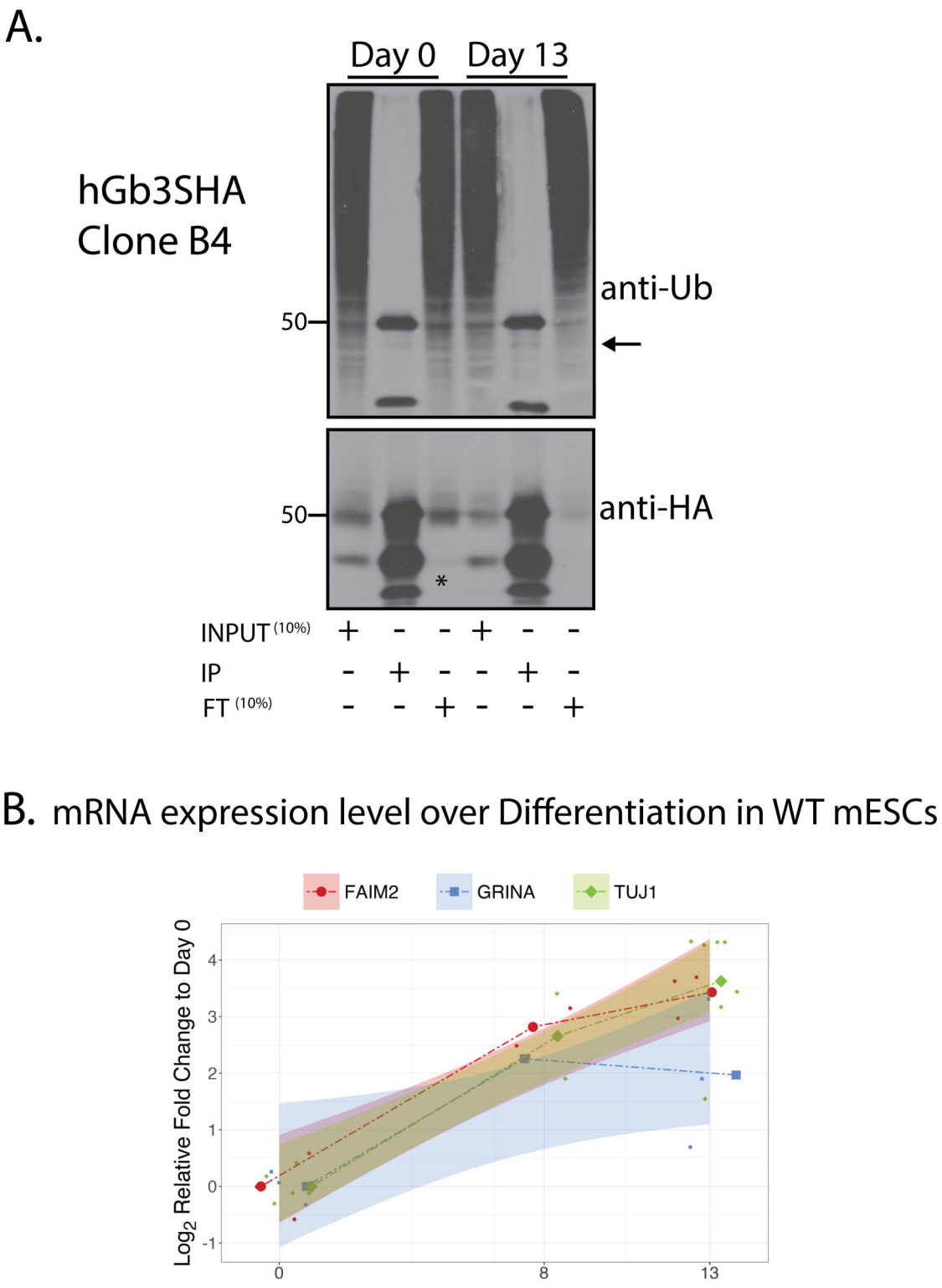

Figure 8.1: A. Representative Western blot image of Immunoprecipitation (IP) of hGB3SHA from Day 0 and Day 13 lysates from hGb3SHA clone B4. Arrow—-> marks the increased bands. * in the anti-HA blot marks the increased IP of high-mannose form.; B. FAIM2 and GRINAmRNA eexpression levels over differentiationin WT mESCs with Neuronal Marker (TUJ1). Data are shown as the mean ± SD of 3 individual experiments.

8. Probing the molecular basis of the Regulation

A second avenue to be investigated was the actual interacting partners of the enzymes and one staring us in the face was FAIM2. The pioneering study by Yamaji et al. had shown that overexpression of the members of TMBIM family of proteins resulted in a significant increase in ShTx resistance in Hela cells(Yamaji, Nishikawa, et al. 2010). The study goes on to show that 2 of these proteins, FAIM2 and GRINA-C (a C-terminal mutant of one of the TMBIM members) confer the greatest resistance and they do this by degrading the Gb3S enzymes in the lysosomes. Our interest in these proteins peaked when a preliminary experiment revealed that mRNA expression for both (FAIM2 and GRINA) increases gradually over neuronal differentiation(Figure-8.1-B). When we contacted Yamaji, he graciously offered to send us some amount of all the TMBIM family plasmids that he had constructed for the project. I was personally most interested in the FAIM2 as it was the only member of the family which conferred the most resistance as a full protein but a concern that Yamaji had mentioned, in communication and publication, was that at least the GRINA-C construct perturbed the localization of TGN46 along with Gb3S which casted a doubt over the integrity of the TGN. Along with all the other HA-tagged constructs of TMBIM family proteins that they had shared with us, they had also donated a FAIM2-FLAG tagged construct and I used this construct for co-transfection studies with our HA-tagged GSL enzyme constructs. Few initial experiments showed that FAIM2 does hGb3SHA protein level but it seemed to have a similar effect on most of the GSE tested and the effect was not rescued by the addition of BAF (3 of the enzymes tested shown in (Figure-8.2). When we looked at the protein through IF we realized that FAIM2 was mis-localizing most of the GSL enzymes along with TGN46(Figure-8.3 to Figure-8.5). This maybe an artifact of overexpression or something else entirely but we decided not to pursue this route further and instead, we focused on designing a screening experiment to look for the players of our regulatory mechanism in its system of origin and hoped to see FAIM2 again if it did play a role in the mechanism.

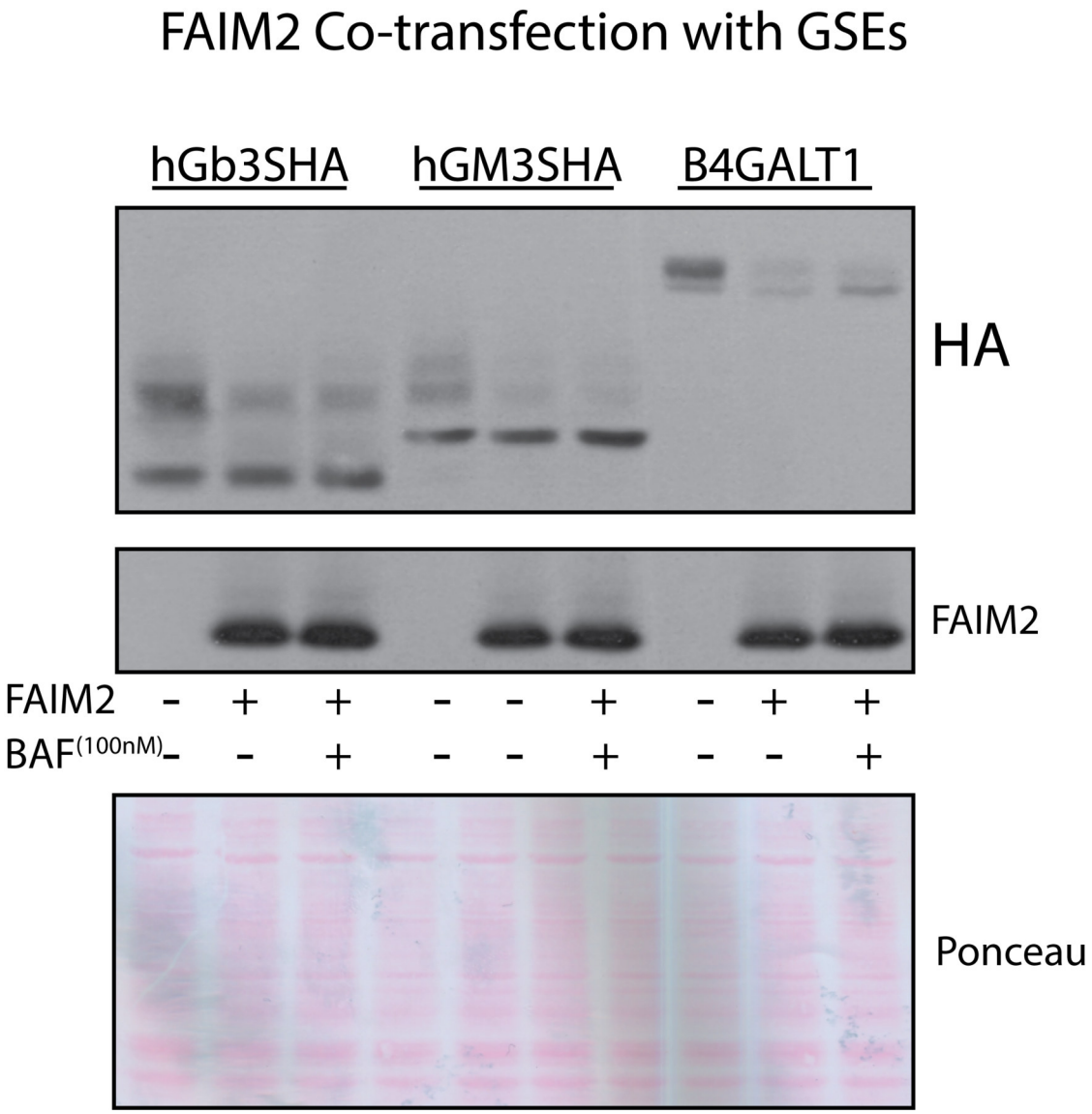

Figure 8.2: Representative western blot image and Ponceau scan of FAIM2–FLAG Co–Transfection with GSEs and treatment with BAF. FAIM2 too seems to have a destabalization effect on all 3 GSEs(hGb3SHA, hGM3SHA and B4GALT1HA) which is not rescued with BAF.

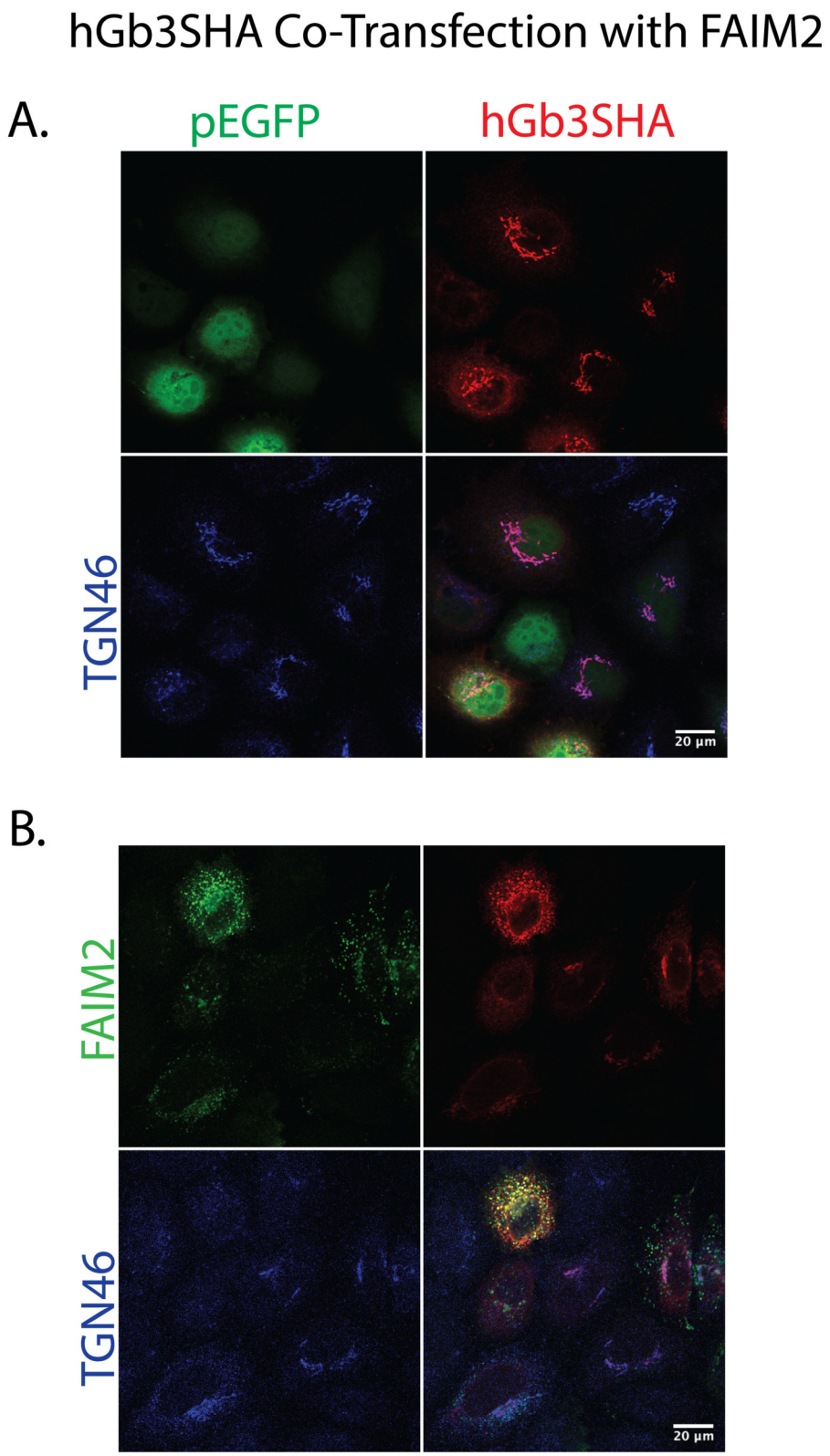

Figure 8.3: Representative confocal images of hGB3SHA localization wpon Co–Transfection with A. pEGFP empty vector and; B. FAIM2–FLAG in HeLa. TGN46 is also mislocalized.

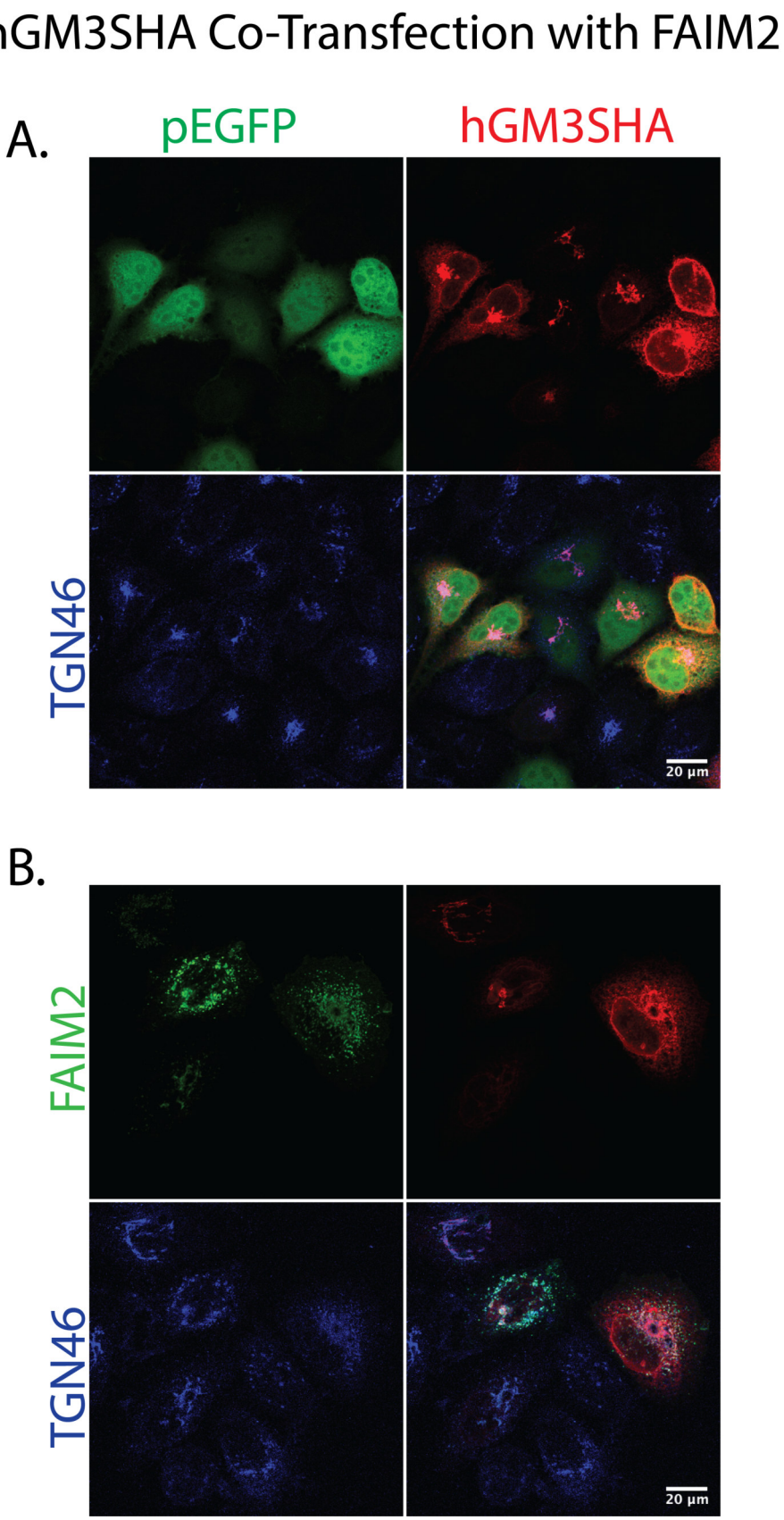

Figure 8.4: Representative confocal images of hGM3SHA localization wpon Co–Transfection with A. pEGFP empty vector and; B. FAIM2–FLAG in HeLa. TGN46 is also mislocalized.

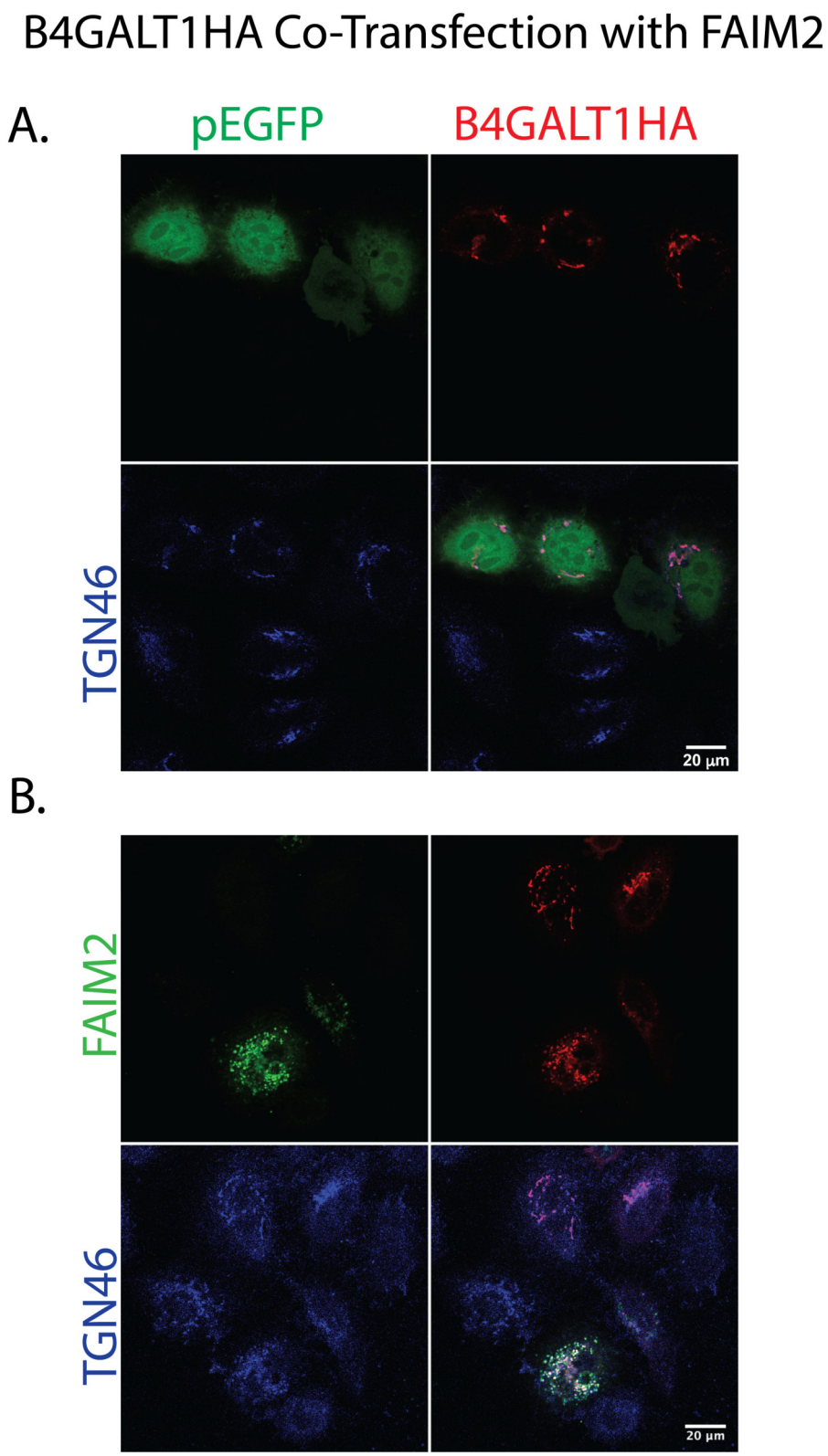

Figure 8.5: Representative confocal images of B4GALT1HA localization wpon Co–Transfection with A. pEGFP empty vector and; B. FAIM2–FLAG in HeLa. TGN46 is also mislocalized.

8.2 Mass-Spec based exploration of interacting partners of Gb3S and GM3S

An acknowledged mechanism of regulation of glycosylation enzymes at the golgi is via the short cytoplasmic 'tail' region, a characteristic feature of GSE's. In fact, unpublished data from our lab and other collaborators had already identified GOLPH3/Vps74 as an interacting partner of Gb3S that strongly interacted with its cytoplasmic tail region and very weakly with GM3S cytosolic tail, in HeLa(Rizzo et al. 2021). GOLPH3/Vps74 has long been understood as being an important player in retention of Golgi resident proteins and we understood that human GOLPH3 differentially interacted with a subset of GSE's in hela cells although the main effector of GOLPH3 mediated GSL perturbations was seen to be LCS (Banfield 2011). In my own differentiation experiments, total levels of GOLPH3 did not change post-differentiation and the protein was not detectable as a Co-IP with HA proteins, which may be more indicative of the antibody than the interaction. We decided to take advantage of one of the experimental setups used for the GOLPH3 project whereby the interactions were validated using biotinylated peptides mimicking the tail region of different GSE's (Rizzo et al. 2021) and instead, we used the same peptides of Gb3S and GM3S to do a more exploratory mass-spec based proteomic analysis by pulling-down their interacting partners at the 2 time points, Day 0 and Day 13. The Pull-Downs were processed for MS as described in methods and a proteomic dataset comprising 2516 identified proteins was obtained.

The dataset was separated by the 2 tail-peptides and a Relative Fold Change(RFC) to Day 0 was calculated from the Total Spectrum Normalized (TSN)values, individually. Statistical analysis revealed 259 proteins and 204 proteins that were significantly changed at Day 13 in Gb3S-T-pd and GM3S-T-pd, respectively and it was apparent that there were similarities in the datasets as similar proteins showed up in similar locations on their respective volcano plots (eg. Map1b, Crabp1)(Figure-8.6). A total of 30 such proteins were identified and although these could be manually filtered out it made logical sense, in light of our recent discoveries,

to calculate a relative-relative fold change R^2FC value between the Day 13 RFC of the 2 tail-peptides using the GM3S-tail dataset as control(

$$R^2FC = \frac{RFCGb3ST^{Day13}}{RFCGM3ST^{Day13}}$$

) (Figure-8.7-A). Such normalization should, in theory, squelch the proteins that follow the same trajectories while at the same time accentuating the differences between the 2 tail-peptides. Out of the 433 unique proteins significantly changed in either of the 2 pull downs, only 136 made it to the 261 significantly changed protein data set obtained with R^2FC values (only 7 proteins were seen to appear in all 3 datasets) which meant other 125 proteins that were not significantly different in the 2 datasets separately had just become much more interesting(Figure-8.7-B and 8.8-A). In fact, this final list of 125 proteins was conceptually most interesting for me because we were most confident of our understanding that at least at day 13 both proteins show starkly opposite phenotypes which meant there was a higher possibility of capturing the regulatory protein in this R2FC list although, there was always a possibility that both the proteins may yet be utilizing similar mechanism/complexes with piloted switching. A really nice testable control for the data transformation was GOLPH3 which was barely changed in the Gb3S-tail dataset alone but becomes much more significant when compared to GM3S-tail which sits nicely with the observed experimental data (Figure-8.8-B).

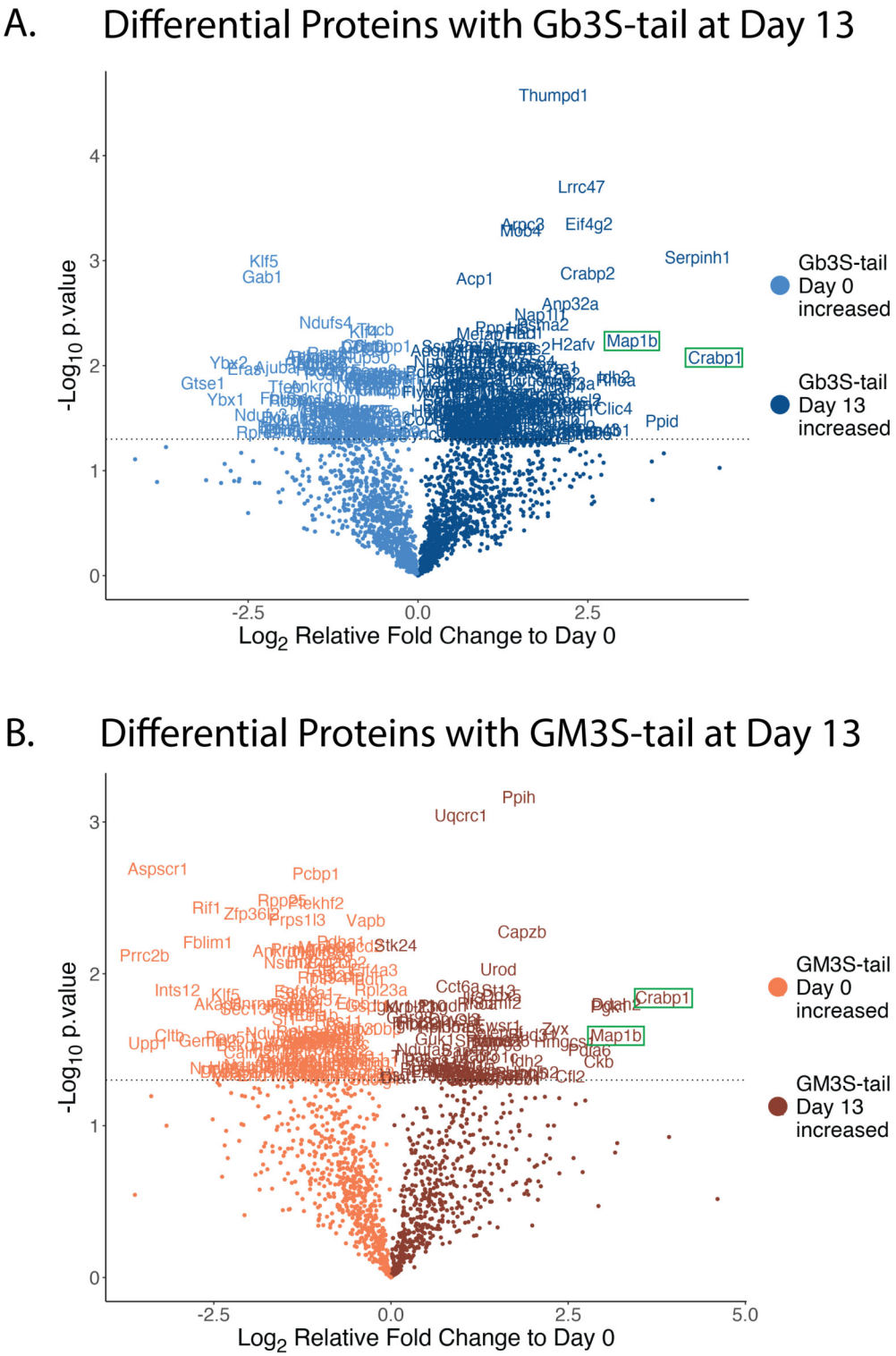

Figure 8.6: Schematic representation of proteomic datasets as Volcano plots with Log2 RFC at x–axis and negative Log10 p.value at y–axis for A. Gb3S–tail(Gb3ST) and; B. GM3S–tail(GM3ST); from 2 biological replicates

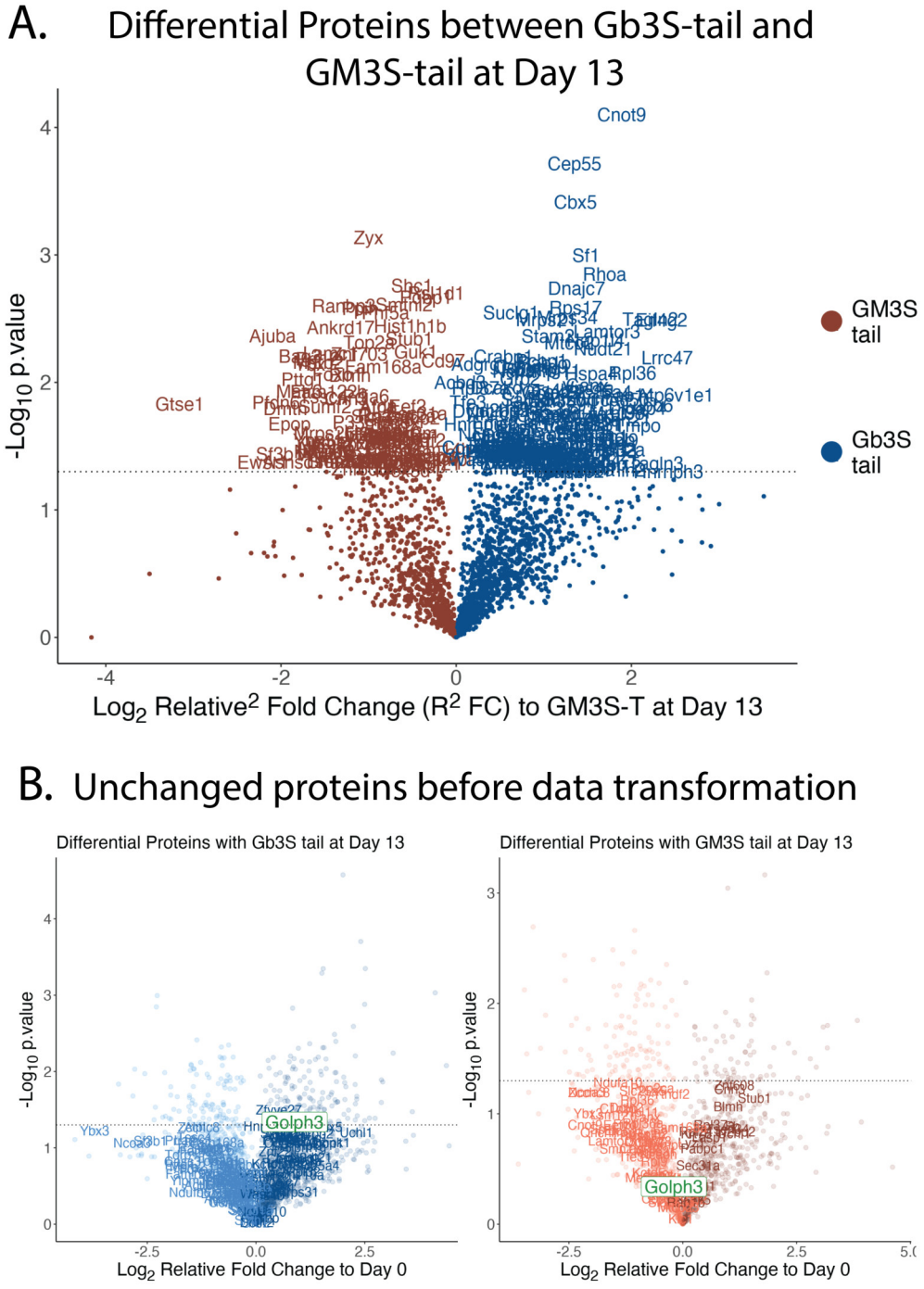

Figure 8.7: A. Volcano plot of differential proteins between Gb3S–tail and GM3S–tail at Day 13 with Log2 relative–relative fold change (R2FC) at x–axis and negative Log10 p.value at y–axis; B. Graphical representaion of 125 proteins unchanged before data transformation in both datasets (Gb3S–tail and GM3S–tail), individually.

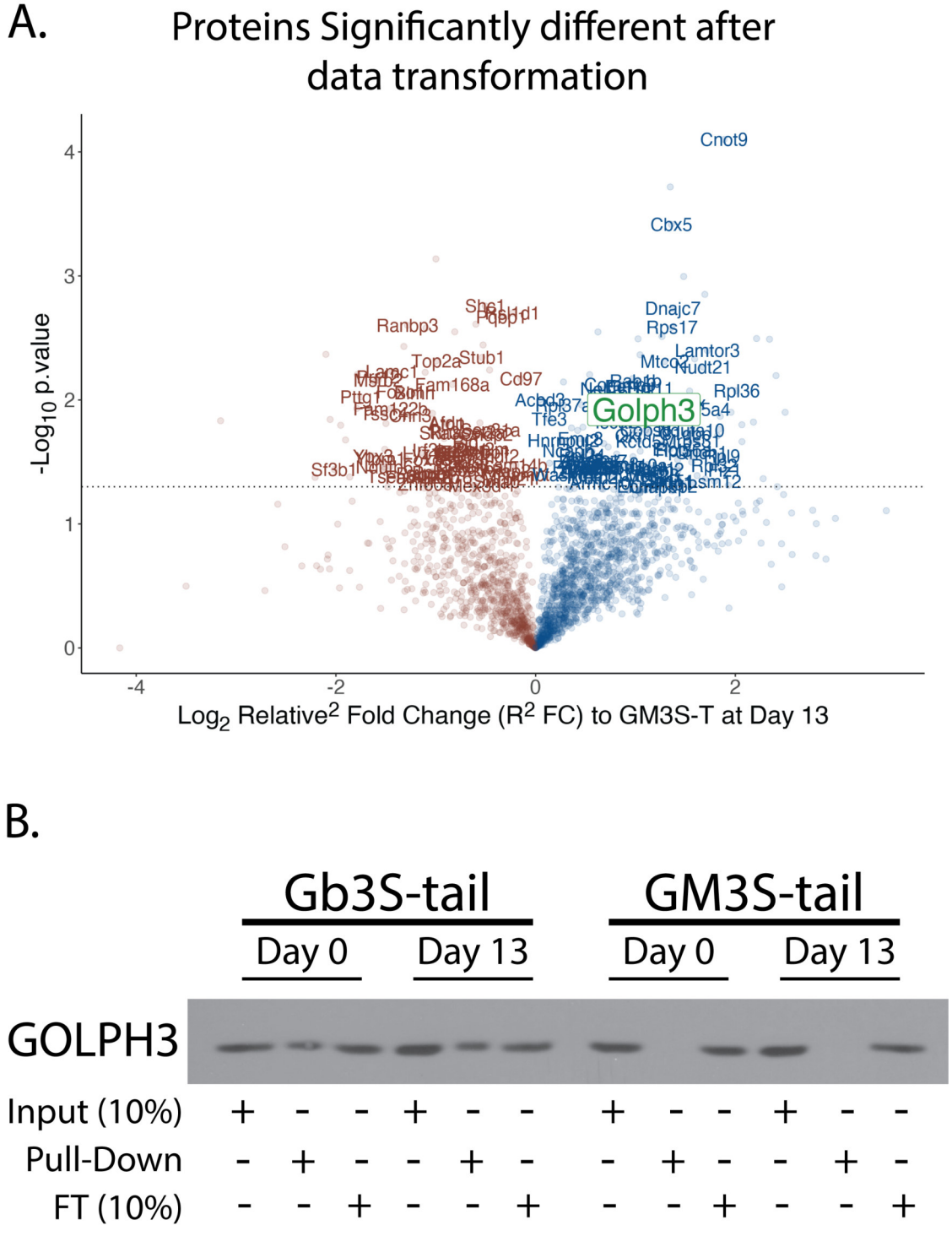

Figure 8.8: A. 125 significantly changed protein in the transformed dataset; B. Validation of the data transformation with Pull–Down of GOLPH3 with both tails from mESC WT Stem(Day 0) and Neuronal(Day 13) stages.

8. Probing the molecular basis of the Regulation

The datasets were explored through DAVID functional annotations clustering and the most significantly enriched clusters of proteins were common to all datasets (Gb3S-tail significant, GM3S-tail significant, R2FC significant), separately and as a single list of 602 proteins but a cluster of 12 and 5 proteins annotated as part of the endosomes and endosomal sorting complex (ESCRT) first piqued our interest even when it appeared as a lowly 0.6 enrichment score cluster ranking 25 out of the 44 clusters recognized, only in the R2FC significant dataset. As the clustering was further gated, the ESCRT cluster went to ranking 11 in proteins significantly increased at Day 13 with Gb3S T in R^2 FC dataset grouping and then, became the third highest ranked cluster in a further gating of proteins changed by at least 2-fold along with all the the other criteria(Figure-8.9-A). The ESCRT complex seemed a prime candidate for the protein transport linked phenotypes that we were witnessing, at least for the hGb3SHA, but a closer look at some of the other clusters revealed other proteins that are annotated according to their primary functions yet other evidences point to interactions in unconventional ways like Cep55 and ESCRT(Schuh and Audhya 2014) complex proteins. Some un-clustered proteins were also seen to be individually possessing characteristics that may explain the phenotype like proteins that directly or indirectly interact with the ubiquitin ligase complexes(like kctd5 (Bayón et al. 2008)). Finally, a couple of really significant clusters of proteins implicated in neurological disorders contained proteins that have interesting post-translational modification properties but the functional role is still murky like UCHL1 in the Parkinson's Disease cluster. All of this was realized after a considerable amount of time spent solely looking at the proteins significantly increased at Day 13 with Gb3S-tail in the R^2FC dataset so, to try and reach some semblance to a conclusion, I decided to manually curate a first list of proteins (23 tests and 1 control)(Figure-8.9-B) from this grouping and start designing a screening protocol focusing on our most understood phenotype, the loss of hGb3SHA.

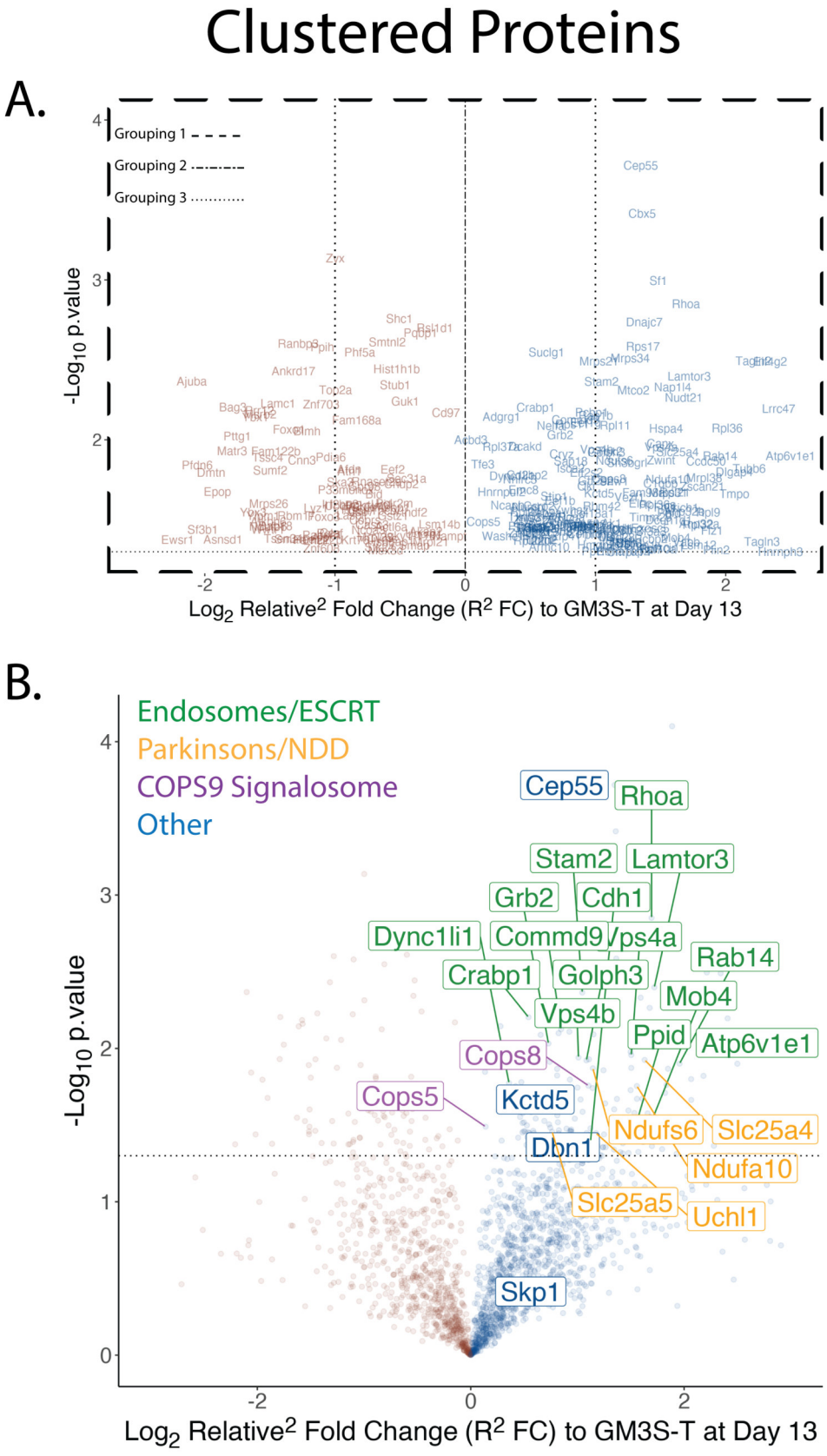

Figure 8.9: Graphical representation of A. grouping gates for DAVID clustering analysis and; B. Manually curated list of 24 proteins for screening.

8.3 First screen: Shooting in the dark;

As I was getting back to the lab in January 2020, we were discussing on a screening strategy and out of the two possible routes that we discussed, one being silencing the candidates over differentiation to rescue the protein and the other attempting to overexpress the candidate proteins in stem cell stage to induce a loss of the hGb3SHA protein, we opted for the latter because it possessed a possibility of narrowing candidates at the stem cell stage. The full strategy proposed was to employ lentiviral vector-based plasmids to do an initial screen in HeLa cells and then, hopefully, a narrower screen with packaged viral titres on stem cells before exploring the full context of a response if observed. I found myself lucky to be at EPFL a second time because of the easy access to resources like the genomics facility although the pLenti library is not one of the more favored vector backbones in the library from the facility which meant we were only able to find 13 out of the original 23 proposed but further 4 were unusable due to sequence mutations. Unfortunately, by the time we received the cultures the pandemic was in full swing and EPFL went under hard lockdown for a couple of months.

As the regulations relaxed for some time, we cautiously started with some screening of the hits on HeLa cells but the prospect of narrowing down candidates in HeLa seemed an unlikely possibility as none of the hits showed any significant effect on hGb3SHA(Figure-8.10-A). There was 1 protein, Lamtor3, that showed a significant effect on hGM3SHA protein with no effect on hGb3SHA, which made me think that maybe this was a protein that was captured in the grouping not because of its increased interaction with Gb3S-t at day 13 but rather because of its significantly increased interaction with GM3S-tail at Day 0 and, in fact, a look at the TSN values revealed exactly that but since we had no strong evidences of what was happening to hGM3SHA we could not do much with this information at that moment. Since the situation was still uncertain, any extensive experiments were out of the question for the time being, so I focused on 2 proteins that had become our prime candidates in discussions over the lockdown; Vps4a and Uchl1.

8. Probing the molecular basis of the Regulation

Although neither of the 2 showed any significant results in the original screen still, they were the only 2 to show a pattern similar to what we hoped i.e. to induce a loss in hGb3SHA with no change or increase in hGM3SHA but, more than data, both the proteins possessed some strong conceptual support. Vps4a for its obvious position in lysosomal degradation pathways like ESCRT(Han and Hill 2019) and, more recently, EGAD(Schmidt et al. 2019). UCHL1, on the other hand, was more or less stumbled upon when I discovered that in the original publication (which stemmed the project) UCHL1 had been used as a positive control to validate the transcriptional regulation of GM3S gene by AUTS2. Apart from the conceptual temptation of closing the loop such that loss of Gb3 perpetuates a cascading effect which increases the expression of GM3S while negatively feeding back into its own loss, UCHL1 is an interesting enigma in its own. It is one of the most abundantly expressed proteins in the brain and yet its functional role is still shrouded in mystery with reports claiming both, deubiquitinating and ubiquitin ligase-like enzymatic activity(Bishop et al. 2016). Although the protein is annotated as a deubiquitinating enzyme, a substrate for its enzymatic activity is yet to be identified and the general consensus, as I understand it, is that independent of UCHL1 enzymatic activity it stabilizes monomeric ubiquitin to make it available for cellular events(Matuszczak et al. 2020). I was able to validate the results of the MS by using the Gb3S-tail and GM3S-tail peptides (LCS-tail and B4GALT1-tail used as controls) to pull down the transfected Vps4a and UCHL1 in Hela cells (Figure-8.10-B) but further co-transfection experiments with Vps4a and UCHLl1 and 6 GSEs in HeLa cells did not show any significant results (only quantification shown (Figure-8.11-A)), staying true to the theme of the project, still UCHL1 and Vps4a seemed the best candidates if a viral transfection were to be carried out on stem cells in the near future.I was also lucky to locate a Vps4a Dominant Negative GFP (Vps4a DN) plasmid that the Gisou Van der Goot Lab had previously used in a publication and were kind enough to donate(Abrami et al. 2013). I decided to do some exploratory experiments with the plasmid on HeLa cells and was quite puzzled with the results as the western

blot showed a drastic loss of both enzymes, hGb3SHA and hGM3SHA, but the IF seemed to say something completely opposite (Figure-8.11-B).

It was quite evident from the IF that the hGb3SHA and hGM3SHA interacted differently with the Vps4a DN as in steady state transfections hGb3SHA was seen to partially co-localize with LAMP1 and Vps4a DN structures whereas hGM3SHA was crisply separated(Figure-8.12) which would suggest that disrupting Vps4a function somehow stops the degradation of hGb3SHA even when in lysosomes and thus one would expect an increase in the total protein level and not the observed decrease. Stranger still was that this 'decrease' was not rescued by BAF even though in IF a considerable amount of both enzymes was seen to colocalize with LAMP1 and Vps4aDN positive vesicles after treatment with BAF (Figure-8.13). A final strange behaviour actually came from the p-Lenti Vps4a that we received from the facility which did not look anything like any reported Vps4a transfection or the Vps4a DN transfection (Figure-8.14). We thus concluded that Vps4a may play a role in the specific mis-localization of hGb3SHA but the p-Lenti plasmids did not seem to be the right approach to test this hypothesis and, regrettably, the donating lab were not able to locate the original control Vps4a plasmid so any further experiments with this Vps4a DN plasmid would be highly suspect.

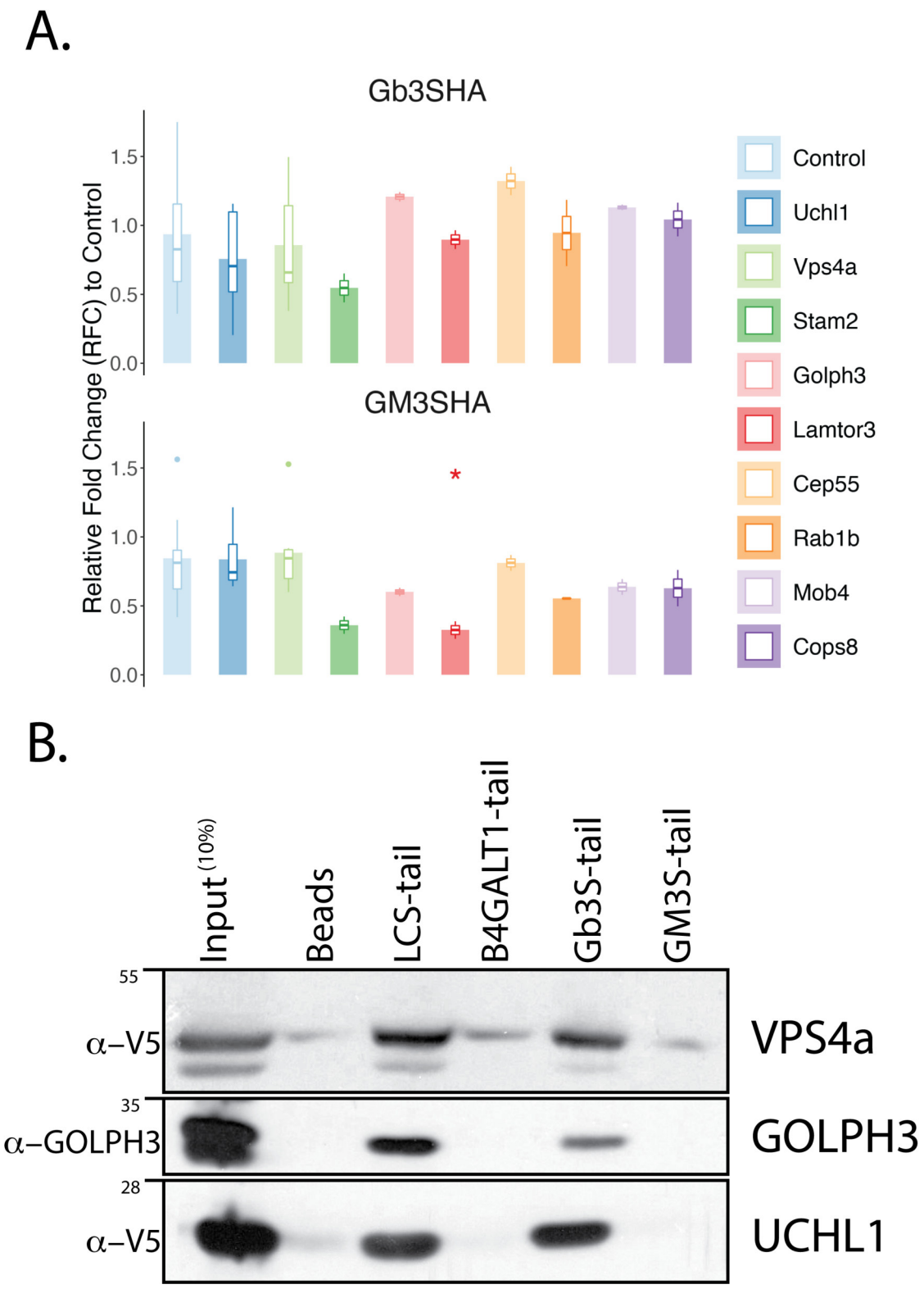

Figure 8.10: A. Quantification of HA protein expression level from Co–Transfection of 9 candidate proteins with hGbSHA and hGM3SHA. Data are shown as the mean ± SD of 3 individual experiments; *p < 0.05 and; B. Representative western blot image of validation of Pull–Down with Gb3S and GM3S tails on HeLa OE Vps4a or UCHL1.

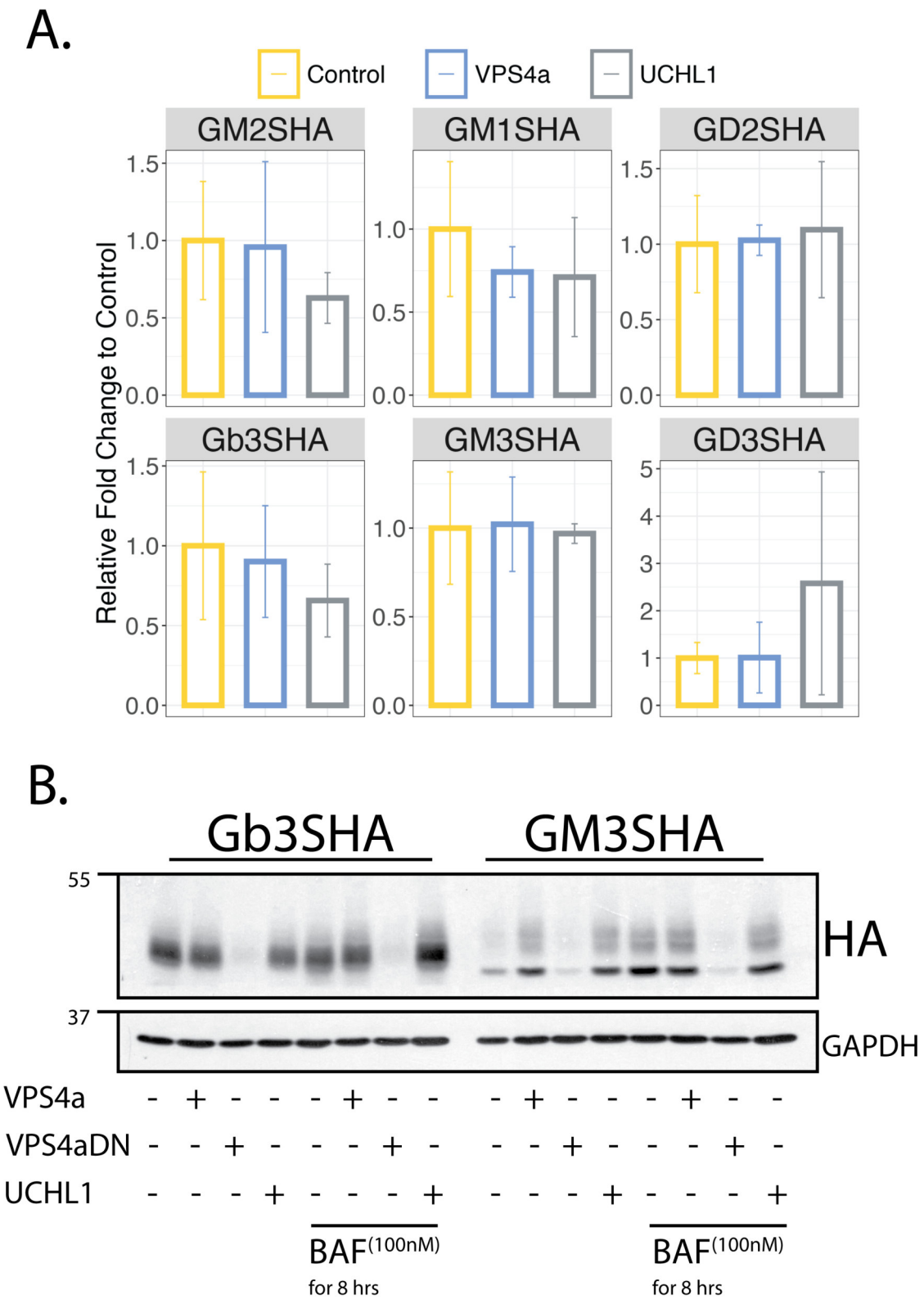

Figure 8.11: A. Quantification of HA protein expression level in Co–Transfection studies with Vps4a and UCHL1 with 6 HA-tagged GSEs (as facet labels). Data are shown as the mean ± SD of 3 individual experiments; *p < 0.05; B. Representative western blot image of effects of BAF on Gb3SHA and GM3SHA protein expression level upon Co–Transfection with Vps4a, Vps4aDN and UCHL1.

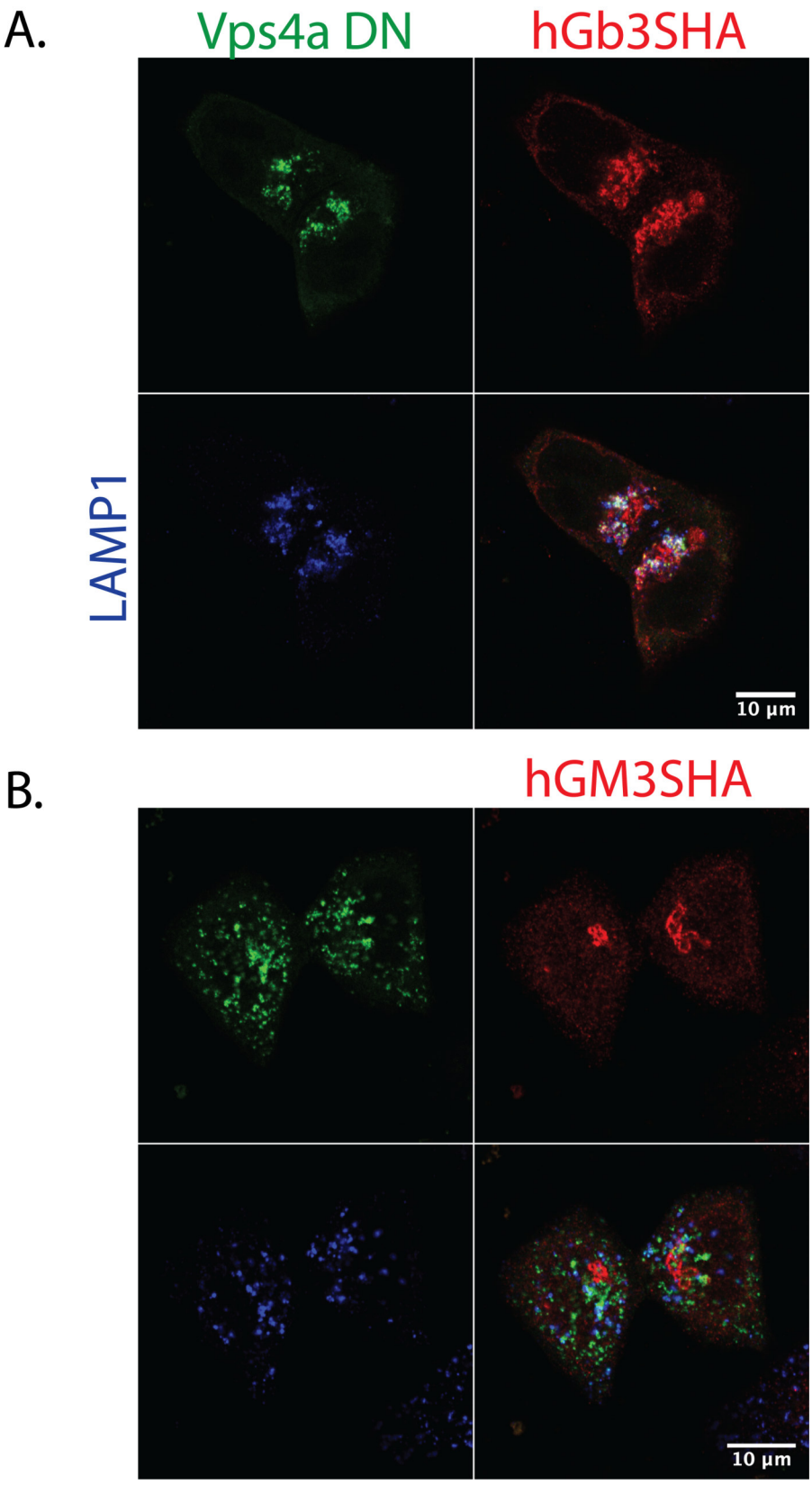

Figure 8.12: Representative Confocal images of Vps4aDN in HeLa cells Co–Transfected with A. hGb3SHA and; B. hGM3SHA. hGB3SHA colocalized with lysosomes(LAMP1) and Vps4aDN puncta whereas hGM3SHA shows a crisp peri-nuclear staining.

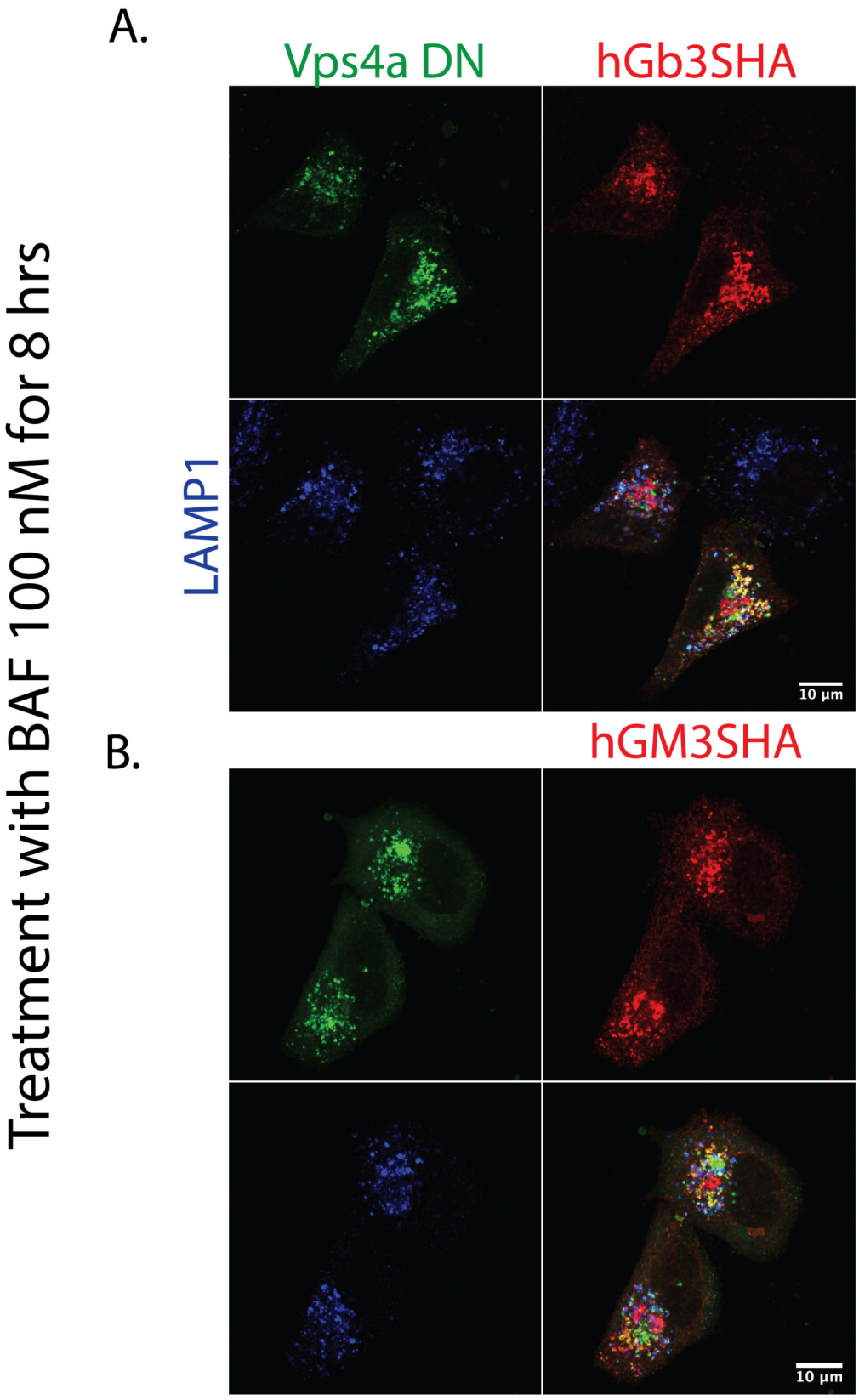

Figure 8.13: Representative Confocal images of BAF treated Vps4aDN transfected HeLa cells Co–Transfected with A. hGb3SHA and; B. hGM3SHA. Both enzymes partially colocalized with lysosomes(LAMP1) and Vps4aDN puncta upon BAF treatment.

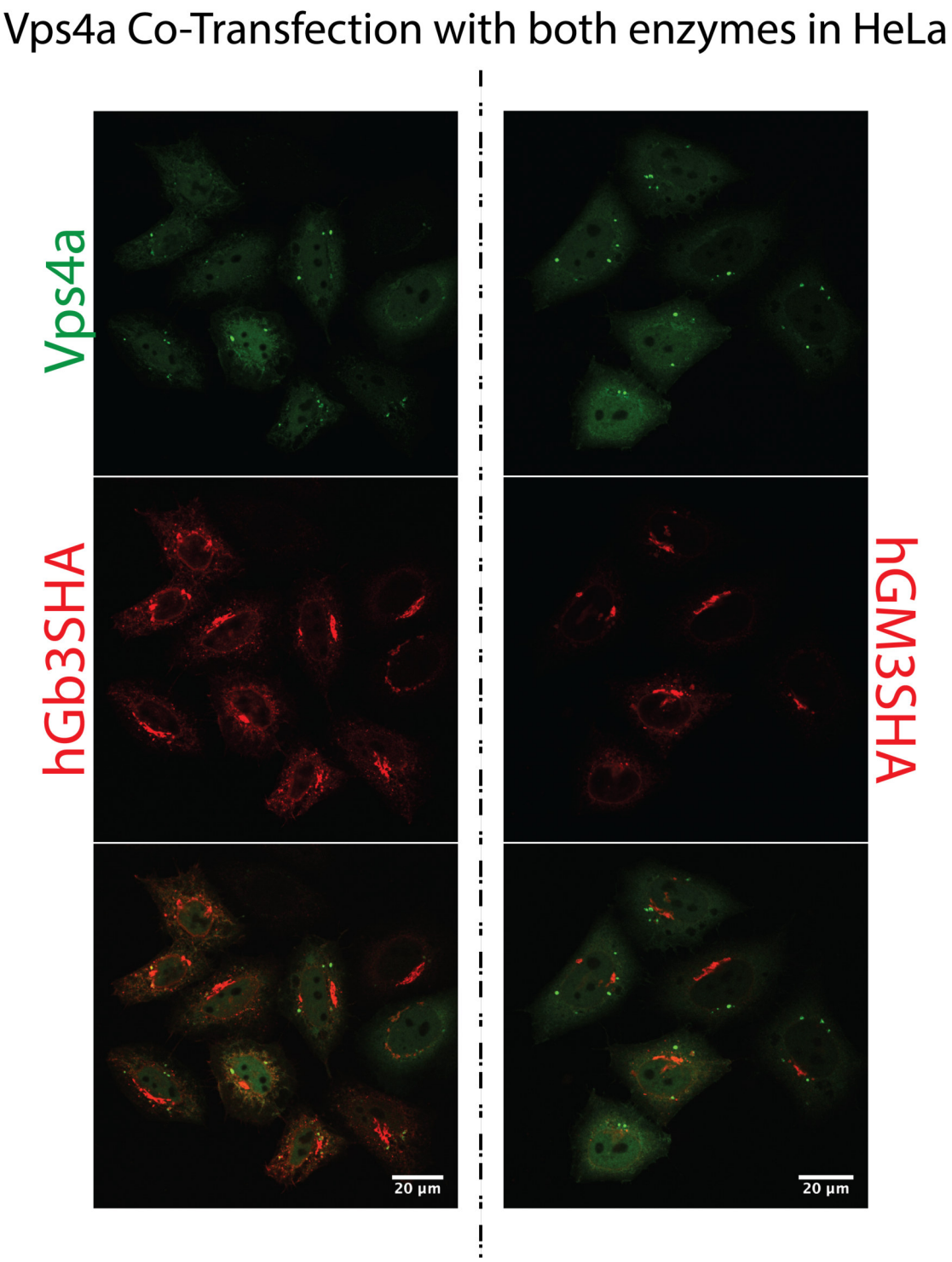

Figure 8.14: Representative Confocal images of Vps4a Co–Transfected with hGb3SHA and hGM3SHA in HeLa.

8.4 UCHL1

While researching UCHL1 we came across a very specific inhibitor called LDN 57444 (LDN) which has been used in >20 publications since its discovery in 2003(Liu, Fallon, et al. n.d.), so before we completely changed tactics, I decided to try an experiment with it using established concentrations for specific inhibiton in neurons ii.e. 10uM for 24hrs (Cartier et al. 2012), on the transfected hela cells and was pleased to see very specific response on hGb3SHA such that only hGb3SHA seemed to respond to LDN treatment irrespective of the Co-transfection with Vps4a or UCHL1(Figure-8.15) . Although there could be other inferences drawn from the experiment the other effects were not reproducible but the effect of LDN on hGB3SHA was very consistent. Spurred on by the positive results, we did the experiments on the clonal cell lines and were taken aback by the severity of the effect seen at both cell stages, stem and neuronal. It seemed that LDN showed a very special kind of rescue of hGb3SHA such that the mature form of the enzyme seemed to be shifted to a slightly higher molecular weight(Figure-8.16-A). Although the rescue was not as strong as BAF but it was the most specific of any of the drugs that we had tested and the shifted band supported our evidences of a membrane trafficking nature of the hGb3SHA phenotype. As UCHL1 is officially annotated as a DUB, instead of doubting this statement if we hold it at face value, a secondary hypothesis would be that instead of directly modifying hGb3SHA, UCHL1 could be switching the function of a membrane transport machinery such that now hGb3SHA spends longer time in the Golgi, either by retention or continual retrieval, and may get hyperglycosylated. The IF seemed to completely support this hypothesis as where BAF rescued the protein in lysosomes, LDN rescued protein in the Gogi (Figure-8.16-B). A quick way to check this would be to chop off the all mature glycosylation using a PnGASE F enzyme(Wang et al. 2014) and see if it could collect all of the enzymes in the single immature band. A second caveat I added to the experiment was to include the shorter time-point of 8hr for treatment with LDN, corresponding to our understanding of the enzyme. The experiment was extremely

informative as it revealed 2 important things; first was that the shifted band was not a glycosylation shift as 2 sharp bands appeared in the LDN treated samples instead of the single Immature band observed in control(Figure-8.17-A). Second, was that LDN was much more potent inhibitor for hGb3SHA degradation than previously seen as a drastic rescue of the protein could be observed at 8hr rather then 24hrs(Figure-8.17-A). The PNGase experiment also gave us a rough estimate of the contaminant band which allowed for a primitive analysis on the percentage makeup of hGb3SHA divided into the 3 most common forms of the protein. The 3 bands were termed E-band (ER-band; lowest molecular weight band ~37kd; high-mannose *Band1* in (Yamaji, Nishikawa, et al. 2010)), GL-band (Golgi-Lower; most abundant mature form at steady state ~ 45kd; lower part of *Band2* in (Yamaji, Nishikawa, et al. 2010)) and GU-band (Golgi-Upper; most increased by LDN treatment ~50kd; upper part of *Band2* in (Yamaji, Nishikawa, et al. 2010)) and only experiments where all 3 bands are clearly visible were considered for this analysis (8 experiments, ~ 16 replicates). The analysis told us that the form of hGb3SHA that drastically increases upon LDN treatment is also naturally increased over differentiation. This increase is directly related to the decrease in the E-band (Figure-8.17-B).

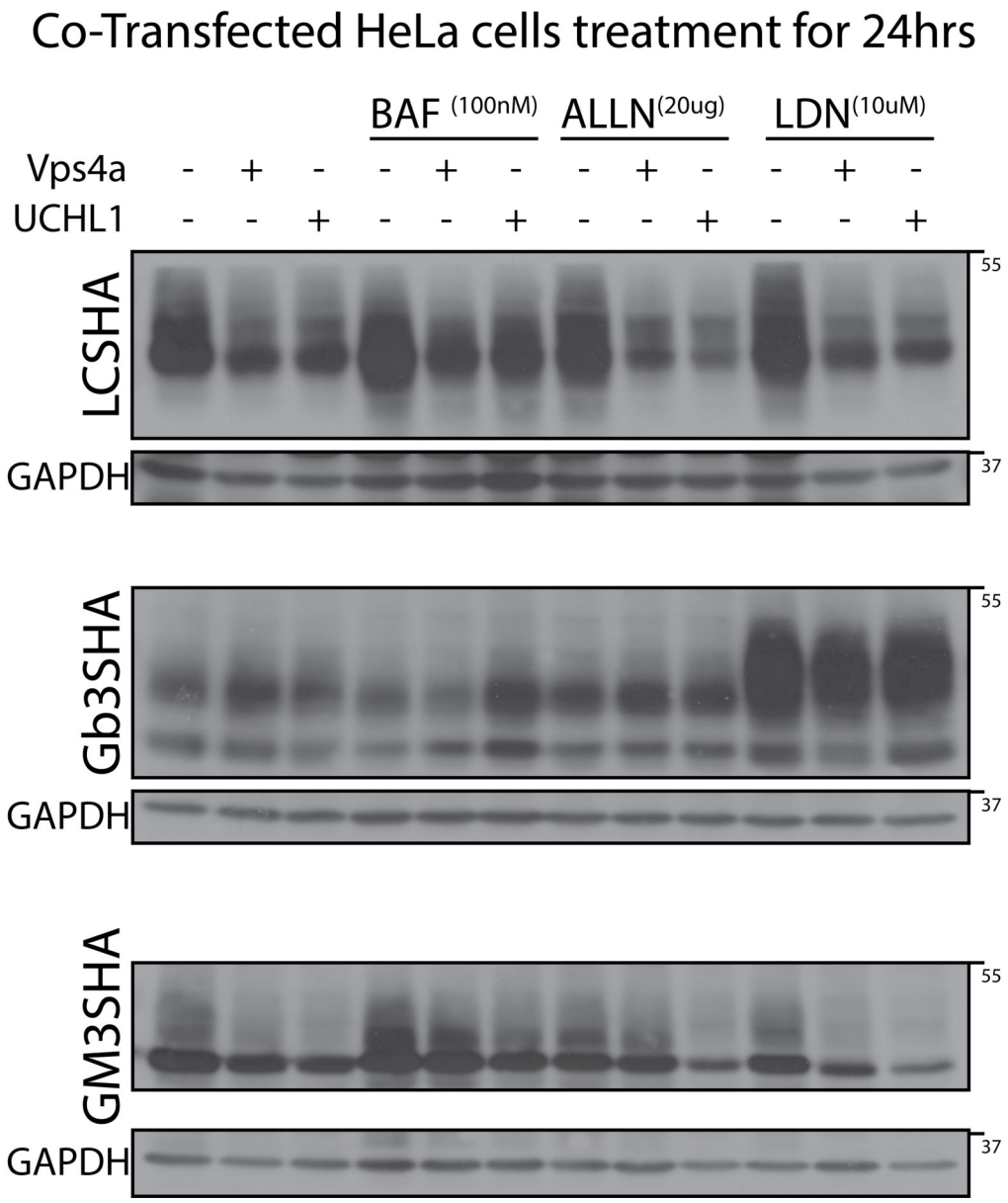

Figure 8.15: Representative western blot image of LCSHA, Gb3SHA and GM3SHA Transfected HeLa cells, Co–Transfected with Vps4a and UCHL1 and treated with Lysosomal(BAF), Proteosomal(ALLN) and UCHL1 (LDN) inhibitors for 24 hrs.

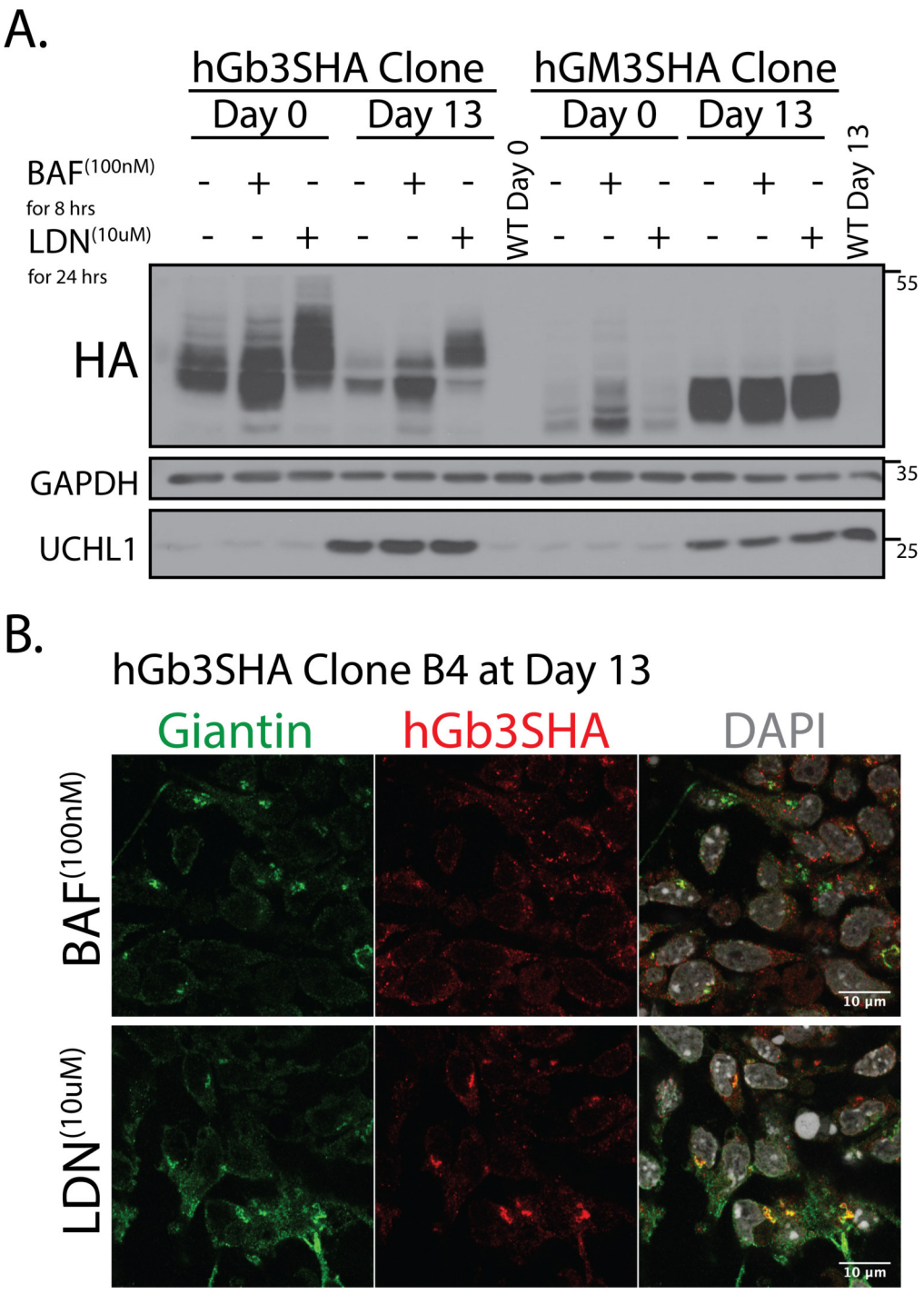

Figure 8.16: A. Representative western blot image of hGb3SHA Clone B4 and hGM3SHA Clone B9 treated with BAF(8hrs) and LDN(24hrs) Post-Differentiation; B. Representative confocal images of differentiated hGb3SHA clone B4 cells treated with BAF and LDN. hGb3SHA is mostly seen in punctas with BAF treatment whereas upon LDN treated, hGb3SHA is rescued at the Golgi(Giantin)

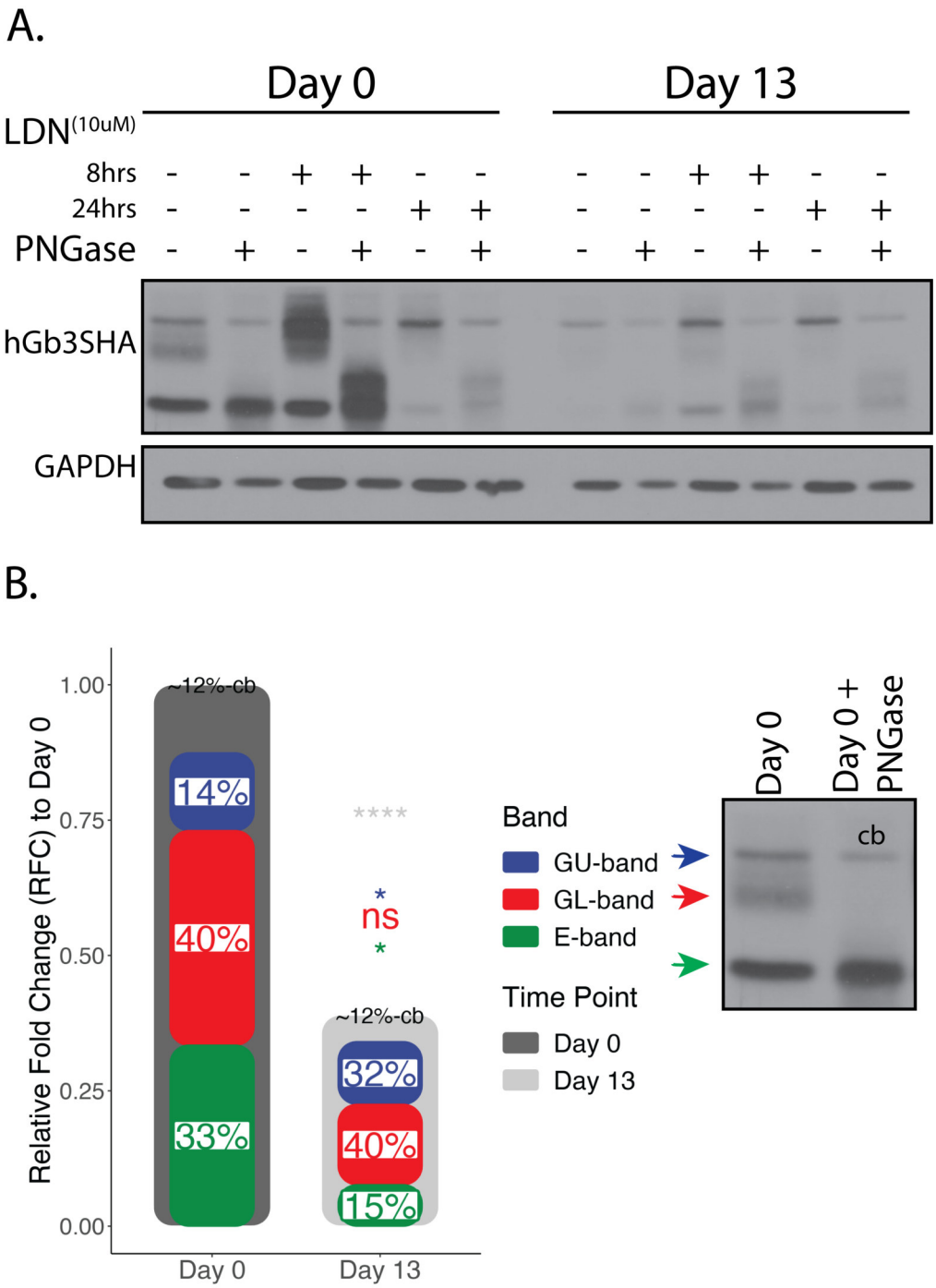

Figure 8.17: A. Representative western blot image of LDN treatment at Day 0 and Day 13 on hGb3SHA clone B4 at 2 time points (8hrs and 24 hrs) with a further treatment with PNGAse to 'deglycosylate' the protein; B. Graphical representation of percentage makeup analysis done on all previous experiments where all 3 bands, GolgiUpper(GU–band), GolgiLower(GL–band) and Endoplasmic reticulum (E–band) were clearly visible (9individual experiments). Corresponding bands are color coded and *cb denotes contaminant band

8. Probing the molecular basis of the Regulation

To further characterize this rescue, we did a time-course experiment with LDN on both cell states and realized that even though the maximum rescue was seen at 8 hrs, LDN was capable of significantly rescuing the protein in as less as 2 hrs at Day 13(Figure-8.18). I was also able to test a UCHL1 antibody that had just arrived and it revealed that although UCHL1 is most definitely a neuronally expressed protein still some amount of UCHL1 was present in our stem cells which may explain the observed rescue of the protein in stem cells (this was also true for HeLa cells). Another thing that was quite evident from the experiment, was that the 'shift' only became significant after 4hrs of treatment from when it became the dominant form of the enzyme(Figure-8.19).

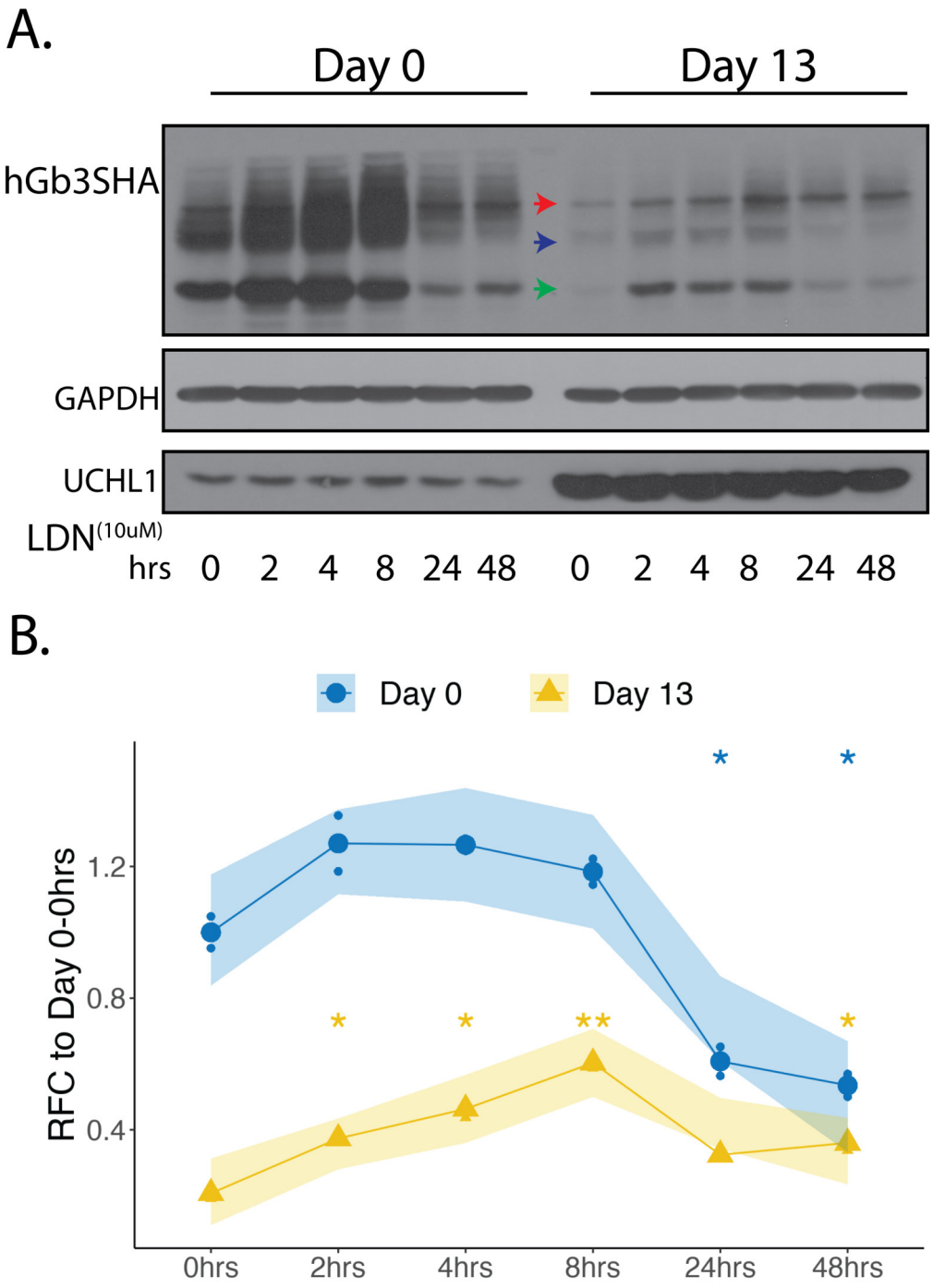

Figure 8.18: A. Representative western blot image of LDN57444 (LDN) time course treatment on hGb3SHA Clone B4 at Day 0 and Day 13 ; B. Quantification of LDN time course. LDN is able to significantly rescue the protein in in Neurons (Day 13) in 2hrs.

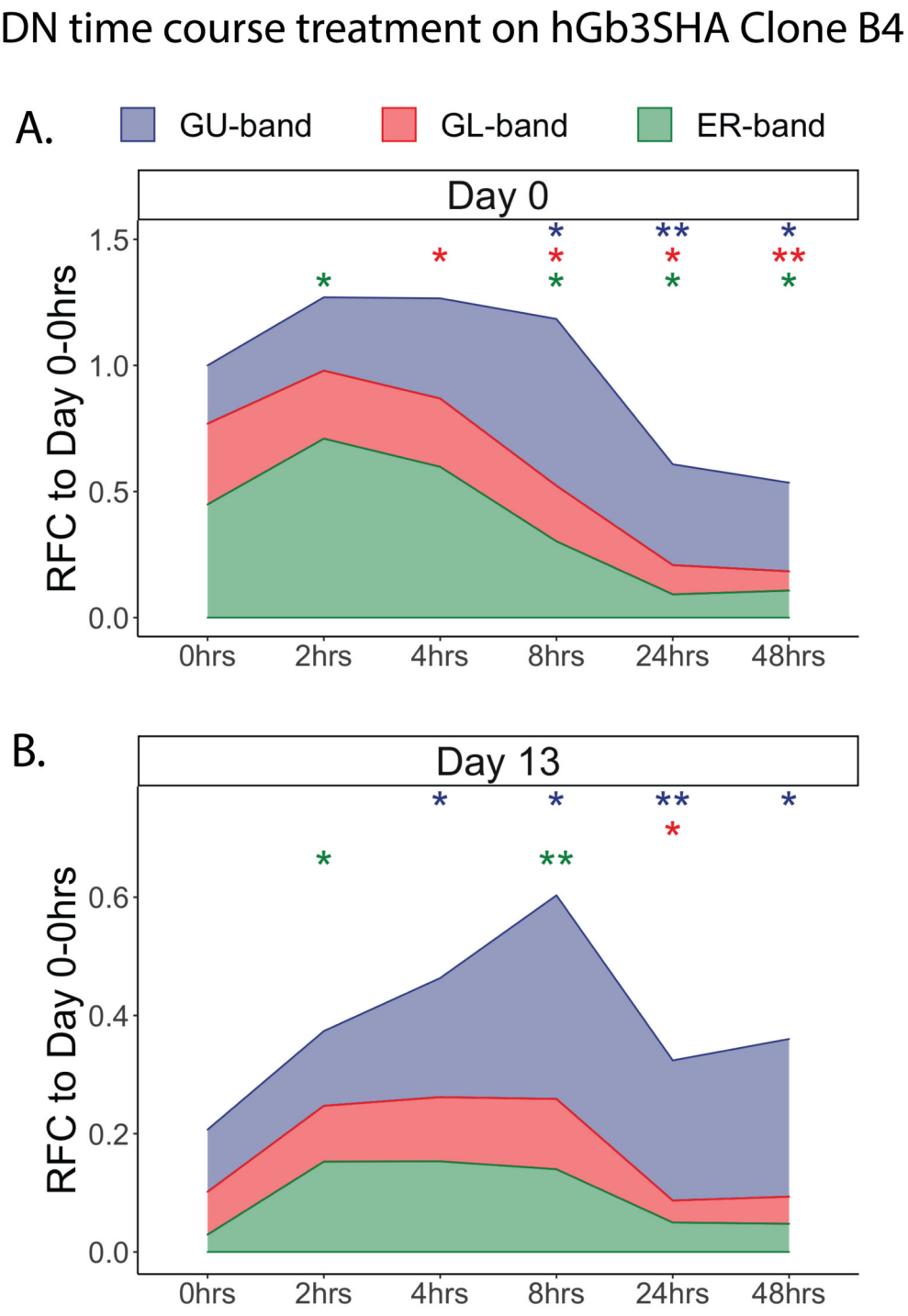

Figure 8.19: Graphical representation of Percentage makeup of the 3 hGb3SHA bands overlayed onto the RFC to Day 0 values for A. Stem (Day0) and B. Neurons (Day 13)

8. Probing the molecular basis of the Regulation

The weird nature of the effect of LDN on hGb3SHA prompted us to look deeper and we came across a very recent publication (Panyain et al. 2020) that casted a doubt on its mechanism of action. The publication reported that they failed to see any significant inhibition by LDN on UCHL1's capability of engaging with labelled Ub fluorescent probes in Fluorescence Polarization (FP) based screenings as well as other biochemical assays and, in fact, that they had identified a compound which they claim to be the most potent and selective inhibitor for UCHL1(Panyain et al. 2020). Our association with Gisou van Der Goot lab came to our rescue once more as we found out that the author of the paper, Nattawadee Panyain, had just joined as post-doc in the lab and through her references we were able to procure some amount of this new compound (Compound2) but due to general disruption of travel and communication in these times I was only able to do my first experiments with the drug in February 2021.

By this time, I had been accustomed to looking at the effect of LDN on hGb3SHA in stem cells and the first experiments using the compound at 100nM did not exhibit any effect on the protein levels in stem cells which may not be indicative of much as uchl1 is really present in miniscule amounts in stem cells relative to day 13 but since the effect of LDN was so clearly visible and discrete, we had hoped for a clearer answer. Before planning a larger differentiation experiment I wanted to test some other concentrations of the inhibitors and decided to run a preliminary experiment testing 4 concentrations of all 3 known UCHL1 specific inhibitors that i had collected by this time i.e. LDN, Compound2 and 6RK73. 6RK73 was a latest addition to the growing collection of uchl1 inhibitors which had also appeared in another original research article published in 2020 (Liu, González-Prieto, et al. 2020) which, yet again, claimed a better inhibition than LDN, but distinctly this is a covalently bonding compound which meant this inhibition should be irreversible. A final drug added to this 'mini-screen' was a UCHL3 inhibitor called TCID (Ouyang et al. 2020), which was only used at a presumably higher concentration of 10uM while the rest of the drugs were tested at identical concentrations to maintain some semblance of a comparison (100nM, 200nM, 500nM and 1uM for 8hrs). The

results from this pilot experiment were promising as all 3 uchl1 specific inhibitors showed a positive response at some concentrations while TCID treated samples were unchanged(Figure-8.20-A) and as soon as I saw the result I started what I hoped to be a final conclusive differentiation experiment for this part of the project. During this time we were further analysing the preliminary experiment and it seemed that the molecular weight shifting peculiarity of LDN treatment was not just limited to the time of treatment but also probably with the concentration(Figure-8.20-B). A second experiment on stem cells with only the 3 uchl1 inhibitors at 2 concentrations (1uM and 10uM,) conclusively validated the results that indeed all 3 inhibitors showed a rescue of the protein in 8 hrs similar to BAF and that the shift in the band is most probably linked to the concentration, at least at stem cell stage as LDN seemed to be perfectly capable of rescuing similar amount of protein at 1uM without the shift(Figure-8.20-B). Compound 2 was showing a weird effect at the higher concentration of 10uM whereby there was an observable decrease in the mature bands which was explained by an additional lower molecular weight band, possibly a degradation product, which was only seen at this concentration with Compound 2.

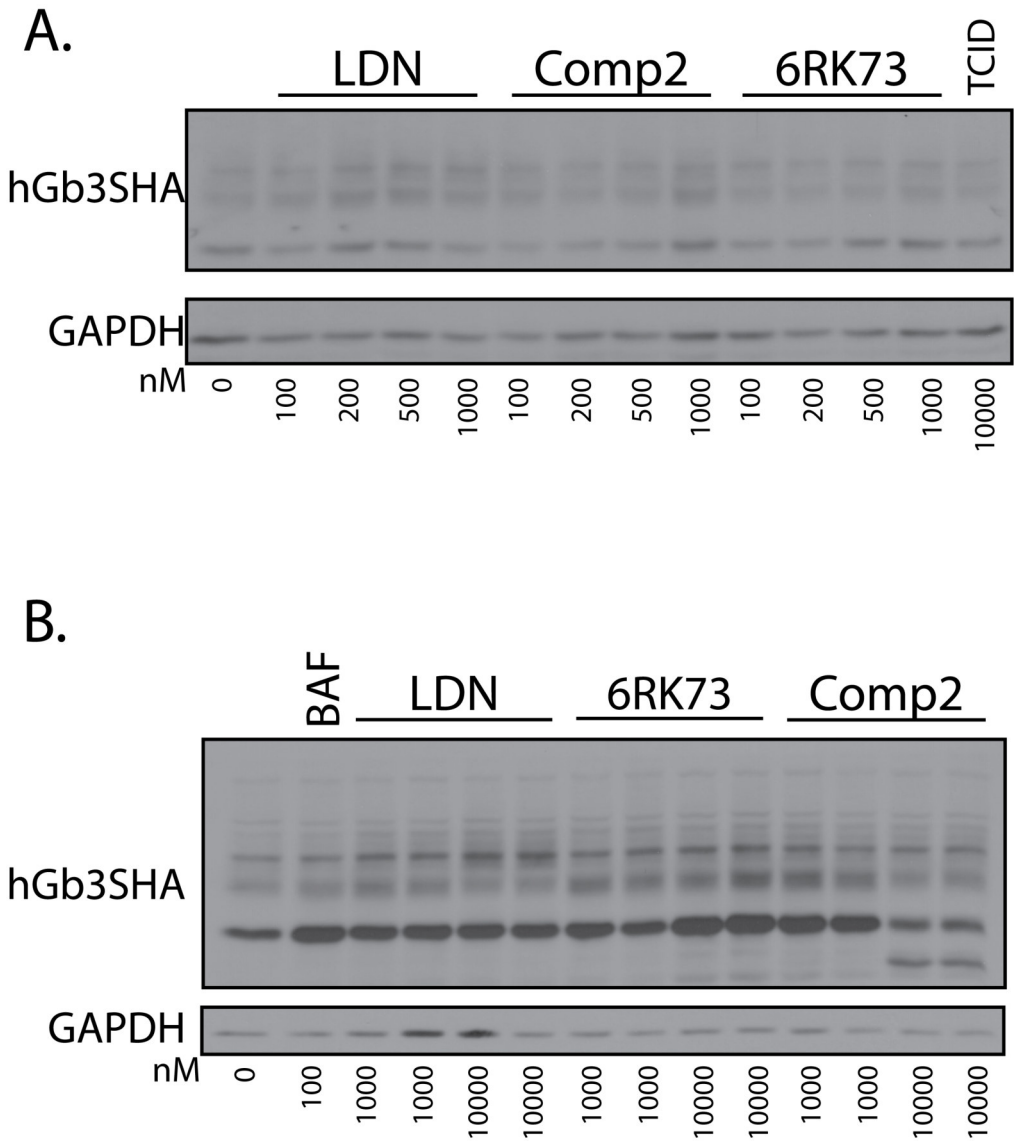

Figure 8.20: A. Representative western blot 'mini–screen' whereby Day 0 hGb3SHA Clone B4 is treated with 3 UCHL1 specific inhibitors LDN57444(LDN), Compound2(Comp2) and 6RK73 and, UCHL3 specific inhibitor(TCID) with increasing concentration of the UCHL1 inhibitors (100, 200, 500 and 1000 nM) and a static concentration of 10uM of TCID; B. hGb3SHA clone B4 Day 0 treated with BAF(100nM) and 3 UCHl1 specific inhibitors at 1uM and 10uM. All treatments for 8hrs.

8. Probing the molecular basis of the Regulation

The final experiment was originally planned for a western blot and IF on differentiated cells using 1uM concentration for all 3 drugs but during the differentiation it was quite evident that the conditions were not optimal as by day 6-7 the culture dishes were already completely confluent which meant an unreliable neuronal differentiation for sure but also an increase in other uncharacterized cell types in the population(Wongpaiboonwattana and Stavridis 2015). From personal experience and based on anecdotal evidences mentioned later, this meant the population can increase in cell types that may naturally retain the enzyme and because the phenotype that we had come to rely upon was so critically linked with the cell state that over the time I had made a rule of prematurely aborting such sub-optimal differentiations so as not to dilute the results. The time constraints were such that a new differentiation experiment would be not be feasible and, my own personal disenchantment with the experiment at this point would be the final nail as i accidentally used the wrong concentrations of LDN(10uM instead of 1uM) and 6RK73 treated 'Day 13' sample was completely lost. I leave the final experiment in its entirety for the reader's consideration. The experiment showed that 2 out of the 3 UCHL1 inhibitors showed a substantial rescue of the protein at day 13, LDN and Compound2, while 6RK only rescued the protein at stem cell stage. Both the inhibitors showed a tendency to rescue significantly more in 'day 13' samples but the evident problem with the experiment is that the phenotypical decrease of hGb3SHA is not observed(Figure-8.21). We thus concluded that UCHL1 almost definitely plays a role in hGb3SHA increased lysosomal degradation at Day 13 but it is not yet clear if it directly modifies the protein itself or it switches the function of some sorting machinery.

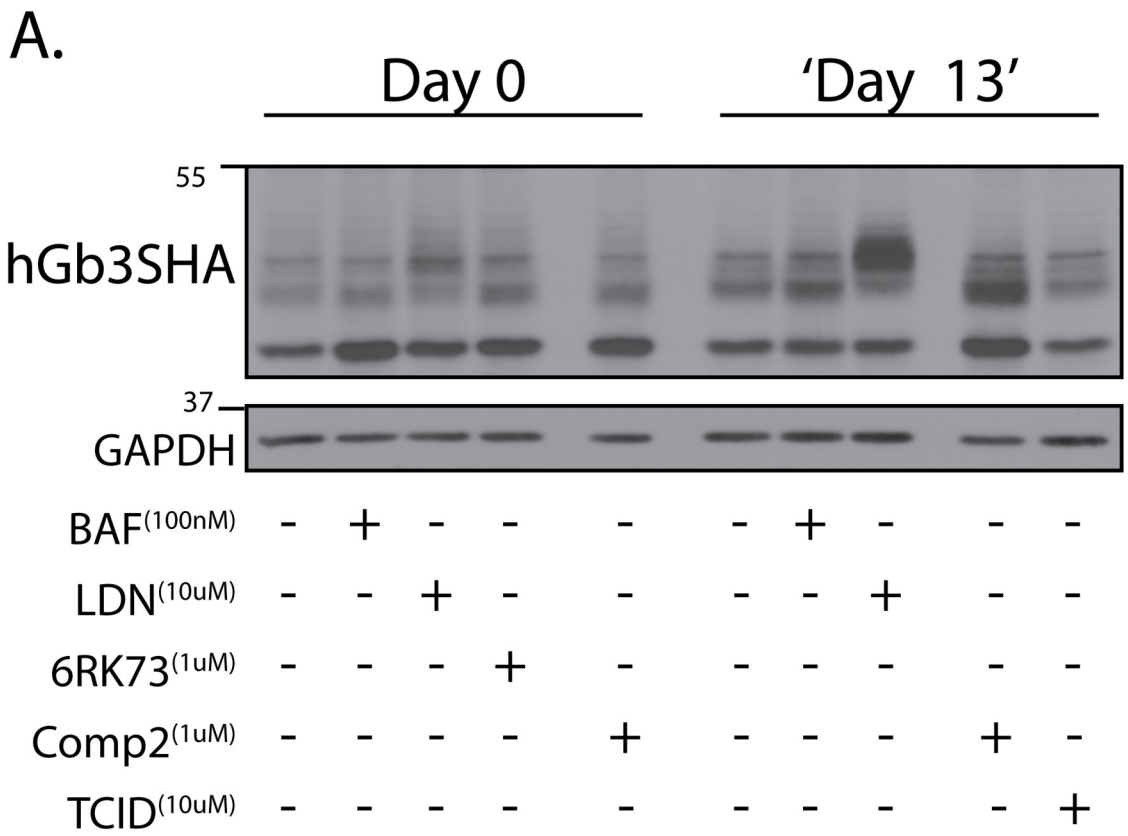

Figure 8.21: A. Western blot image of treatment at Day 0 and Day 13 on hGb3SHA clone B4 with all 3 UCHL1 inhibitors at Day 0 and only LDN57444 (LDN) and Compound2 (Comp2) at 'Day 13'. **Note–Technical problems with the experiment i.e. not a canonical Day 13 differentiation as mentioned in text.**

9

Anecdotal evidences:

The predictable nature of the machinery was truly tested when during a routine lab meeting my long time colleague, Laura Capolupo, told us about her latest exciting finding of an FGFR-DN fibroblastic cell line being completely devoid of globosides, as revealed by FACS analysis(under review(Capolupo et al. 2021)). The experiment that Laura was conducting had her looking at transformations in human fibroblast and 2 cell lines established from these cells, a TGFBR2DN (TGF(DN)) and an FGFR1DN (FGF(DN))(Bordignon et al. 2019). She was gracious enough to provide me with a pristine immunoblot to look for UCHL1 expression in an experiment where she had used a general GSL synthesis inhibitor Fumonisin B1 (FB1) on all 3 cell types. For this project, the experiment conclusively placed UCHL1 directly under the regulation of the TGFR-FGFR duelist pathway as well as confirming that its expression is affected by the lipids as it was observed that UCHL1 expression was significantly increased in FGF(DN) cell line and significantly decreased in TGF (DN) cell line. The expression is further impacted upon by the loss of GSLs upon treatment with FB1.

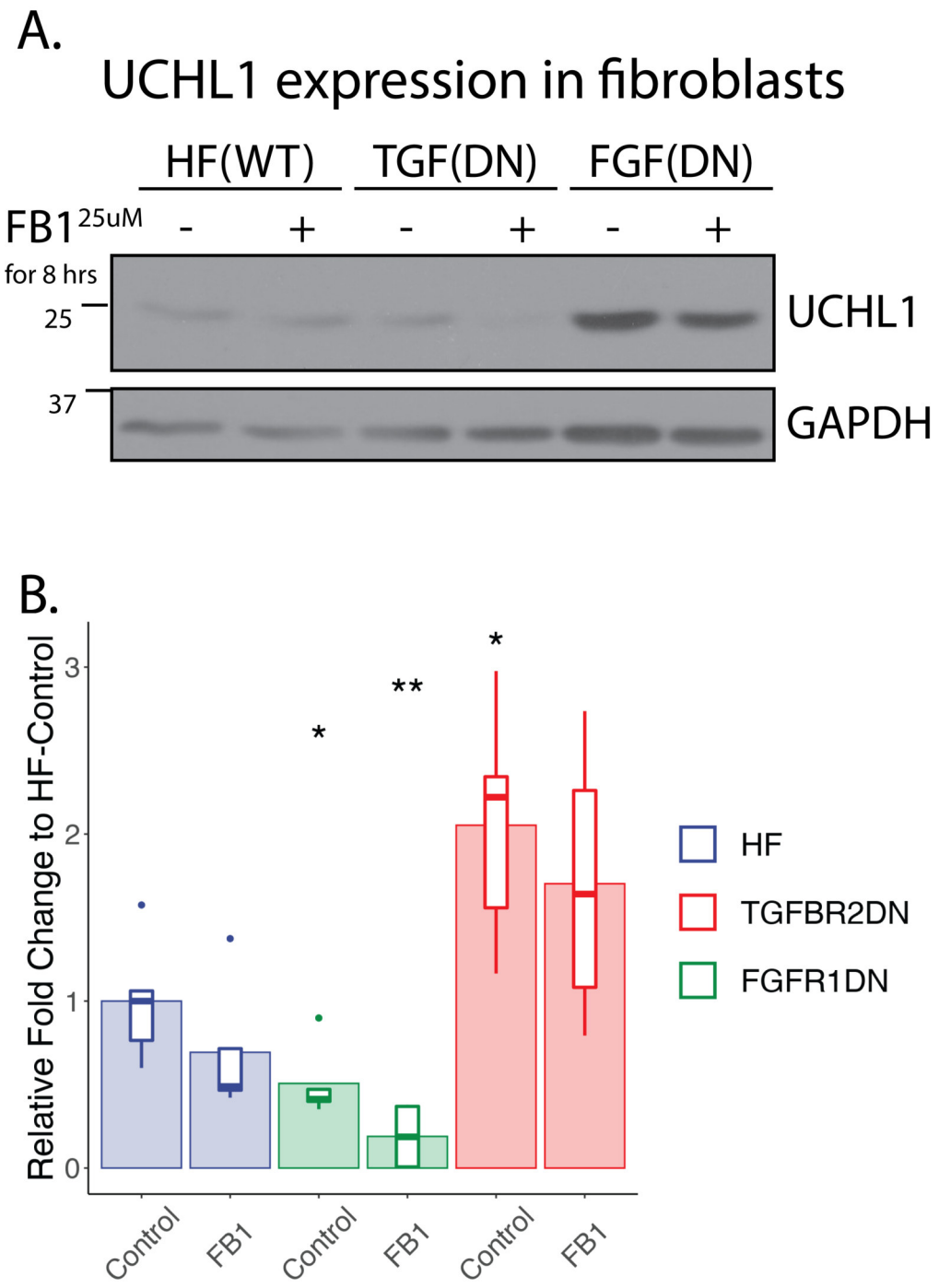

Figure 9.1: A. Representative western blot image of UCHL1 expression in Human Fibroblast (HF(WT)) and TGFBR2 dominant negative (TGF(DN)) and FGFR1 dominant negative (FGF(DN)) cell lines treated with GSL synthesis inhibitor (FB1) for 8hrs. B. Quantification shows a significant effect of TGF-FGF duelist pathway of UCHL1 expression. FGF(DN) cell line was devoid of Globosides. Data are shown as the mean ± SD of 3 individual experiments; *p < 0.05

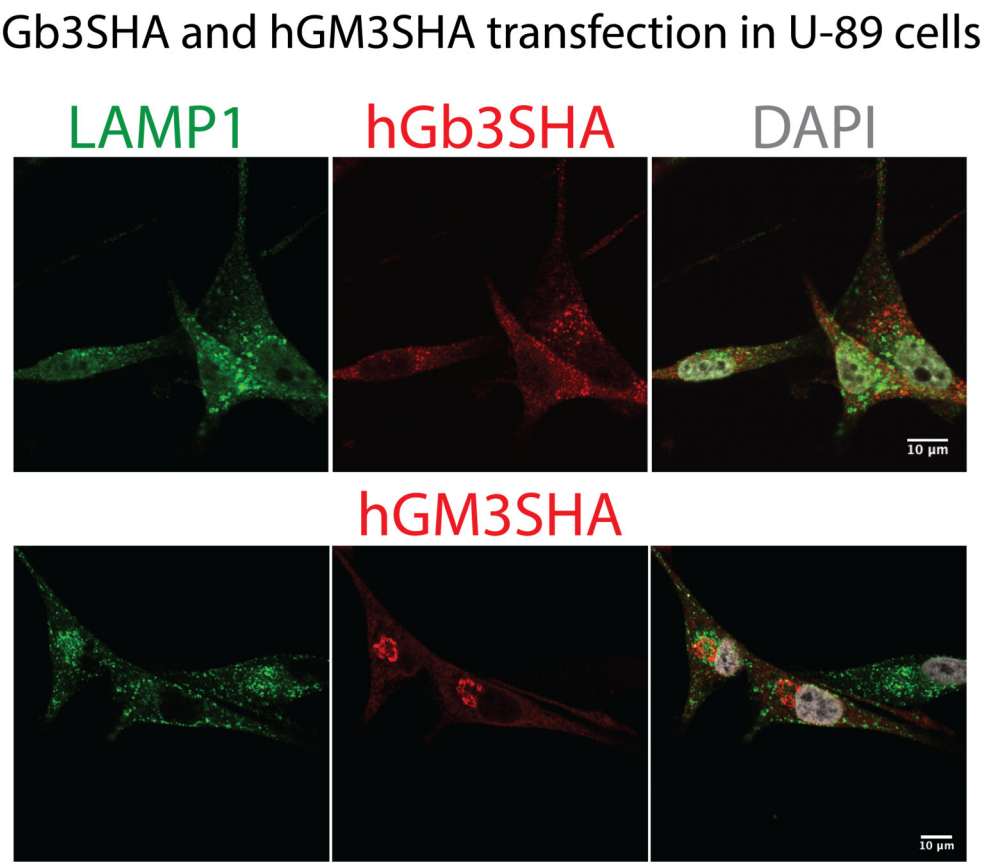

Figure 9.2: Representative Confocal images of hGb3SHA and hGM3SHA transfection in endogenously UCHL1 expressing neuroglioblastoma cell lines(U-89)

A final piece of anecdotal evidence worth mentioning is the localization of transfected hGb3SHA and hGM3SHA in a neuroglioblastoma cell line called U-89. While trying to look for a less demanding experimental system for our regulation, I looked into cell lines that endogenously overexpress UCHL1. We were lucky to find this cell line in EPFL itself and just a preliminary steady state transfection of hGb3SHA and hGM3SHA revealed that this cell line was readily hGb3SHA staining was completely punctated whereas hGM3SHA was strictly in the golgi.

10 Discussion

Our understanding of GSLs has been continually evolving towards a much more active role of the lipids, especially in cell- fate determination. This has driven the development of technology to study them better or vice-versa. GSEs, on the other hand, are notorious for the incessant lack of antibodies against them and this has led to a large gap in their understanding. Moreover, most evidence of their regulation is also largely based upon indirect evaluation of their products [Yu et al. (2016). Our strategy of trying to force stem cells to overproduce Gb3 at the 'wrong' time unknowingly positioned us in a very unique situation to witness a massive transformation event from the point of view of a GSE for the first time. The actual transformation event i.e. stem cell to neurons also made it more special as it is a physiological example of a drastic remodeling of the GSL profile and one that we had the most understanding about in terms of lipid and GSE expression, or so we thought. Studies on stem cells focusing on lipid changes(Liang et al. 2010) had attributed this remodeling to the transcriptional switch observed in the mRNA expression level of the core GSE i.e. Gb3S gets downregulated by ~50% whereas GM3S expression is increased >10 fold but, our study conclusively points towards an extra layer of post-translational regulation that degrades Gb3S on one hand while stabilizing GM3S on the other. Besides the fact that it would

explain the discrepancy between the mRNA expression and the almost complete loss of Gb3 upon differentiation, on first glance, this extra layer of regulation would seem redundant until we look into the actual nature of GSL synthesis regulation. According to current understanding, GSL synthesis is dependent upon the correct compartmentalization of precursors and corresponding GSE in the Golgi(Pothukuchi et al. 2020; Rizzo et al. 2021). This is ensured by a series of membrane trafficking events, both anterograde and retrograde(Huang and Wang 2017), and 'adaptors' which provide the specificity to these events. In our attempt to force the system we seem to have stumbled upon a similar membrane trafficking event that almost exactly doubles the rate of degradation of Gb3S in 'neuronal' cells but whether it is through an inability of Ggolgi retention or an active translocation to the lysosome is not really clear though anecdotal data suggests the latter. The data also shows that this event is one of earliest events in development thereby pointing towards a causative nature of the phenotype or at least it puts Gb3S in the same category of precisely regulated canonical stem markers as Notch, REST and SOXB1, each of which also show a dual nature of regulation whereby their mRNA expression downregulation is complemented with Post-Translationa modifications and, in fact, the Notch signalling downregulation is directly dependant wpon the targeted degradation of and effector protein called Hes1 (Saritas-Yildirim and Silva 2014). This elevates the position of Gb3S in the Waddington Landscape ideology such that Gb3S would assume a similar position as any other remodeling gene through its potential to regulate major signaling pathways at the plasma membrane. The emergence of ESCRT pathway as a potential candidate seemed inevitable retrospectively although the potential bias of Vps4a (as inferred by Vps4a DN GFP plasmid) towards Gb3S and the prospect of the 3 independent forms of Gb3S present naturally are both very intriguing results but, the most remarkable finding from the study would have to be the definite role of UCHL1 in specific degradation of Gb3S.

UCHL1 seems to be a highly studied protein with little details. A direct quote from uniprot which states," Ubiquitin-protein hydrolase involved both in the processing of ubiquitin precursors and of ubiquitinated proteins (Probable)" (along

with several cautions ,3 when last checked), perfectly defines my time researching UCHL1. Despite the obvious dubious nature of its enzymatic activity, its role in protein degradation machinery cannot be discredited and it has long been a potential pharmaceutical target due to its role in tumour progression (Liu, Fallon, et al. n.d.). Most notably UCHL1 has been convincingly linked with a-synucleopathies like familial Parkinsons Disease (PD) when an autosomal dominant point mutation (I93M) was first identified in two siblings with a strong family history of PD, but later studies show it is not through inhibition of its hydrolase activity as previously thought (Liu, Fallon, et al. n.d.). This is an important point of convergence for both enzymes as recent evidences also positively links a-Gal A defect to increased accumulation of a-synuclein(Nelson et al. 2018) and a-Gal A defects directly results in accumulation of Gb3 which is a hallmark of a rare X-linked lysosomal storage disorder called Fabry Disease (Hannun et al. 2015). Fabry disease itself shares many clinical symptoms with PD and patients of Fabry have been known to be diagnosed with extrapyramidal symptoms of Parkinsonism but a "no classic less severe" form of Fabry disease(Arends et al. (2017)) does not occur through a defect in a-Gal A. Our study would suggest that the mystery of UCHL1 mediated a-syn nucleopathy revolves around its association with Gb3S and may also explain the type II Fabry Disease whereby an accumulation of Gb3 is not directly due to a defect in a-Gal A but rather due to a defect in UCHL1 activity. A hypothetical scenario would be if increased Gb3 production would result in an incremental increase in lysosomal accumulation of Gb3 over a long period as the steady state amount of a-Gal A is not able to cope up, which also sits nicely with the late-onset of the disease. The most prospective element of the study is its potential specific druggability and the very least it demands is a reinvestigation into the effects of UCHL1 and other lipid storage disorders through the perspective of GSEs.

The increase in GM3S is much harder to comment upon as the true nature of its increase still evades us. It is still not clear if it is a true increase in the stability of the protein or if the protein is being lost at the stem cell stage as blocking protein degradation did not reveal any major difference in degradation

rate but it did reveal that at least there is no translational block. It would also seem that post-differentiation, GM3S is exported more efficiently from the ER and some of the increase could be attributed to the decrease in the high-mannose band (E-band) of the enzyme. It almost looks like even though we electroporated the M3 isoform, it shows an M2 phenotype at stem cell stage and then switches back to an M3 phenotype over differentiation. As our understanding of the transcript variants for GM3S is continually growing with efforts from Inokuchi et. al, and others, this study points to a possible mechanism that may exploit some of this variation. A very naive hypothetical may also be that the GM3S is somehow being secreted at the stem cell stage and the increase is not a true increase but these would be confirmed in future studies.

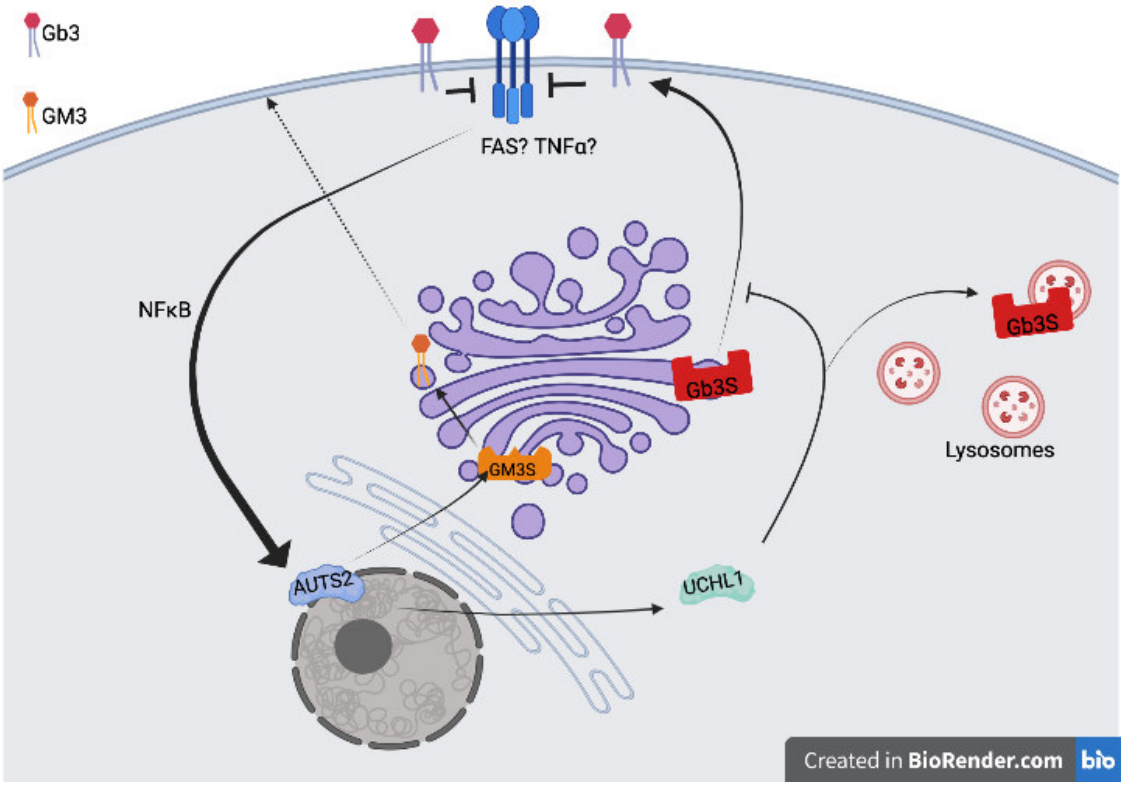

Figure 10.1: Final Model. Gb3 inhibits the expression of AUTS2 via NFKB signalling pathway. AUTS2, in turn, starts the expression of GM3S and UCHL1. Finally, UCHL1 directs Gb3S from the Golgi to the lysosomes thereby feeding back into the loss of Gb3S.

10.0.1 Final Comment:

It would seem that the initial circuit that Domenico Russo discovered may be truly deterministic event for a particular cell as the loss of Gb3 negatively feeds back onto itself. Loss of Gb3 leads to the activation of the NFKB, most probably via the FasR, which tranlates into AUTS2 expression, among other things. AUTS2 further induces the expression of GM3S, on one hand, and UCHL1 on the other thereby ensuring a swift change of GSL profile. It would be interesting to see if AUTS2 also induces a 3 factor that may be responsible for the 50% decrease in mRNA which would truly seat AUTS2 as the master regulator of this switch. The full regulatory machinery, in my opinion, would be a key driving factor of cellular transformation like EMT/MET with the glycosphingolipids themselves fueling its perpetuation and even amplification. UCHL1 adds another dimension to the GSL circuit such that reports suggesting unconventional secretion of UCHL1 via neurons (Öhrfelt et al.

2016) and, more recently, UCHL1 dependant exosome cargo selection mediated by ESCRT (Kobayashi et al. 2018) cements the idea that UCHL1 is critically linked with membrane trafficking and may exert its effect via GSL.

Materials and Methods

Contents

10.1 Cell Lines and Maintenance and 2d-Differentiation:

HeLa cells were obtained from the American Tissue Type Collection (ATTC,USA); E14 mESCs were provided by the laboratory of Maurizio D'Esposito, (IGBCNR, Naples, Italy). HeLa cells were grown in Dulbecco's modified Eagle's medium (Gibco) supplemented with 4.5 g/L glucose, 2 mM L-glutamine, 100U/mL penicillin and streptomycin, and 10% (v/v) foetal calf serum (FCS). mESCs were cultured feeder-free either in gelatin-coated culture vessels or on poly-Dlysine/ laminin-coated glass slides. Standard gelatin coating was performed using a filter sterilised 0.1% (w/v) gelatin solution (Sigma-Aldrich, Germany) in sterile phosphate-buffered saline (PBS) for at least 30 min at room temperature. Glass slides were coated by incubation with 0.01 mg/mL poly-D-lysine (Sigma-Aldrich, USA) for 30 min at 37 °C, followed by two brief washes in PBS. Subsequently, the slides were incubated for 16 h in 2 µg/mL laminin (Sigma-Aldrich, Germany) in PBS at room temperature. Undifferentiated

stem cells were maintained in expansion medium consisting of Glasgow minimal essential medium (SigmaAldrich, Germany) supplemented with 2 mM glutamine (Life Technologies Germany), 1 mM sodium pyruvate (Life Technologies, Germany), 100 µM nonessential amino acids (Life Technologies, Germany), 10% (v/v) FBS (Euroclone, Italy), 0.05 mM 2-mercaptoethanol (Sigma-Aldrich, USA), 100 U/mL penicillin/streptomycin (Life Technologies, Germany), and 1,000 U/mL leukaemia inhibitory factor (LIF; Millipore, USA). The expansion medium was replaced every 24 h, and the cells were split every second day. For neural differentiation according to (Fico et al., 2008), 103 cells/cm2 were seeded on either gelatin or poly-D-lysine/ laminin-coated glass slides (see above) and maintained for 24 h in expansion medium. Differentiation was induced by LIF deprivation in LIF-free knock-out Dulbecco's minimal essential medium (Life Technologies, USA) supplemented with 15% knock-out serum replacement (Life Technologies, USA), 2 mM glutamine (Life Technologies, USA), 100 U/mL penicillin/streptomycin, and 0.1 mM 2-mercaptoethanol (Sigma-Aldrich, USA). During the differentiation, the medium was replaced every day, and the cells were fixed for immunostaining or processed for biochemical procedures on days 0 and 13, or processed for RNA extraction on days 0, 8, and 13 (day 0, undifferentiated cells before LIF deprivation). All of the cells were maintained in a humidified incubator in 5% CO2 and 95% air at 37 °C.

10.2 Differentiation of mESCs in the Neuroepithelial Cyst Model

A total of 50,000 single ESCs resuspended in 10 ml N2B27 were embedded in 150 ml Matrigel and distributed equally over five 3.5 cm2 glass bottom dishes (MatTek). After gelling at 37°C for 15 min, the embedded cells were cultured in N2B27. In separate experiments, laminin/entactin gels (Corning), diluted with chilled N2B27 to 10 mg/ml, or PEG gels (see below) were used instead of Matrigel. The laminin/entactin matrix was allowed to gel for 30 min at 37_0_C. For posteriorization, 250 nM all-trans RA (Sigma) was added to the differentiation mediumon day 2 for 18 hr. For ventralization to FP, 1 mM smoothened agonist

SAG (Calbiochem) was added on day 3 for 24 hr. To inhibit FP formation, 1 mMor5 mMcyclopamine (Tocris) was added on day 2 for 18, 72, or 120 hr to the culture medium. The medium was replaced with fresh cyclopamine after the RA pulse (day 3) and on day 5 of cyst growth. **Our clonal cell lines were first adapted to their media for a couple of generations before cyst generation**

10.3 Immunofluorescence

HeLa or mESC cells were grown on 24-mm coverslips. At the time of observation, the cells were washed with PBS, fixed in 4% paraformaldehyde for 10 min, and quenched with 50 mM NH4Cl in PBS. The cells were permeabilised for 10 min with 0.3% Triton X-100 in PBS and blocked in PBS containing 5% FCS and 0.05% Triton X-100 for 1 h. The cells were then incubated with primary antibodies for 1 h at room temperature and washed three times with 0.1% Triton X-100 in PBS. The appropriate isotype-matched, AlexaFluor-conjugated secondary antibodies (Invitrogen, USA) were used, and coverslips were mounted with Mowiol (Calbiochem, Germany).

10.4 Stable cell line generation:

mESCs were electroporated using the LONZA 4-D Nucleofector system. Electroporation was done according to manufacturers instruction for the P3 Primary Cell Kit with a predefined. protocol code CG-104. Electroporated cells were plated back on Gelatinized culture dishes and let to grow for 24 hrs. Puromycin selection media is added according to previous mortality curve of WT cell (1.5ug/ml for 72 hrs results in 100% mortality). 72hrs later, individual colonies were plated on gelatinized 96-well plates and explanded.

10.5 RNA extraction and real-time PCR

Total RNA was isolated from HeLa cells and mESCs using RNeasy Mini kits (Qiagen, Germany) according to the manufacturer instructions. The yield and

the integrity of the RNA were determined using a spectrophotometer (NanoDrop 2000c; Thermo Scientific, USA), by TAE agarose gel electrophoresis, and with an Agilent 2100 Bioanalyser (Agilent Technologies, USA). RNA (1 µg) was reverse transcribed using QuantiTect Reverse Transcription kits (Qiagen, Germany) according to the manufacturer instructions and subjected to real-time qPCR with gene-specific primers (Appendix Table S4) in the presence of LightCycler® 480 SYBR Green I Master Mix (Roche, Switzerland) on a LightCycler® 480 II detection system (Roche, Switzerland). Relative abundance of mRNA was calculated by normalization to GAPDH.

10.6 SDS-PAGE and western blotting

10.6.1 SDS-PAGE

Two 16 x 18 cm plates were used for assembling standard gels. The plates were assembled to form a chamber using two 1.5 mm plastic spacers aligned along the lateral edges of the plates. The plates were then fixed using two clamps and mounted on a plastic base, which sealed thebottom. All of the materials were from Hoefer Scientific Instruments. The running gel was prepared by mixing H2O, 30% (w/v) acrylamide-bisacrylamide solution, 1.5M Tris-HCl (pH 8.8), 10% (w/v) SDS, 10% ammonium persulfate (APS) and N,N,N',N'-tetramethylethylene diamine(TEMED) in different amount according to gel percentage. Soon after pouring, the gel wascovered with a layer of water and left at RT for about 1 h. The water layer was removed. The stacking gel was prepared by mixing H2O, 30% (w/v) acrylamide-bisacrylamide solution, 0.5M Tris-HCl (pH 6.8), 10% (w/v) SDS, 10% (w/v) APS and TEMED, and the solution was pipetted and poured onto the running gel. Immediately, a 15-well comb was inserted between the glass plates and it was left 1 hour at RT. For sample preparation, after treatment, the cells were washed three times with PBS and lysed in RIPA buffer (150 mM NaCl, 1% Triton X-100, 0.5% sodium deoxycholate, 0.1% SDS, 25 mM Tris-HCl, pH 7.4), supplemented with protease cocktail inhibitor. The lysates were clarified by centrifugation, and

quantified using a commercially available BCA kit (Pierce™ BCA Protein Assay Kit, ThermoFisher) according to the manufacturer instructions. Samples were prepared by adding an equal volume of 2x SDS sample buffer, incubating at 95°C for 5 min, briefly centrifuging and then loading onto the gel. The gel was then transferred into the electrophoresis apparatus and the electrophoresis was carried out under a constant current of 7 mA overnight

10.6.2 Western blotting

The polyacrylamide gel was soaked for 15 min in transfer buffer, placed on a sheet of 3MM paper (Whatman, NJ, USA) and covered with a nitrocellulose filter. The filter was covered with a second sheet of 3MM paper, to form a "sandwich" which was subsequently assembled into the blotting apparatus. Protein transfer occurred at 400 mA for 4 hours. At the end of the run, the sandwich was disassembled and the nitrocellulose filter was soaked in 0.2% Ponceau red and 5% (v/v) acetic acid, to visualize the protein bands, and then rinsed. The strips containing the proteins of interest were blocked in TBS-T/5% BSA for 45 min at RT, and then with the primary antibody diluted at its working concentration in the blocking solution buffer overnight at 4 °C. After Washing with TBS-T, the strips were next incubated for 1 h with the appropriate HRP-conjugated secondary antibody, diluted in antibody dilution buffer and washed twice in TTBS, for 10 min each. After washing, the strips were incubated with the ECL solution for 3 minutes and exposed to x-ray films, which were then scanned. The intensity of the bands and preparation of images was done using ImageJ and Adobe Illustrator 2020.

10.6.3 Transfections:

HeLa cells were plated at 50% confluence in 24-well, 12-well or 6-well plates and transfected, for 24 h with 0.3 ug/well to 2 ug/well of plasmid, with LTX-Lipofectamine (Invitrogen, USA), according to manufacturer instructions.

10.7 Statistical Analysis:

All statistical analyses was done in R using rstatix pacakge and ggplot.

Real-Time primers	...2	...3	...4
Human	Forward	Reverse	NA
gb3s	GATCCCCACCTCTCTGCAAT	TTGGACATGGTATCCCCAGA	NA
p65	ATGTGGAGATCATTGAGCAGC	CCTGGTCCTGTGTAGCCATT	NA
ikba	GCCATTGTAGTTGGTAGCCTTCA	GCCATTGTAGTTGGTAGCCTTCA	NA
auts2	TGGCGTTTCTCCACACGTTC	TGGCGTTTCTCCACACGTTC	NA
gm3s	TGGTTATTGGAAGCGGAGG	TCTGAATATCCCTCAACTGGT	NA
gapdh	GGCTGTTGTCATACTTCTCATGG	GGCTGTTGTCATACTTCTCATGG	NA
Mouse	Forward	Reverse	NA
gb3s	TCCTCAAGAACCTGCTCAAC	CACAGTGCCAAGAACTCATG	NA
auts2	GCCATGACCAGCTTTGTTAC	TCTGTCGTTTCTCCGCAC	NA
gm3s	TCAGAGCCTCAGTCAAGATTC	GATGTGTAGCCAAGACAACG	NA
tuj1	ATCAGCAAGGTGCGTGAGGAG	ATGGACAGGGTGGCGTTGTAG	NA
auts2	TTCGGCTGAGGTGGACTCT	TTCGGCTGAGGTGGACTCT	NA
nurr1	GAGGGTCTGTGCGCTGTTTG	TGTCCGTGCGAACCACTTCT	NA
gm2s	TGGATAAACTCAACCGGCAG	GTGTCTTACGAGGATGGTGAAG	NA
gm1s	CTGTGTCAAATTGGCTGGTG	CAGTCCTCTCCCCATTCATG	NA
gapdh	AGGTCGGTGTGAACGGATTTG	GGGGTCGTTGATGGCAACA	Nested
PCR primers	Forward	Reverse	AGTGGTGTTCCATCCGCAG
Gb3S	GGAATTCatgtccaagccCCCCG	CGAATTCGTCACCGGTTAATTAACCGG	GATCTCAGTGGAGGCATTGATCGTG
GM3S	GGAATTCatgagaaggcccagcttgt	CGAATTCTTAACCGGTGGCGTAGTCTG	NA
drugs	company	NA	NA
BMS-345541	Tocris Cat. No. 4806	NA	NA
BAF	sigma 88899-55-2	NA	NA
ALLN	sigma 208719	NA	NA
LDN	sigma L4170	NA	NA
6RK	medchempress HY-133118	NA	NA
TCID	calbiochem CAS 30675-13-9	NA	NA
Comp2	donated by Edward Tate	NA	NA
FB1	simga F1147	NA	NA
PnGase	simgma EMS0001	NA	NA
anitbody	company	NA	NA
GAPDH	Abcam ab9485	NA	NA
auts2	Sigma HPA00039	NA	NA
p65	Santa Cruz Biotechnology catalog: sc-8008	NA	NA
IkBA	Santa Cruz Biotechnology catalog: sc-8404	NA	NA
HA	BioLegend catalog: 803101	NA	NA
golph3	Abcam catalog: ab98023	NA	NA
tuj1	Covance MMS-435P	NA	NA
oct3/4	rndsystems MAB1759	NA	NA
nanog	Millipore SC1000	NA	NA
phalloidin	Thermo: : A22287	NA	NA
LAMP1	BioLegend catalog: 328608	NA	NA
TGN46	Invitrogen catalog: MA3-063	NA	NA
antiFLAG	sigma f1804	NA	NA
FAIM2	Abcamcatalog: ab64187	NA	NA
V5	Thermo Fisher R96025	NA	NA
Giantin	BioLegend catalog: 924302	NA	NA
HUMAN	siRNA	NA	NA
Gb3S	AGAAAGGGCAGCUCUAUAAUU	NA	NA
Gb3S	GGACACGGACUUCAUUGUUUU	NA	NA
Gb3S	UGAAAGGGCUUCCGGGUGGUU	NA	NA
Gb3S	GCACUCAUGUGGAAGUUCGUU	NA	NA
p65	CAUCAGAGCUGCGGAUUUG	NA	NA
p65	GCAGAAAGAGGACAUAUCA	NA	NA
p65	GCCCGUCUAUGACAAGAAA	NA	NA
p65	GCACAGAUGAAUUGGAGAU	NA	NA

10.7.1 Appendix

Works Cited

Abrami, Laurence et al. (Nov. 2013). "Hijacking Multivesicular Bodies Enables Long-Term and Exosome-Mediated Long-Distance Action of Anthrax Toxin". In: *Cell Reports* 5.4, pp. 986–996. DOI: 10.1016/j.celrep.2013.10.019. URL: https://linkinghub.elsevier.com/retrieve/pii/S2211124713006037 (visited on 06/07/2021).

Allende, Maria Laura and Richard L. Proia (Dec. 2014). "Simplifying complexity: genetically resculpting glycosphingolipid synthesis pathways in mice to reveal function". In: *Glycoconj J* 31.9, pp. 613–622. DOI: 10.1007/s10719-014-9563-5. URL: http://link.springer.com/10.1007/s10719-014-9563-5 (visited on 06/07/2021).

Arends, Maarten et al. (May 2017). "Characterization of Classical and Nonclassical Fabry Disease: A Multicenter Study". In: *J Am Soc Nephrol* 28.5. Edition: 2016/12/15 Publisher: American Society of Nephrology, pp. 1631–1641. DOI: 10.1681/ASN.2016090964. PMID: 27979989. URL: https://pubmed.ncbi.nlm.nih.gov/27979989.

Banfield, D. K. (Aug. 1, 2011). "Mechanisms of Protein Retention in the Golgi". In: *Cold Spring Harbor Perspectives in Biology* 3.8, a005264–a005264. DOI: 10.1101/cshperspect.a005264. URL: http://cshperspectives.cshlp.org/lookup/doi/10.1101/cshperspect.a005264 (visited on 06/07/2021).

Bayón, Yolanda et al. (2008). "KCTD5, a putative substrate adaptor for cullin3 ubiquitin ligases". In: *FEBS Journal* 275.15, pp. 3900–3910. DOI: 10.1111/j.1742-4658.2008.06537.x.

Bishop, Paul, Dan Rocca, and Jeremy.M. Henley (Aug. 15, 2016). "Ubiquitin C-terminal hydrolase L1 (UCH-L1): structure, distribution and roles in brain function and dysfunction". In: *Biochemical Journal* 473.16, pp. 2453–2462. DOI: 10.1042/BCJ20160082. URL: https://portlandpress.com/biochemj/article/473/16/2453/49243/Ubiquitin-Cterminal-hydrolase-L1-UCHL1-structure (visited on 06/07/2021).

Bordignon, Pino et al. (Aug. 2019). "Dualism of FGF and TGF-B Signaling in Heterogeneous Cancer-Associated Fibroblast Activation with ETV1 as a Critical Determinant". In: *Cell Reports* 28.9, 2358–2372.e6. DOI: 10.1016/j.celrep.2019.07.092. URL: https://linkinghub.elsevier.com/retrieve/pii/S2211124719310083 (visited on 06/07/2021).

Burke, James R. et al. (2003). "BMS-345541 is a highly selective inhibitor of IκB kinase that binds at an allosteric site of the enzyme and blocks NF-κB-dependent transcription in mice". In: *Journal of Biological Chemistry* 278.3, pp. 1450–1456. DOI: 10.1074/jbc.M209677200. URL: http://dx.doi.org/10.1074/jbc.M209677200.

Capolupo, Laura et al. (Feb. 23, 2021). *Sphingolipid Control of Fibroblast Heterogeneity Revealed by Single-Cell Lipidomics*. preprint. Biochemistry. DOI: 10.1101/2021.02.23.432420. URL: http://biorxiv.org/lookup/doi/10.1101/2021.02.23.432420 (visited on 06/07/2021).

Cartier, Anna E. et al. (Apr. 13, 2012). "Differential Effects of UCHL1 Modulation on Alpha-Synuclein in PD-Like Models of Alpha-Synucleinopathy". In: *PLoS ONE* 7.4. Ed. by Philipp J. Kahle, e34713. DOI: 10.1371/journal.pone.0034713. URL: https://dx.plos.org/10.1371/journal.pone.0034713 (visited on 06/07/2021).

Chakrabandhu, K et al. (2008). "The extracellular glycosphingolipid-binding motif of Fas defines its internalization route, mode and outcome of signals upon activation by ligand." In: *Cell death and differentiation* 15.12, pp. 1824–37. DOI: 10.1038/cdd.2008.115. URL: http://www.ncbi.nlm.nih.gov/pubmed/18670435.

Cheung, T. C. and C. F. Ware (2013). *Tumor Necrosis Factor Receptors*. 2nd ed. Vol. 4. Elsevier Inc., pp. 454–459. DOI: 10.1016/B978-0-12-378630-2.00358-3. URL: http://dx.doi.org/10.1016/B978-0-12-378630-2.00358-3.

D'Angelo, Giovanni et al. (Dec. 2013). "Glycosphingolipids: synthesis and functions". In: *FEBS J* 280.24, pp. 6338–6353. DOI: 10.1111/febs.12559. URL: http://doi.wiley.com/10.1111/febs.12559 (visited on 06/07/2021).

Fisher, Peter et al. (Apr. 2019). "Modeling Glycan Processing Reveals Golgi-Enzyme Homeostasis upon Trafficking Defects and Cellular Differentiation". In: *Cell Reports* 27.4, 1231–1243.e6. DOI: 10.1016/j.celrep.2019.03.107. URL: https://linkinghub.elsevier.com/retrieve/pii/S2211124719304541 (visited on 06/07/2021).

Han, Han and Christopher P. Hill (Feb. 28, 2019). "Structure and mechanism of the ESCRT pathway AAA+ ATPase Vps4". In: *Biochemical Society Transactions* 47.1, pp. 37–45. DOI: 10.1042/BST20180260. URL: https://portlandpress.com/biochemsoctrans/article/47/1/37/131/Structure-and-mechanism-of-the-ESCRT-pathway-AAA (visited on 06/07/2021).

Hannun, Yusuf A. et al., eds. (2015). *Bioactive Sphingolipids in Cancer Biology and Therapy*. Cham: Springer International Publishing. DOI: 10.1007/978-3-319-20750-6. URL: http://link.springer.com/10.1007/978-3-319-20750-6 (visited on 06/07/2021).

Hicke, Linda (Mar. 2001). "Protein regulation by monoubiquitin". In: *Nat Rev Mol Cell Biol* 2.3, pp. 195–201. DOI: 10.1038/35056583. URL: http://www.nature.com/articles/35056583 (visited on 06/07/2021).

Huang, Shijiao and Yanzhuang Wang (Nov. 27, 2017). "Golgi structure formation, function, and post-translational modifications in mammalian cells". In: *F1000Res* 6, p. 2050. DOI: 10.12688/f1000research.11900.1. URL: https://f1000research.com/articles/6-2050/v1 (visited on 06/07/2021).

Inokuchi, Jin-ichi et al. (2018). "Biology of GM3 Ganglioside". In: *Progress in Molecular Biology and Translational Science*. Vol. 156. Elsevier, pp. 151–195. DOI: 10.1016/bs.pmbts.2017.10.004. URL: https://linkinghub.elsevier.com/retrieve/pii/S1877117317301412 (visited on 06/07/2021).

Kobayashi, E. et al. (Feb. 7, 2018). "C-Terminal Farnesylation of UCH-L1 Plays a Role in Transport of Epstein-Barr Virus Primary Oncoprotein LMP1 to Exosomes". In:

mSphere 3.1. Ed. by James M. Pipas, e00030–18. DOI: 10.1128/mSphere.00030-18. URL: https://msphere.asm.org/content/3/1/e00030-18 (visited on 06/07/2021).

Liang, Y.-J. et al. (Dec. 28, 2010). "Switching of the core structures of glycosphingolipids from globo- and lacto- to ganglio-series upon human embryonic stem cell differentiation". In: *Proceedings of the National Academy of Sciences* 107.52, pp. 22564–22569. DOI: 10.1073/pnas.1007290108. URL: http://www.pnas.org/cgi/doi/10.1073/pnas.1007290108 (visited on 06/07/2021).

Liu, Sijia, Román González-Prieto, et al. (Mar. 15, 2020). "Deubiquitinase Activity Profiling Identifies UCHL1 as a Candidate Oncoprotein That Promotes TGFB-Induced Breast Cancer Metastasis". In: *Clin Cancer Res* 26.6, pp. 1460–1473. DOI: 10.1158/1078-0432.CCR-19-1373. URL: http://clincancerres.aacrjournals.org/lookup/doi/10.1158/1078-0432.CCR-19-1373 (visited on 06/07/2021).

Liu, Yichin, Lara Fallon, et al. (n.d.). "The UCH-L1 Gene Encodes Two Opposing Enzymatic Activities that Affect ␣-Synuclein Degradation and Parkinson's Disease Susceptibility". In: (), p. 10.

Matuszczak, Ewa et al. (July 2020). "Ubiquitin carboxy-terminal hydrolase L1 – physiology and pathology". In: *Cell Biochem Funct* 38.5, pp. 533–540. DOI: 10.1002/cbf.3527. URL: https://onlinelibrary.wiley.com/doi/abs/10.1002/cbf.3527 (visited on 06/07/2021).

Meinhardt, Andrea et al. (Dec. 2014). "3D Reconstitution of the Patterned Neural Tube from Embryonic Stem Cells". In: *Stem Cell Reports* 3.6, pp. 987–999. DOI: 10.1016/j.stemcr.2014.09.020. URL: https://linkinghub.elsevier.com/retrieve/pii/S2213671114003051 (visited on 06/07/2021).

Merrill, Alfred H. (Oct. 12, 2011). "Sphingolipid and Glycosphingolipid Metabolic Pathways in the Era of Sphingolipidomics". In: *Chem. Rev.* 111.10, pp. 6387–6422. DOI: 10.1021/cr2002917. URL: https://pubs.acs.org/doi/10.1021/cr2002917 (visited on 06/07/2021).

Nelson, Michael P. et al. (Feb. 2018). "The lysosomal enzyme alpha-Galactosidase A is deficient in Parkinson's disease brain in association with the pathologic accumulation of alpha-synuclein". In: *Neurobiology of Disease* 110, pp. 68–81. DOI: 10.1016/j.nbd.2017.11.006. URL: https://linkinghub.elsevier.com/retrieve/pii/S0969996117302723 (visited on 06/07/2021).

Öhrfelt, Annika et al. (July 15, 2016). "Increased Cerebrospinal Fluid Levels of Ubiquitin Carboxyl-Terminal Hydrolase L1 in Patients with Alzheimer's Disease". In: *Dement Geriatr Cogn Disord Extra* 6.2, pp. 283–294. DOI: 10.1159/000447239. URL: https://www.karger.com/Article/FullText/447239 (visited on 06/07/2021).

Ouyang, Lianlian et al. (2020). "The deubiquitylase UCHL3 maintains cancer stem-like properties by stabilizing the aryl hydrocarbon receptor". In: *Signal Transduction and Targeted Therapy* 5.1. DOI: 10.1038/s41392-020-0181-3. URL: http://dx.doi.org/10.1038/s41392-020-0181-3.

Pacheco, Alline R. et al. (July 5, 2018). "CRISPR Screen Reveals that EHEC's T3SS and Shiga Toxin Rely on Shared Host Factors for Infection". In: *mBio* 9.3. Ed. by Eric J. Rubin. In collab. with Cammie Lesser and Laurie Comstock. DOI:

10.1128/mBio.01003-18. URL: https://journals.asm.org/doi/10.1128/mBio.01003-18 (visited on 06/07/2021).

Panyain, Nattawadee et al. (July 15, 2020). "Discovery of a Potent and Selective Covalent Inhibitor and Activity-Based Probe for the Deubiquitylating Enzyme UCHL1, with Antifibrotic Activity". In: *J. Am. Chem. Soc.* 142.28, pp. 12020–12026. DOI: 10.1021/jacs.0c04527. URL: https://pubs.acs.org/doi/10.1021/jacs.0c04527 (visited on 06/07/2021).

Pothukuchi, Prathyush et al. (May 3, 2020). *Regulated compartmentalization of enzymes in Golgi by GRASP55 controls cellular glycosphingolipid profile and function*. preprint. Cell Biology. DOI: 10.1101/2020.05.03.074682. URL: http://biorxiv.org/lookup/doi/10.1101/2020.05.03.074682 (visited on 06/07/2021).

Purich, Daniel L. (July 20, 2017). *The Inhibitor Index: A Desk Reference on Enzyme inhibitors, Receptor Antagonists, Drugs, Toxins, Poisons & Therapeutic Leads*. 1st ed. CRC Press. DOI: 10.1201/9781315184289. URL: https://www.taylorfrancis.com/books/9781351730686 (visited on 06/07/2021).

Rizzo, Riccardo et al. (Apr. 15, 2021). "Golgi maturation-dependent glycoenzyme recycling controls glycosphingolipid biosynthesis and cell growth via GOLPH3". In: *EMBO J* 40.8. DOI: 10.15252/embj.2020107238. URL: https://onlinelibrary.wiley.com/doi/10.15252/embj.2020107238 (visited on 06/07/2021).

Russo, Domenico, Laura Capolupo, et al. (Dec. 15, 2018). "Glycosphingolipid metabolism in cell fate specification". In: *Journal of Cell Science* 131.24, jcs219204. DOI: 10.1242/jcs.219204. URL: https://journals.biologists.com/jcs/article/131/24/jcs219204/77044/Glycosphingolipid-metabolism-in-cell-fate (visited on 06/07/2021).

Russo, Domenico, Floriana Della Ragione, et al. (Apr. 3, 2018). "Glycosphingolipid metabolic reprogramming drives neural differentiation". In: *EMBO J* 37.7. DOI: 10.15252/embj.201797674. URL: https://onlinelibrary.wiley.com/doi/10.15252/embj.201797674 (visited on 06/07/2021).

Saritas-Yildirim, Banu and Elena M. Silva (Apr. 2014). "The role of targeted protein degradation in early neural development: Protein Degradation and Neurogenesis". In: *genesis* 52.4, pp. 287–299. DOI: 10.1002/dvg.22771. URL: http://doi.wiley.com/10.1002/dvg.22771 (visited on 06/07/2021).

Schmidt, Oliver et al. (Aug. 2019). "Endosome and Golgi-associated degradation (EGAD) of membrane proteins regulates sphingolipid metabolism". In: *EMBO J* 38.15. DOI: 10.15252/embj.2018101433. URL: https://onlinelibrary.wiley.com/doi/10.15252/embj.2018101433 (visited on 06/07/2021).

Schuh, Amber L. and Anjon Audhya (May 2014). "The ESCRT machinery: From the plasma membrane to endosomes and back again". In: *Critical Reviews in Biochemistry and Molecular Biology* 49.3, pp. 242–261. DOI: 10.3109/10409238.2014.881777. URL: http://www.tandfonline.com/doi/full/10.3109/10409238.2014.881777 (visited on 06/07/2021).

Tamm, Christoffer, Sara Pijuan Galitó, and Cecilia Annerén (2013). "A comparative study of protocols for mouse embryonic stem cell culturing". In: *PLoS ONE* 8.12, pp. 1–10. DOI: 10.1371/journal.pone.0081156.

Vu, Don et al. (2013). "A structural basis for selective dimerization by NF-κB RelB". In: *Journal of Molecular Biology* 425.11, pp. 1934–1945. DOI: 10.1016/j.jmb.2013.02.020.

Wang, Ting et al. (Dec. 1, 2014). "Discovery and characterization of a novel extremely acidic bacterial N-glycanase with combined advantages of PNGase F and A". In: *Bioscience Reports* 34.6, e00149. DOI: 10.1042/BSR20140148. URL: https://portlandpress.com/bioscirep/article/doi/10.1042/BSR20140148/56284/Discovery-and-characterization-of-a-novel (visited on 06/07/2021).

Wongpaiboonwattana, Wikrom and Marios P. Stavridis (May 14, 2015). "Neural Differentiation of Mouse Embryonic Stem Cells in Serum-free Monolayer Culture". In: *JoVE* 99, p. 52823. DOI: 10.3791/52823. URL: http://www.jove.com/video/52823/neural-differentiation-mouse-embryonic-stem-cells-serum-free (visited on 06/07/2021).

Yamaji, Toshiyuki, Kiyotaka Nishikawa, and Kentaro Hanada (Nov. 2010). "Transmembrane BAX Inhibitor Motif Containing (TMBIM) Family Proteins Perturbs a trans-Golgi Network Enzyme, Gb3 Synthase, and Reduces Gb3 Biosynthesis". In: *Journal of Biological Chemistry* 285.46, pp. 35505–35518. DOI: 10.1074/jbc.M110.154229. URL: https://linkinghub.elsevier.com/retrieve/pii/S0021925820468917 (visited on 06/07/2021).

Yamaji, Toshiyuki, Tsuyoshi Sekizuka, et al. (Jan. 2019). "A CRISPR Screen Identifies LAPTM4A and TM9SF Proteins as Glycolipid-Regulating Factors". In: *iScience* 11, pp. 409–424. DOI: 10.1016/j.isci.2018.12.039. URL: https://linkinghub.elsevier.com/retrieve/pii/S2589004218302694 (visited on 06/07/2021).

Yu, Alice L. et al. (2016). "Alterations of glycosphingolipids in embryonic stem cell differentiation and development of glycan-targeting cancer immunotherapy". In: *Stem Cells and Development* 25.20, pp. 1532–1548. DOI: 10.1089/scd.2016.0138.

Zhang, Yonggang and Wenhui HU (2012). "NFκB signaling regulates embryonic and adult neurogenesis". In: *Front Biol (Beijing)* 23.1, pp. 1–7. DOI: 10.1016/j.acthis.2007.10.016.Image. URL: https://www.ncbi.nlm.nih.gov/pmc/articles/PMC3624763/pdf/nihms412728.pdf.

Zhao, Mingming et al. (2018). *Transcriptional outcomes and kinetic patterning of gene expression in response to NF-κB activation*. Vol. 16. 9. DOI: 10.1371/journal.pbio.2006347.